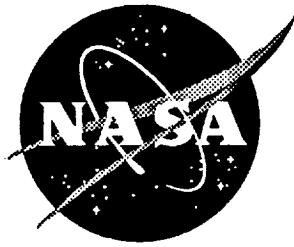


NASA Contractor Report 194982 (Revised Copy)



Computer Modeling the Fatigue Crack Growth Rate Behavior of Metals in Corrosive Environments

Edward Richey III, Allen W. Wilson, Jonathan M. Pope, and Richard P. Gangloff
University of Virginia, Charlottesville, Virginia

(NASA-CR-194982-Rev) COMPUTER
MODELING THE FATIGUE CRACK GROWTH
RATE BEHAVIOR OF METALS IN
CORROSIVE ENVIRONMENTS Final Report
(Virginia Univ.) 180 p

N95-15918

Unclas

G3/26 0033911

Grant NAG1-745

September 1994

National Aeronautics and
Space Administration
Langley Research Center
Hampton, Virginia 23681-0001

Table of Contents

List of Illustrations	iii
List of Tables	vi
Executive Summary	viii
Introduction	1
Section I: Data Collection and Preparation (Jonathan Pope)	
I.1: Data Collection	9
I.2: Digitizing the Graphs	12
I.3: Data File Transformations	15
I.4: Digitization and Transformation Example	19
I.5: Error Analysis	23
I.6: Conclusions for Data Collection and Preparation	34
Section II: Interpolative Model (Edward Richey,III)	
II.1: Crack Growth Rate Equations	37
II.2: Interpolative Computer Modeling Program	49
II.3: Data Testing and Results for the Interpolative Model	54
II.4: Conclusions for the Interpolative Model	82
Section III: Linear Superposition Model (Allen W. Wilson)	
III.1: Introduction to the Linear Superposition Method	85
III.2: Implementation of the Linear Superposition Model	91
III.3: Data Testing and Results for the Linear Superposition Model	99

III.4: Conclusions for the Linear Superposition Model	106
References	109
Appendix A: Data File Directory	112
Appendix B: Procedure for Creating Data Files from Graphs	115
Appendix C: DIGITIZE Program Listing	121
Appendix D: Examples for the Interpolative Model	126
Appendix E: Superposition Program Verification - Integration	146
Appendix F: Examples for the Superposition Model	152
Appendix G: Computer Models for Fatigue Analysis	159

List of Illustrations

Figure 1: Schematic of three regimes of fatigue crack growth	2
Figure 2: Effect of frequency on crack growth in Ti-8Al-1Mo-1V alloy	3
Figure 3: Static load environmental crack growth	5
Figure 4: Schematic illustrating the method of linear superposition	7
Figure 5: Typical da/dN vs. ΔK graph	12
Figure 6: Digitized data example	16
Figure 7: Crack growth data for Ti-6Al-4V	19
Figure 8: Digitized and transformed Ti-6Al-4V data	24
Figure 9: Transformation test, original data	25
Figure 10: Transformation test, digitized data	26
Figure 11: Transformation test, photocopied data	29
Figure 12: Original data with error band	35
Figure 13: Crack closure function as a function of stress ratio	40
Figure 14: Schematic drawing of a hyperbolic sine (SINH) curve	41
Figure 15: Schematic drawing of a sigmoidal curve	43
Figure 16: Comparison of curves fit by Haritos and interpolative model	56
Figure 17: Fit of fatigue data for Ti-6Al-4V in air with $R = 0.1$	61
Figure 18: Fit of fatigue data for Ti-6Al-4V in air with $R = 0.4$	62
Figure 19: Fit of fatigue data for Ti-6Al-4V in air with $R = 0.7$	63
Figure 20: Fit of fatigue data for Ti-6Al-4V in 1.0% NaCl with $R = 0.1$	64

Figure 21: Fit of fatigue data for Ti-6Al-4V in 1.0% NaCl with $R = 0.4$	65
Figure 22: Fit of fatigue data for Ti-6Al-4V in 1.0% NaCl with $R = 0.7$	66
Figure 23: Interpolated data using Forman Equation with closure (C,n fit)	71
Figure 24: Interpolated data using Forman Equation with closure (C,n,p,q fit)	73
Figure 25: Interpolated data using Forman Equation without closure (C,n fit)	74
Figure 26: Interpolated data using Forman Equation without closure (C,n,p,q fit) ...	76
Figure 27: Interpolated data using Hyperbolic Sine (SINH) Equation	78
Figure 28: Interpolated data using Sigmoidal Equation	80
Figure 29: Wei and Landes corrosion fatigue plot	87
Figure 30: Corrosion fatigue plot of AA 7079-T651 - frequency dependent	88
Figure 31: AA 7079-T651 corrosion fatigue plot at different frequencies	89
Figure 32: Corrosion fatigue plot of IN 718 - frequency dependent	90
Figure 33: IN 718 corrosion fatigue plot with various hold times	90
Figure 34: Sinusoidal loading wave form	95
Figure 35: Ramp loading with hold time	95
Figure 36: Ramp loading with no hold time	96
Figure 37: Square loading wave form	96
Figure 38: Computer predictions for Wei and Landes data at 150 Hz	101
Figure 39: Computer predictions for Wei and Landes data at 5 Hz	102
Figure 40: Computer predictions for Speidel data - frequency dependent	104
Figure 41: Computer predictions for Speidel data at various frequencies	105
Figure 42: Computer predictions for Ashbaugh data for $R = 0.1$ and 0.5	107

Figure F.1: Materials on file for Forman Equation constants	154
Figure F.2: Input of data modeled by Forman Equation	155
Figure F.3: Specifications for determining Forman Equation Constants	156

List of Tables

Table I.1: Error analysis for original graph (Figure 9)	27
Table I.2: Error analysis for photocopied graph (Figure 11)	30
Table I.3: Summary of test results	33
Table II.1: Bench marking of linear regression algorithm	54
Table II.2: Bench marking of non-linear regression algorithm	55
Table II.3: Forman Equation with closure (C,n fit)	57
Table II.4: Forman Equation with closure (C,n,p,q fit)	58
Table II.5: Forman Equation without closure (C,n fit)	58
Table II.6: Forman Equation without closure (C,n,p,q fit)	59
Table II.7: Hyperbolic Sine Equation	59
Table II.8: Sigmoidal Equation	60
Table II.9: Coefficients of determination	67
Table II.10: Average coefficients of determination	68
Table II.11: Forman Equation with closure (C,n fit)	69
Table II.12: Forman Equation with closure (C,n,p,q fit)	70
Table II.13: Forman Equation without closure (C,n fit)	72
Table II.14: Forman Equation without closure (C,n,p,q fit)	75
Table II.15: SINH Equation parameters	77
Table II.16: Sigmoidal Equation parameters	79
Table E.1: Program predictions for $n = 1$	149

Table E.2: Program predictions for $n = 2$	150
Table E.3: Program predictions for $n = 3$	150
Table E.4: Program predictions for $n = 4$	151

Executive Summary

The fatigue crack growth resistance of aerospace alloys is generally reduced by concomitant cyclic plastic deformation and exposure to a wide range of aggressive environments at ambient and elevated temperatures. Notable examples are iron and nickel-based superalloys in high pressure gaseous hydrogen, high strength alloy steels in water vapor, as well as aluminum, titanium and ferrous alloys in aqueous chloride solutions. Despite substantial advances over the past 30 years, the fracture mechanics approach to damage tolerant fatigue life prediction has not been adequately developed to enable incorporation of environmental effects on fatigue in codes such as NASA FLAGRO.

Research, conducted at the University of Virginia (UVa) over the past four years and under NASA grant sponsorship, has aimed to develop the data, methods and understanding necessary to incorporate descriptions of environment-enhanced fatigue crack propagation (FCP) into NASA FLAGRO. The first phase produced a literature review of monotonic load stress corrosion cracking and environmental FCP (or corrosion fatigue) of a variety of structural alloys and environments relevant to aerospace applications.¹ The second phase of this research included three projects, conducted by undergraduates in the Department of Mechanical and Aerospace Engineering at UVa to fulfill the thesis-project requirement of the BS degree. This report documents the results of this team research. One student, Edward Richey III, has continued this work in conjunction with a Master of Science degree program in Mechanical Engineering. He was responsible for integrating the results of each undergraduate project into this report and the accompanying software package, and is continuing experimental work on corrosion fatigue crack propagation in the Ti-6Al-4V/aqueous chloride system.

The underlying objective of the second phase of the research was to establish the foundation to incorporate deleterious environmental effects on fatigue crack propagation laws into NASA FLAGRO. Known methods to interpolate and potentially extrapolate

¹ R.P. Gangloff and S.S. Kim, *Environment Enhanced Fatigue Crack Propagation in Metals*, NASA Contractor Report 4301, NASA Scientific and Technical Information Division, 1990.

environmental FCP data were emphasized, including linear superposition and empirical curve-fitting descriptions of fatigue crack growth rate (da/dN) versus applied or effective stress intensity range (ΔK). The third approach, mechanism-based predictions of environmental FCP, is beyond the scope of this project and is being examined elsewhere.²

The results of the undergraduate projects were incorporated into a single computer program.³ This program contains elements that were extracted from the NASA FLAGRO source code, particularly library data on material fatigue and fracture properties, as well as the Forman equations for calculations of fatigue crack growth rate versus stress intensity relationships, including the effect of crack closure. The program was written in Fortran and is executed by entering *MENU* from the DOS prompt on an IBM-compatible personal computer. The user can then select one of the following three options that resulted from each undergraduate project.

Digitization of Crack Growth Rate Data (Jonathan M. Pope)

The objective of this task was to develop a method to digitize FCP kinetics data, generally presented in terms of extensive da/dN - ΔK pairs, to produce a file for subsequent linear superposition or curve-fitting analysis. The method that was developed is specific to the Numonics 2400 Digitab and is comparable to commercially available software products such as DigimaticTM.⁴ Experiments demonstrated that the errors introduced by the photocopying of literature data, and digitization, are small compared to those inherent in laboratory methods to characterize FCP in benign and aggressive environments. The digitizing procedure was employed to obtain fifteen crack growth rate data sets for several aerospace alloys in aggressive environments.

² R.P. Gangloff, *Corrosion Fatigue Crack Propagation in Metals*, in Environment Induced Cracking of Metals, R.P. Gangloff and M.B. Ives, eds., NACE, Houston, TX, pp. 55-109, 1990.

R.P. Gangloff, *NASA-UVa Light Aerospace Alloy and Structures Technology Program*, UVA Report No. UVA/528266/MSE94/114, March, 1994.

³ A copy of this program may be obtained from the NASA Grant monitor, Dr. R.S. Piascik, in the Mechanics of Materials Branch at the NASA-Langley Research Center.

⁴ DigimaticTM is available from Famous Engineer Brand Software located in Richmond, Virginia.

Interpolation Modeling of Environmental FCP Data (Edward Richey, III)

The objective of this task was to develop curve-fitting procedures for several well-known relationships between da/dN and ΔK , and to employ algorithms to interpolate the effects of loading frequency, hold time and stress ratio on the constants in these crack growth rate equations. Equations include the simple Paris power-law, the Forman Equation (with and without closure as developed in NASA FLAGRO), the Hyperbolic Sine Equation, and the Sigmoidal Equation. The program allows the user to select the form of the crack growth rate equation, as well as which constants to fix and which to optimize based on an input da/dN - ΔK data set. Interpolation is accomplished based on a logarithmic function, however, additional research is required to improve this approach by incorporating known results on time-cycle-dependent environmental FCP. Once the equation constants are determined as a function of frequency, hold-time and stress ratio based on several sets of input data for a given material and environment system, da/dN versus ΔK relationships can be interpolated.

This empirical approach was assessed for Ti-6Al-4V in aqueous NaCl at several loading frequencies. The Forman, Hyperbolic Sine and Sigmoidal equations each reasonably described non-power-law crack growth rate behavior. The program incorporates statistical parameters (the coefficient of determination, r^2 , and a confidence interval estimate for each constant) to evaluate the goodness of fit for each crack growth rate equation. On this basis, r^2 was generally above 0.90 for each of these three equations applied to six da/dN - ΔK data sets for Ti-6Al-4V in air and NaCl at three stress ratios. The Forman Equation (with or without closure) yielded the highest r^2 for three cases, the Hyperbolic Sine Equation yielded the highest r^2 for two cases, and the Sigmoidal Equation yielded the highest r^2 for three cases. The Forman Equation and the Sigmoidal Equation yielded identically high average r^2 values for all data. The program contains the graphics capability to plot da/dN versus ΔK data with the superimposed curve fits.

Linear Superposition Modeling of Environmental FCP Data (Allen W. Wilson)

The basic linear superposition model put forth by Wei and Landes was implemented in the computer program, with improved analysis features. This approach enables the user

to input material property data on fatigue crack propagation in a benign environment, as well as data on monotonic load stress corrosion cracking for the embrittling environment of interest, coupled with the time and stress intensity dependence of the loading function. Material property data can be either extracted from the NASA-FLAGRO library, or entered as specific da/dN - ΔK or da/dt - K pairs and fit to the various equations described above. The portion of the fatigue load-cycle where environment is damaging must be determined by the user. With this input, the linear superposition program provides an output file and graphical representation of environmental fatigue crack growth rate versus ΔK , as a function of loading frequency, hold time, waveform, and stress ratio. The accuracy of the program was confirmed by comparisons with published linear superposition calculations.

The results of this research augment the capability of NASA-FLAGRO. Example calculations demonstrating each element of the program are presented in several appendices to this report. Additional research is, however, required. The linear superposition approach is only accurate and relevant to a limited class of aerospace alloys that are exceptionally prone to environmental crack growth under monotonic loading. Those alloys that are properly selected to resist such cracking are likely to be sensitive to environmental FCP, however, the basic linear superposition approach will substantially underpredict da/dN . The curve fitting approach provides reasonable interpolations of the constants in the crack growth rate equations, however, the form of the interpolation functions must be explored and coupled with physical understanding of time-cycle-dependent environmental FCP. This approach is not well suited for extrapolations outside of the input data base that was used to define the equation constants. These undergraduate projects further confirm the necessity to couple engineering estimation with fundamental understanding of environmental fatigue damage mechanisms.⁵

⁵

R.P. Wei and R.P. Gangloff, *Environmentally Assisted Crack Growth in Structural Alloys: Perspectives and New Directions*, in *Fracture Mechanics: Perspectives and Directions*, ASTM STP 1020, R.P. Wei and R.P. Gangloff, eds., ASTM, Philadelphia, PA, pp. 233-264 (1989).

Introduction

Overview

One major problem when designing or analyzing a structural component is determining the behavior under cyclic loads, which cause cracking by fatigue, particularly coupled with corrosive environments. NASA would like to obtain an effective method of estimating environmental effects on fatigue crack propagation (FCP) rates in metals for use in damage tolerant codes such as FLAGRO. The objective of this research is to accomplish this task through a group undergraduate project within the Materials Science and Engineering Department at the University of Virginia. The method that will be developed for NASA will estimate the rate at which a crack grows when a structural alloy is exposed to cyclic loads in a corrosive or embrittling environment. Data from previous tests will be analyzed.

Fatigue Behavior of Metals

One methodology that has been developed for fatigue analysis is linear elastic fracture mechanics (LEFM). LEFM assumes that all metal parts contain preexisting cracks of engineering size. The speed with which these cracks propagate depends on the type of load, operating conditions, and environment. Cracks grow in a slow, stable manner until a critical crack size is reached, the crack becomes unstable, and the part catastrophically fractures.

Linear elastic fracture mechanics is primarily concerned with predicting conditions

under which unstable crack growth will occur. The theory revolves around a relation involving the nominal stress (σ), crack length (a), and stress intensity factor (K). The stress intensity factor is defined as:

$$K = \sigma \sqrt{\pi a} Y \quad (1)$$

where Y is a correction factor which depends on crack geometry. Failure of the part is assumed to occur when the stress intensity factor exceeds a critical value which marks the onset of fast fracture. When fast fracture occurs, cracks in the part unstably grow at the speed of sound in the material, causing catastrophic failure. The critical value is usually the fracture toughness of the material, K_C , or K_{IC} .

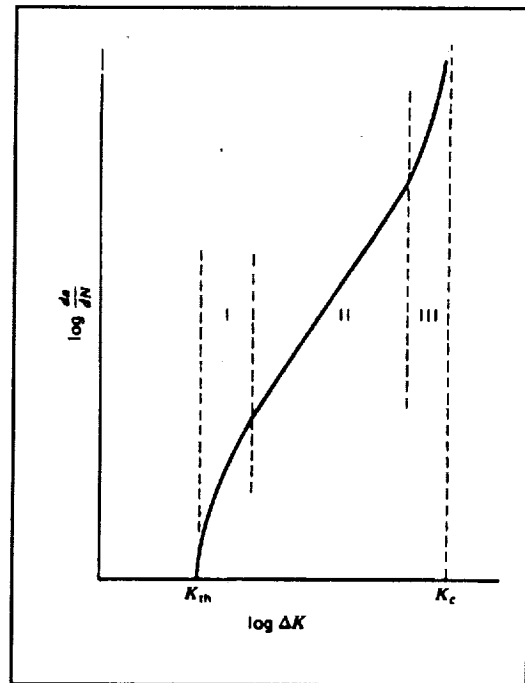


Figure 1: Schematic of three regimes of fatigue crack growth ¹.

A typical fatigue crack growth rate curve is shown in Figure 1. The curve is divided into

three regions. Region I is the near threshold region where a decrease in ΔK ($\Delta K = K_{max} - K_{min}$) results in a sharp decrease in da/dN as the threshold value ΔK_{th} is reached.

Cyclic loads which produce ΔK less than ΔK_{th} do not cause crack propagation. Region

III is the near critical region where a small increase in ΔK produces a large increase in da/dN as K_{max} approaches K_C . Region II is a transition region between Regions I and

III, and can often be characterized by a simple power-law relationship between da/dN and ΔK .

Environmental Effects on Crack Growth

The rate at which fatigue crack growth occurs is strongly dependent on the environment in which the part is operated. An inert or benign environment does not affect fatigue crack growth. A corrosive or embrittling environment affects the fatigue crack growth.

In an inert environment, the rate of fatigue crack growth, $(da/dN)_{\text{fatigue}}$, is generally only a function of the stress intensity factor range, ΔK , and the stress ratio, R ($R = K_{\min}/K_{\max}$). Load characteristics such as frequency, wave form, and hold time do not greatly affect

the behavior. In a corrosive environment, the load characteristics do affect the rate of crack growth. Frequency becomes an important factor because at lower frequencies "more time is allowed for environmental attack during the fatigue process."¹ This effect is illustrated in Figure 2. The lower the frequency and the longer the hold time, the more time the environment has to attack the metal during each load cycle, thus the faster the crack grows. Additionally, environmental fatigue crack propagation can

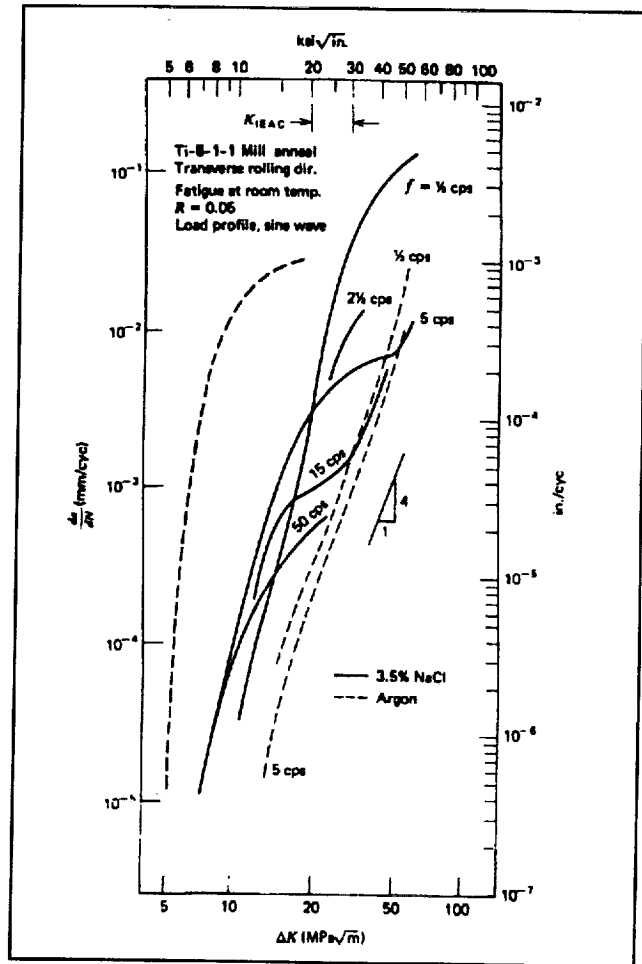


Figure 2: Effect of frequency on crack growth in Ti-8Al-1Mo-1V alloy ¹.

involve complex dependencies of da/dN on ΔK and R ; this behavior is unique compared to that typical of inert environment crack growth.

Environmental subcritical crack growth occurs in corrosive environments without necessarily involving cyclic loads. The stress intensity is held constant and a time-based crack growth rate for the metal in the corrosive environment is determined. This crack growth rate has the form $(da/dt)_{\text{environment}}$, which is the change in the crack length, a , per unit time, t ($da/dt = 0$ in a vacuum and without crack tip creep damage). There is no relevance of stress ratio or frequency since there are no cyclic load patterns and the stress intensity, K , is constant. Time is the main concern.

Stress corrosion describes the growth of cracks due to static loads on a metal in environments which enhance crack growth. The static load causes localized plasticity at the crack tip. A chemical reaction between the material and its environment causes crack propagation when none would occur in the absence of the environment. Because of the chemical reaction at the crack tip, the term corrosion is used to describe this mode of crack growth, although the surrounding material may not show typical signs of corrosion².

Figure 3 is a graphical depiction of the power laws that dictate the static load environmental crack growth rate.

$$(da/dt)_{\text{environment}} = D K^y \text{ below } K^* \quad (2)$$

$$(da/dt)_{\text{environment}} = B K^z \text{ above } K^* \quad (3)$$

where B , D , y , z and K^* are material constants.

Experiments can give accurate estimates of the material property coefficients in

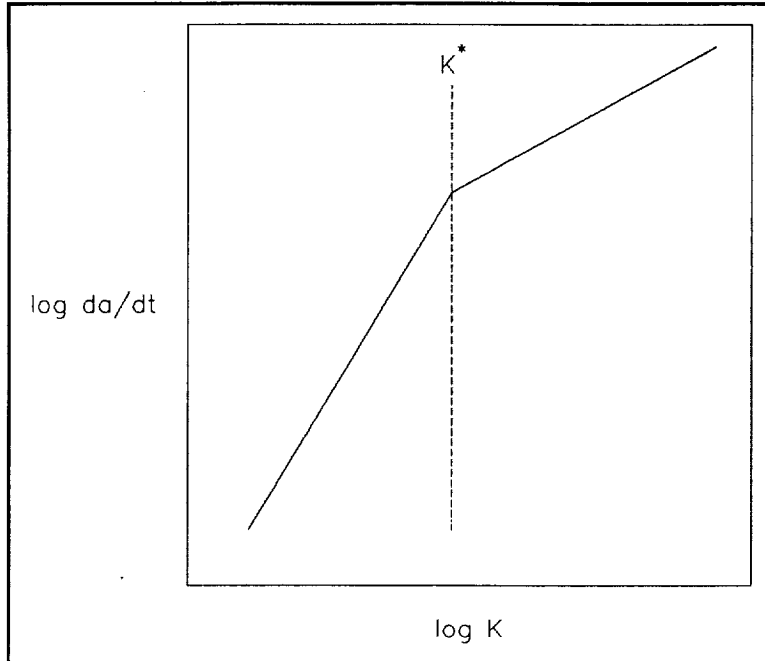


Figure 3: Static load environmental crack growth. K^* is the critical stress intensity between the two power laws for time-based crack growth in a corrosive environment.

the static load environmental crack growth rate laws. However, simple power laws do not apply when both fatigue crack growth and static load environmental crack growth occur simultaneously. This situation is known as environmental fatigue crack growth (or corrosion fatigue), and the rate of crack growth is represented by $(da/dN)_{total}$. Several factors are pertinent in describing the conditions of environmental crack growth. These factors are the stress ratio (R), the frequency of the applied load (f in Hertz), and the environment. Other test factors which have an effect on crack growth rate, but are not addressed in this paper, are environment chemistry, temperature and metallurgical variables.

$(da/dN)_{total}$ is not generally described by a simple power law. For example, Wei and Landes³ outlined a method for predicting $(da/dN)_{total}$ based on superposition of the effects of the crack growth rates, $(da/dN)_{fatigue}$ and $(da/dt)_{environment}$, to yield the total crack growth rate after integration:

$$(da/dN)_{total} = (da/dN)_{fatigue} + \int_{\tau} [da/dt(K)_{environment}] [K(t)] dt \quad (4)$$

where for example:

$$K(t) = K_{min} + (K_{max} - K_{min}) (1 - \cos \omega t) / 2 \quad (5)$$

with

$$\omega = 2 \pi f \text{ (rad/sec)}$$

$$\tau = 1 / f \text{ (seconds)}$$

$K(t)$ may be any time dependent function for a given application. A graphical depiction of superposition is given in Figure 4. The integration term in Equation 4 is often termed the stress corrosion crack growth rate, $(da/dN)_{stress \text{ corrosion}}$. The total crack growth rate, $(da/dN)_{total}$ in Equation 4, is both time and cycle dependent. Gallagher and Wei⁴ note that crack growth is dominated by environmental effects at low frequencies and by mechanical fatigue at high frequencies.

$(da/dN)_{total}$ may also be described by more complex empirical equations such as the Forman, Hyperbolic Sine (SINH), and Sigmoidal Equations. These equations can all be fit to sets of $(da/dN)_{total}$ data and the constants in the equations determined by least squares regression. The fitted constants in the equations can be related to the load characteristics such as frequency, hold time, and stress ratio using empirical relationships. Using these empirical relationships, the equation constants can be determined for any combination of loading frequency, hold time and stress ratio for a given material-environment system. Once these constants have been determined for the desired load characteristics, $(da/dN)_{total}$ can be calculated for any value of ΔK .

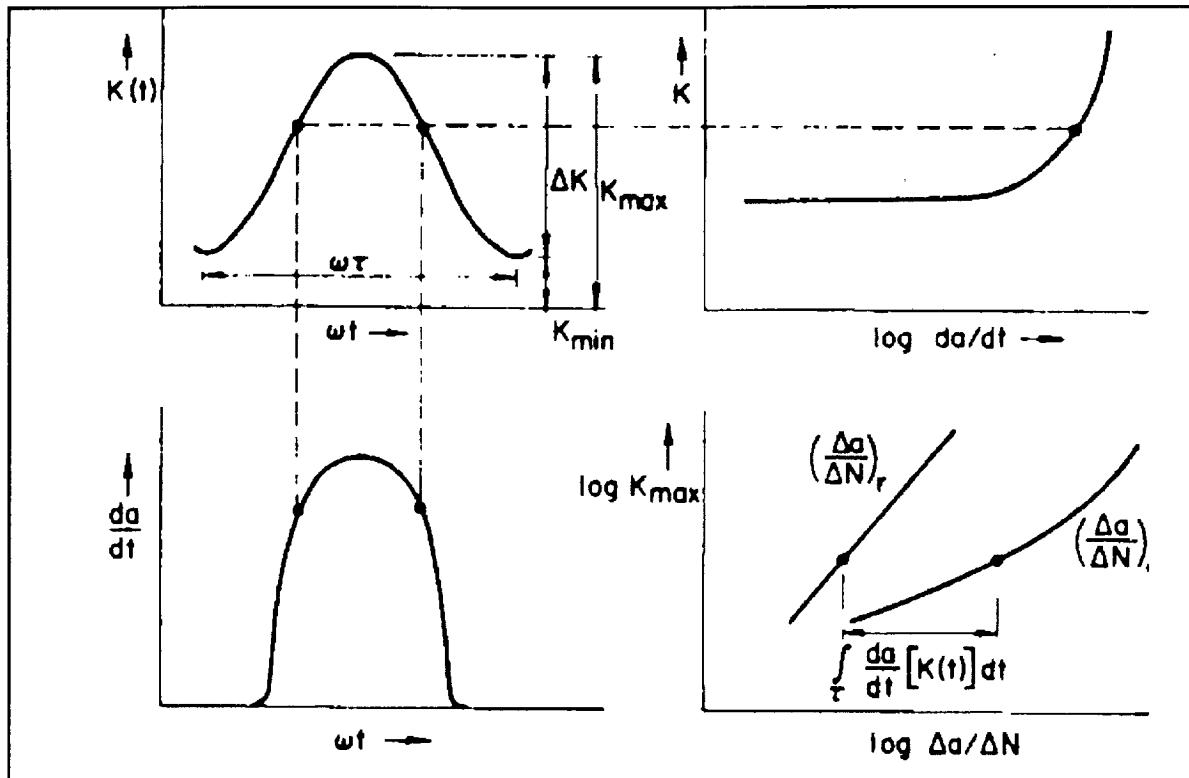


Figure 4: Schematic diagram illustrating the Wei and Landes method of linear superposition analysis. (a) Stress intensity spectrum in fatigue (top left); (b) rate of crack growth under constant load in a corrosive environment (top right); (c) environmental contribution to crack growth in fatigue (bottom left); (d) predicted environmental fatigue crack growth rate (bottom right)³

Project Organization

Two different mathematical schemes were used to develop a method for predicting fatigue crack growth rates in corrosive environments. Allen Wilson developed a FORTRAN program to determine the crack growth rates with a linear superposition model which combines static load environmental cracking time-rate $((da/dt)_{\text{environment}})$ data with inert environment mechanical fatigue cycle-rate $((da/dN)_{\text{fatigue}})$ data. Edward Richey modified the NASA FORTRAN program FLAGRO which contains curve fitting functions that relate crack growth rates to ΔK and the stress ratio, R . Though both programs attempt to generate the same output, different input data and different calculative methods are employed. The results may not be similar because of

known deficiencies in each approach, at least for some material-environment systems.

Jonathan Pope developed a method for collecting, organizing, and preparing data for use in the testing and development of the two computer programs.

The main benefit of this project is the reduction of testing. If fatigue crack growth rates are required for a specific set of conditions that have not been tested, time consuming laboratory experiments are needed. The computer programs can supplement these experiments. The results of the computer programs will then be applied to different machine components that NASA uses so that the lifetime of the component can be accurately predicted. Expensive and exhaustive tests will not be necessary in obtaining a reasonable estimate of the component life.

The following project report is divided into three sections. The first section discusses the digitization process for preparing data files. The second section discusses the interpolative computer model, while the third section discusses the linear superposition model.

Section I: Data Collection and Preparation

I.1: Data Collection

The two computer models for environmental FCP rates require different types of input data. The superposition model combines $(da/dt)_{\text{environment}}$ and $(da/dN)_{\text{fatigue}}$ to arrive at $(da/dN)_{\text{total}}$. The interpolative model starts with several variations of $(da/dN)_{\text{total}}$ data and uses power law approximations to account for the differences in the variables that affect fatigue crack growth in a corrosive environment. The interpolative model can also describe $(da/dt)_{\text{environment}}$ and $(da/dN)_{\text{fatigue}}$ data with equations. Therefore, all three types of crack growth rate data are needed to create a database for the two computer programs. These data will come from laboratory tests during the last twenty-five years. Each graph that is collected often has more than one set of useful data. For a specific alloy, an experimenter has varied either the environment, frequency of the load, or the stress ratio.

Crack growth rate data are typically in the form of graphs with individual points specified and trend lines through the points, but only the data points are the results of laboratory testing. Unfortunately, the common practice is to only publish the graphs with the data points, while the precise numerical values of these data are required for the computer models. These values are often not retained by the experimenters, so searching for values from the authors of the tests would be a hopeless endeavor. As many as 200 test points may be represented on one graph, which makes it impractical to

handle all the numbers that would need to be published along with the graph. The intended outcome of collecting and digitizing a number of graphs is to provide a varied and complete set of data to be used in the computer programs. This was accomplished by recording copies of typical graphs that showed variations in the controlling characteristics on which the modeling programs would focus. The graphs were collected for specific aerospace alloys, environments, and variables.

The database that is compiled is not a complete tool for crack growth rate prediction, but rather provides a realistic test of the computer models. For this reason, a large number of alloys are not examined. A more significant aspect of the database is whether or not it encompasses a wide array of variables. These variables include the stress ratio, frequency, yield strength, and environment. The alloys should be structural materials, fully characterized by fracture mechanics methods. Ti-6Al-4V, a common titanium alloy, and 4340 steel each fit these two criteria. Data for 7075 aluminum have also been recorded.

Data from four different environments were collected. Air with 40% relative humidity, distilled water, a 3.5% sodium chloride solution, and argon make up the environments. Argon is used as an equivalent to vacuum for $(da/dN)_{fatigue}$ data. These four environments are represented in both the Ti-6Al-4V and 4340 steel databases. Stress ratio variations are also included.

One factor which affects fatigue crack growth in corrosive environments is the frequency of the applied load. More so than any other factor, frequency is altered to generate different growth rate laws for a material-environment system. In other words

the metal, environment, and stress ratio are constant throughout a set of tests, but the frequency is changed. At lower frequencies, larger crack growth rates per cycle are experienced than for high frequencies. This occurs because the crack growth rate is measured in length per cycle; at a lower frequency there is a longer period of time that the metal is exposed to the corrosive environment for one cycle. $(da/dt)_{\text{environment}}$ plays a more dominant role in crack growth for this situation.

In the 4340 steel database, yield strength is also important. 4340 steel has a large range of possible yield strengths controlled by tempering. A factor of 100 can separate the $(da/dt)_{\text{environment}}$ rates for 4340 steels of different yield strengths. Therefore, careful attention has been paid to the yield strength of the specimens used in the various experiments. All graphs in the database are for 4340 steel with a yield strength of 1300 to 1700 MPa.

The graphs that have been collected are from a wide range of sources. Most of the data originated in papers in various journals. The graphs have since been duplicated and reprinted in other texts, compendia, and papers. In the data search, several sources presented graphs of the same data. Sometimes the overall appearance of the graph was changed while others looked exactly alike. Searches for specific data were often directed at journal articles, but the most productive manner of acquiring considerable amounts of data was to use compendiums. The Atlas of Fatigue Curves⁵ was very helpful, as were the Aerospace Structural Metals Handbook⁶ and the Structural Alloys Handbook⁷.

A complete list of the data file names and the characteristics that describe each file are given in Appendix A. These files have been sent through the digitization process

that is described in the following text.

I.2: Digitizing the Graphs*

The database consists of fourteen graphs that have the same basic form as that shown in Figure 5. This plot has a large number of data points for each curve. The different curves have different characteristics and each need an individual data file.

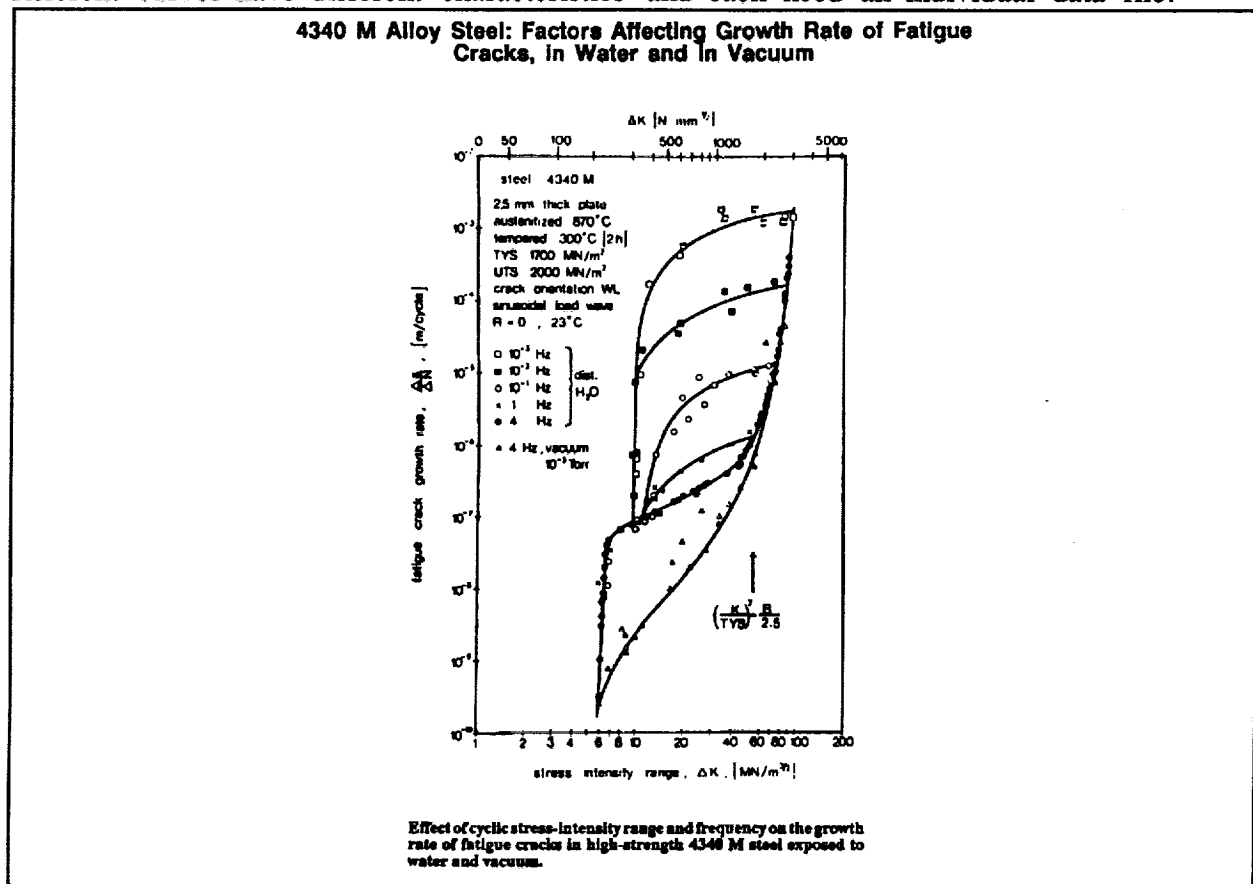


Figure 5: Typical da/dN vs. ΔK graph ⁸.

* A commercial program, DIGIMATIC, has recently been marketed for PC operation under Windows. This product presumably provides similar results to the approach described here but was not tested in this study.

The computer models need input in the form of X and Y coordinates for each da/dN and ΔK . One could try to read each point off the graph with a ruler or a similar technique, but that would be foolhardy. The results would be relatively inaccurate and the process would be tedious and time consuming. A better method is needed.

The method of choice is to electronically read the data points. This can be done using the Numonics 2400 Digitablet. Its primary use is associated with map reading and architectural dimensioning, but it meets our needs. The digitablet has an electromagnetic mechanism with a hand controlled cursor and keypad.⁹ A microprocessor and display console are also part of the digitablet system. The digitablet has many graphical functions, but it is used here only to accept data points. The origin of the graph is set as a zero point to enter data. The user then clicks on each data point to send it to a data file. Unfortunately, absolute distances, which are correlated to graphical data values, are measured only in centimeters or inches. Another problem arises from the set up of the graphs. The scales of the graphs are almost always logarithmic, but the digitablet is not capable of handling log scales. The data that are accepted by the digitablet in the form (X,Y) are meaningless when they stand alone. Section I.3 corrects these problems and creates accurate $(da/dN)-\Delta K$ or $(da/dt)-K$ data files.

A step by step procedure for using the digitablet is included in Appendix B. It covers several necessities such as properly aligning the axes, setting the origin, and selecting the reference points. A steady hand is required for good results, but the manual work that needs to be done in entering a set of points is minimal. Setting up the

system to receive the data is more complicated.

When using the digitablet, an editor must be initiated by an external source and the local source where data are to be retained. It is suggested that the UNIX system and the JOVE editor be used to receive data.⁹ The manual in Appendix B provides a set of guidelines. A user familiar with other editors or systems can work out an alternate method. The local source mentioned above is the computer terminal to the right of the digitablet. The external source can be any network computer.

Assuming that UNIX is the system of choice, the first step is to get a UNIX account. Becoming familiar with the UNIX system can be accomplished with the help of Academic Computing Center documents.¹⁰⁻¹³ It is important to note that a UNIX account can be logged onto from more than one machine at the same time. This feature will be needed to receive data from the digitablet.

The external source opens the UNIX session, and the local source connects to the session. This order of operation must be followed or the data file that is created will not be recorded. Next the JOVE editor is evoked only on the digitablet terminal.¹¹ The data points can now be entered with the keypad. Digitablet values will appear on the screen with other messages. The strange format of this information should be ignored. The data will be in a neat format when the acquisition process is complete.

After data entry is finished and the file has been saved, JOVE is terminated. The file now appears on the external source in a sensible form, a column of X values and a column of Y values. Once the file appears on the external source, the digitablet terminal can close its UNIX session.

Attention now turns to moving the data file to a place where it can be used. The FTP mode (File Transfer Protocol) can be entered while still in UNIX¹², and used to export the UNIX file to DOS. The A:, B:, or hard drive should be specified as the destination for the file. After the transfer, a data file consisting of two columns of numbers exists on a PC disk. The process of assigning real values to these data lies ahead. The manual in Appendix B states the specific steps needed to prepare for this transformation process.

The end result of the digitization and transformation process is the values of the graph points. With the values of the points, it is possible to recreate the graph seen in Figure 5, as illustrated in Figure 6.

I.3: Data File Transformations

The transformation process is necessary because the Numonics 2400 Digitablet does not allow the user to set the scale of the axes. All Digitablet measurements are calibrated in inches or centimeters relative to an input origin, rather than the values on the axes of the graph that is being digitized. The Digitablet output needs to be transformed to the correct values whether the graph has linear or logarithmic scales.

Originally, four FORTRAN programs were written to transform the raw data files into accurate, meaningful data files. The four programs were similar in setup and mathematical logic. The differences between the programs dealt with the orientations of

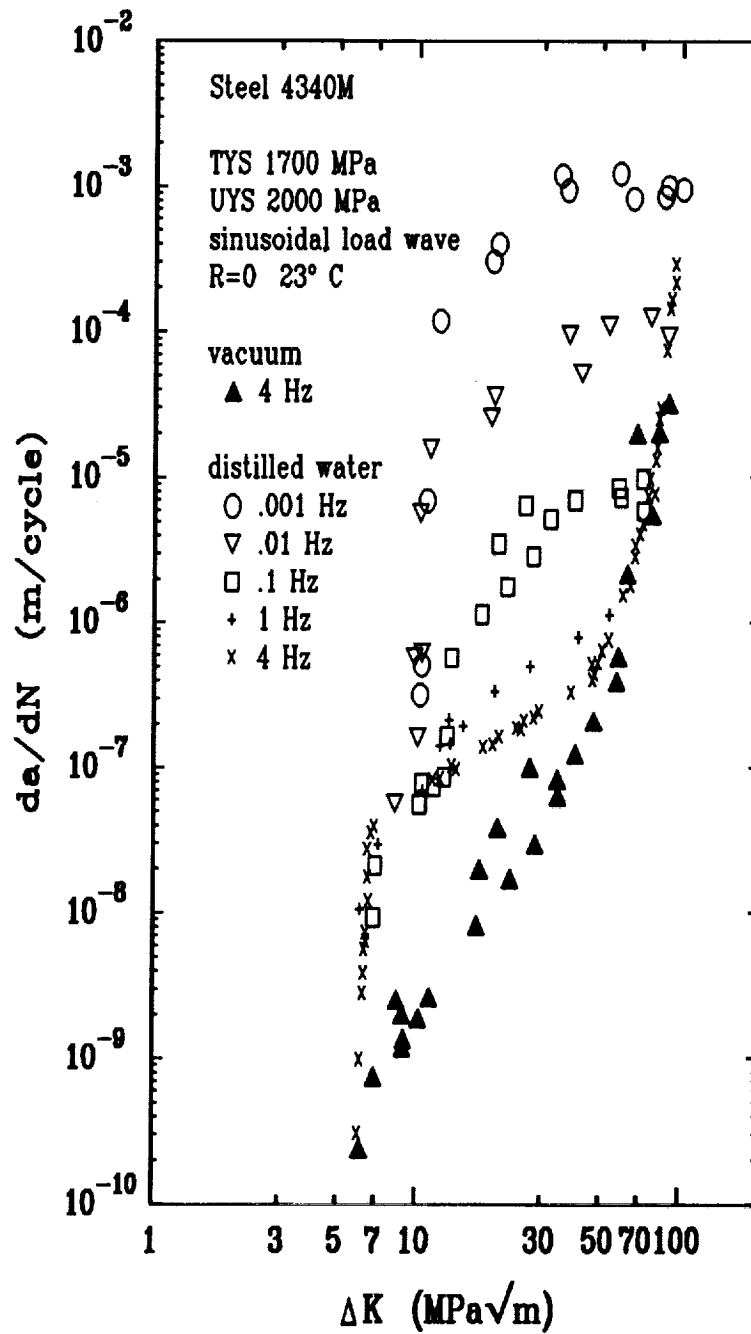


Figure 6: The graph from Figure 5 digitized and plotted with SigmaPlot.

the axes. Different combinations of logarithmic and linear scales on the X and Y axes created the need for more than one program.

An error analysis of the digitization and transformation process is presented in Section I.5. One result of a preliminary error analysis was the exposure of inadequacies in the four FORTRAN programs. One executable program which prompts the user for information about the graph was developed to replace the other programs. Either logarithmic or linear scales on any or both axes can be handled by the program DIGITIZE.EXE. All the functions that the four FORTRAN programs were capable of performing are included in the single executable program.

From the original plot, the user must input the following information for each axis:

1. Logarithmic or linear scale.
2. The graph value at the Digitablet origin.
3. The graph value at an arbitrary reference point far from the origin.
4. The absolute distance between the origin and the reference point as displayed on the Digitablet console.

Two purposes are served by recording information about the graphs. First, the graph origin is related to the zero point of the Digitablet output. For linear scales this is a number that is added to the digitized numbers, but this would also be a multiplying factor if the scales were logarithmic. The numbers in the data file are given meaning by scaling the axes. This is done with two values. One number is the graph value at a reference point, and the second number is the distance to the reference point as

reported on the Digitablet console. For example, on a log axis, the following data might be recorded.

Origin: Digitablet reads 0, graph reads 10.0 ksi/in

Reference point: Digitablet reads 6.000 cm, graph reads 80.0 ksi/in

If the digitablet value of 4.0 cm is entered for a point, x, the transformation is

$$X = (10.0) (80.0/10.0)^{(4.0/6.0)} = \text{a graphical value of } 40.0 \text{ ksi/in}$$

A similar function is set up to calculate values for linear scales. For the same graph data as in the example above,

$$X = 10.0 + (4.0/6.0)(80.0 - 10.0) = \text{a graphical value of } 56.67 \text{ ksi/in}$$

The digitization manual in Appendix B includes a description of all the characteristics of the graph that need to be recorded. The program source code in Appendix C, DIGITIZE.FOR, is easily modified, so the user may set up the transformation in the manner that will yield the most accurate output for different situations. Adaptations to the programs should be considered for applications other than crack growth rate data. For typical crack growth rate graphs, the program will run accurately as it exists.

Section I.4 will move step by step through the digitization process beginning with

a graph. Section I.5 discusses the error that can be expected in the results. These errors come not just from the reference point readings, but from many sources such as photocopying of graphs, shifting of the graph during digitization, and other human errors.

I.4: Digitization and Transformation Example

To illustrate the digitization and transformation process, one of the graphs from the database is presented as an example. One set of data is selected from the graph, and the results from the digitizer and

transformation program are shown. All four sets of digitized data will be re-plotted at the end of the example. The original literature graph is shown in Figure 7, and the specific series that will be the focus of the example is defined by the inverted triangles. The defining characteristics of the data are:

stress ratio = 0.1

frequency = 1 Hertz

environment = 0.6 M NaCl

units are in/cycle and $\text{ksi}\sqrt{\text{in}}$

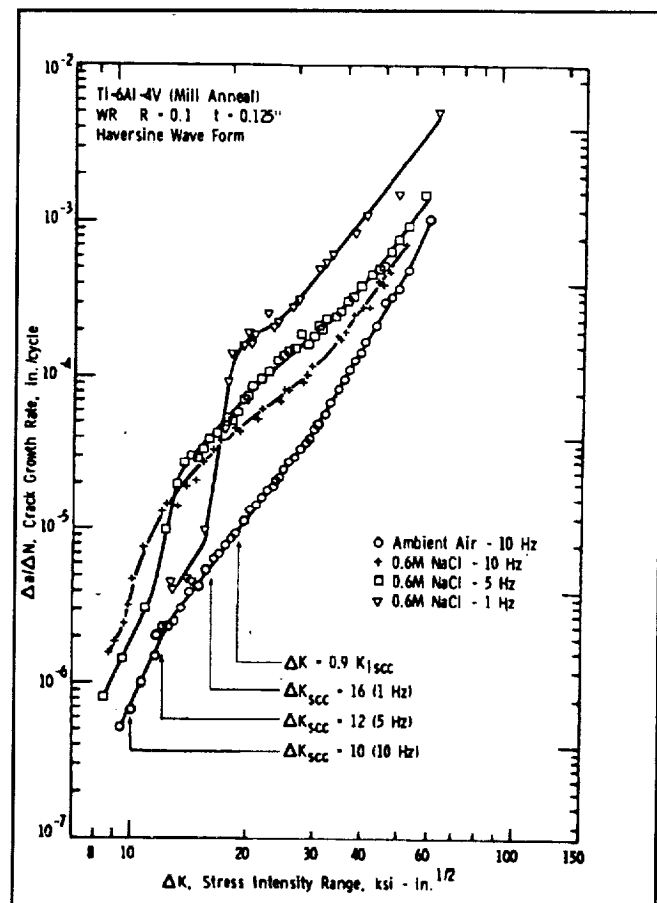


Figure 7: Crack growth data for Ti-6Al-4V¹⁴.

For the programmers who will use the data from these graphs, a list of the data files and their characteristics was created. This list appears in Appendix A. The data file which corresponds to the points in this example is TT1D.DAT. The first T in this name stands for transformed, the second T for titanium, the 1 for the first titanium graph, and the D for the fourth data set in the graph.

During the digitization process, the information that is needed for the transformation process was recorded. The information that was recorded was:

Digitablet origin: X axis value = 8 ksi $\sqrt{\text{in}}$

Y axis value = 10^{-7} in/cycle

Reference point: X axis value = 150 ksi $\sqrt{\text{in}}$

digitizer console = 6.492

Y axis value = 10^{-2} in/cycle

digitizer console = 10.375

All console units are in centimeters. The basis for choosing centimeters was to have the units consistent through all the digitized graphs. The following data file is the output from the digitizer.

<u>X</u>	<u>Y</u>
1.038	3.333
1.025	3.420
1.270	3.455
1.328	3.428
1.498	4.135
1.783	5.467
1.793	6.155
1.845	6.515
2.010	6.628

<u>X</u>	<u>Y</u>
2.113	6.645
2.135	6.765
2.050	6.800
2.403	6.898
2.433	6.943
2.313	7.082
2.653	7.153
2.715	7.262
2.963	7.662
3.060	7.733
3.153	7.855
3.448	8.125
3.635	8.340
4.057	8.645
4.598	9.735
-3.170	-2.843

The last two numbers in this series are negative to signal the end of the data to the transformation program. This point is mentioned in the digitization manual. This set of numbers was saved in the data file RT1D.DAT where the R stands for raw as opposed to transformed.

The data file RT1D.DAT is ready to be transformed. DIGITIZE.EXE is run with the information that was taken from the graph. Both axes have log scales. The only other input for the program is the filename for the transformed data file. After execution, the output file contains the finished set of data seen below.

ΔK <u>(ksi$\sqrt{\text{in}}$)</u>	$(da/dN)_{\text{total}}$ <u>(in/cycle)</u>
12.782	4.038 E-06
12.708	4.448 E-06
14.194	4.624 E-06
14.571	4.488 E-06
15.733	9.835 E-06
17.894	4.312 E-05
17.975	9.253 E-05
18.402	1.380 E-04
19.825	1.564 E-04
20.768	1.594 E-04
20.976	1.821 E-04
20.186	1.893 E-04
23.674	2.110 E-04
23.997	2.218 E-04
22.731	2.588 E-04
26.502	2.800 E-04
27.255	3.161 E-04
30.484	4.926 E-04
31.849	5.330 E-04
33.214	6.103 E-04
38.638	8.235 E-04
41.289	1.045 E-03
49.955	1.466 E-03
63.776	4.916 E-03

Since the original values of the data are not known, there is no way of gauging the accuracy of the digitization and transformation processes. The data can be checked by comparing the points on the graph to these values, but it is difficult to read numbers off

the axes. Another method is to replot the transformed data and compare the shapes of the curves. Figure 8 is the graph of the digitized data points.

The differences between the original and the second version are small; no noticeable discrepancies can be identified when specific points are compared. Section I.5 establishes a range to the expected errors associated with the data acquisition technique.

I.5: Error Analysis

While digitizing and transforming a graph from the database, it became apparent that there is no way to quantify the error since the original graph values are not known. In an effort to define the accuracy of the method, a test has been conducted. The results of the test will give a range of error for the entire process which can then be compared to the typical uncertainty that comes from laboratory experimentation.

A set of $(da/dN)_{total}$ data for aluminum alloy 2024 in moist air was acquired in both graphical and numerical form.¹⁵ The graph was digitized and transformed, and the numbers from the transformation process were compared with the values of the original data. Figure 9 shows the original graph and Figure 10 shows a graph of the digitized and transformed data. Table I.1 compares the results for specific points at the beginning and end of the graph. The average errors are for all the points in the data file (approximately forty).

The data supplied to the modelling programs were often photocopied from

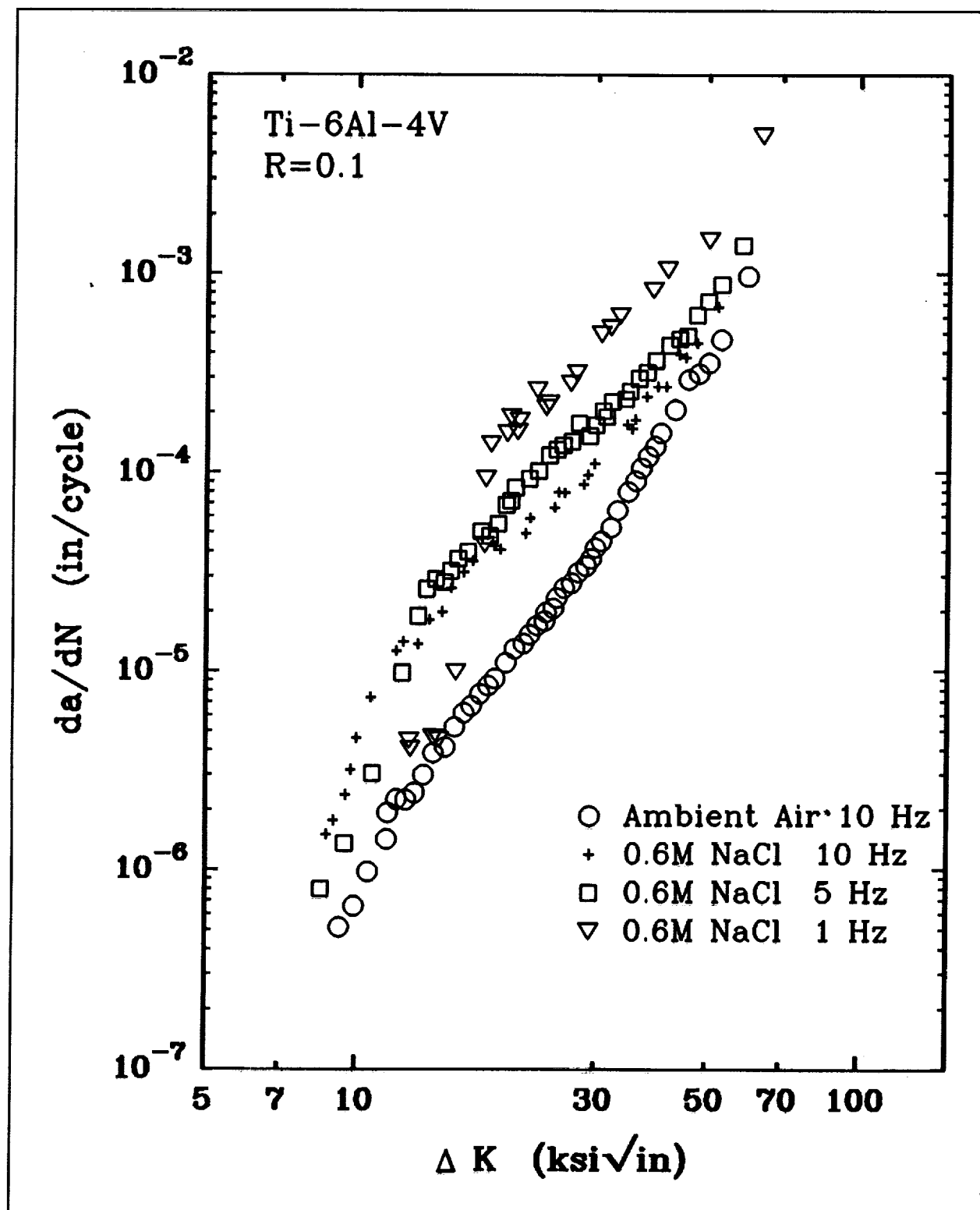


Figure 8: Digitized and transformed set of data from Figure 7.

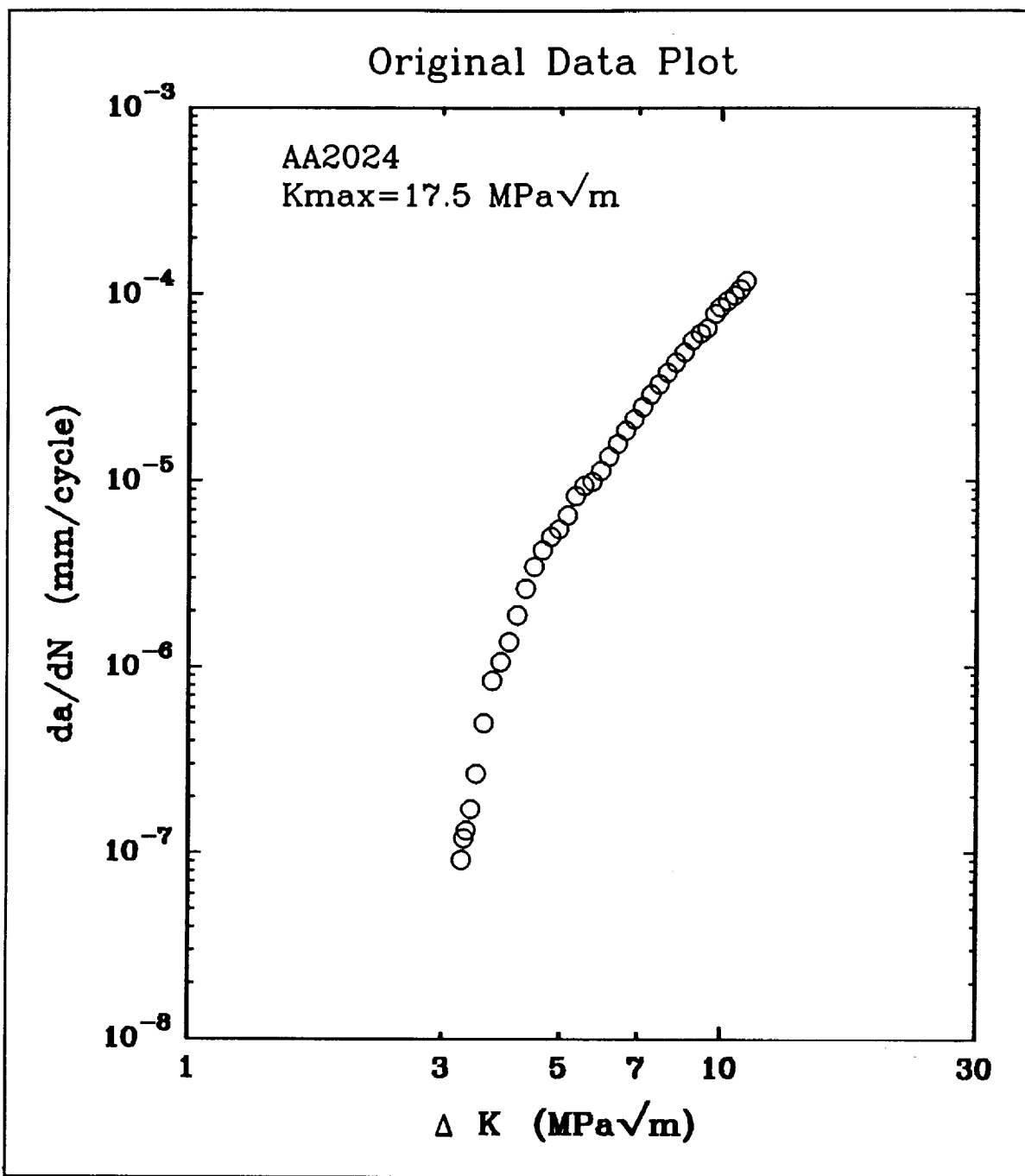


Figure 9: Plot of data obtained in digital form for aluminum alloy 2024 tested in moist air at a constant K_{max} .

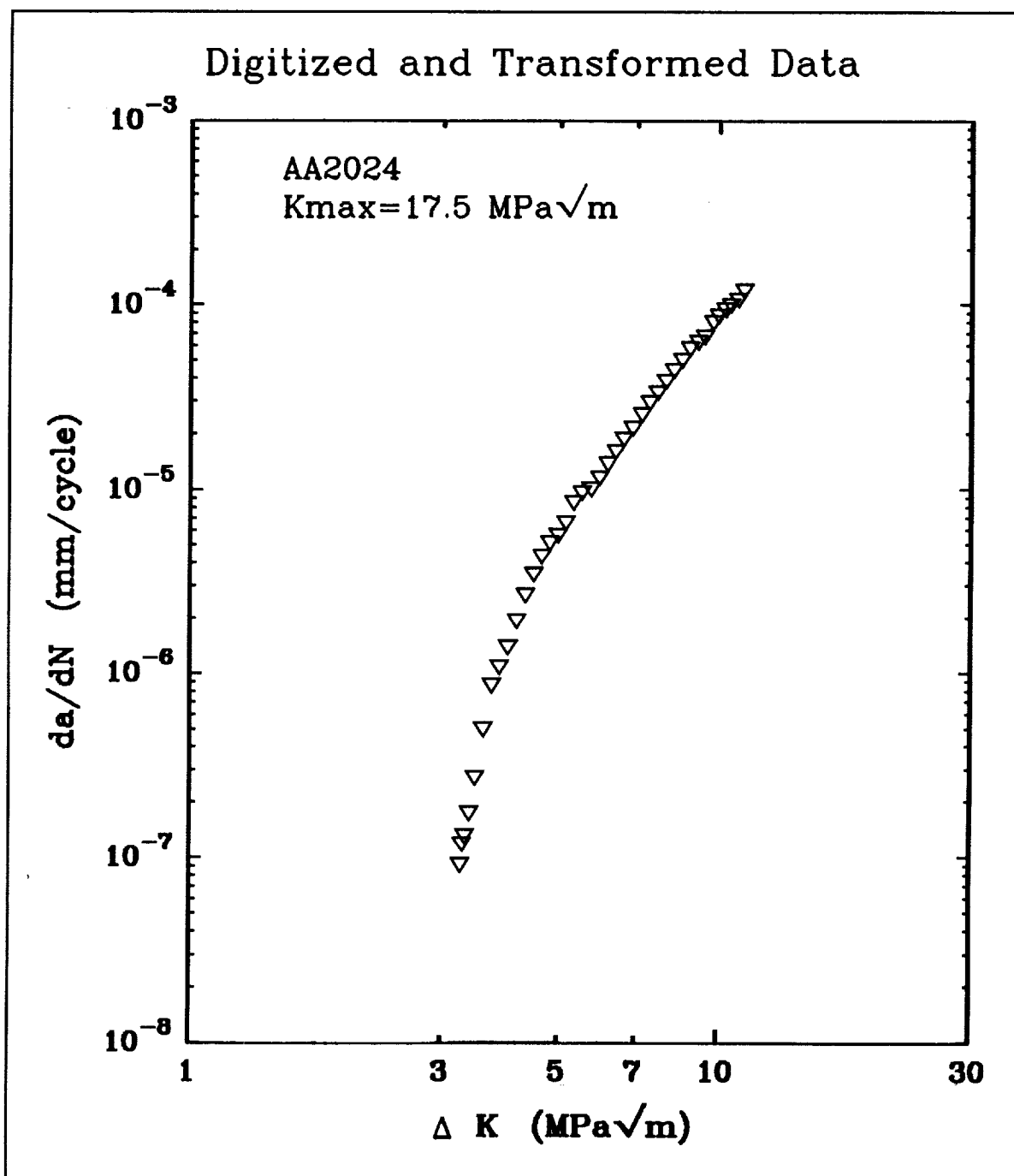


Figure 10: Digitized and transformed set of data from Figure 9.

Table I.1: Error analysis for original graph (Figure 9)

	X original MPa√m	X measured MPa√m	% error	Y original mm/cycle	Y measured mm/cycle	% error
1	3.26197	3.26090	0.033 %	9.77e-8	9.08e-8	0.273 %
2	3.29374	3.28984	0.118 %	1.19e-7	1.18e-7	0.866 %
3	3.32718	3.32704	0.004 %	1.31e-7	1.30e-7	1.03 %
4	3.39286	3.38745	0.160 %	1.71e-7	1.73e-7	0.785 %
5	3.47126	3.47286	0.046 %	2.65e-7	2.69e-7	1.54 %
6	3.58530	3.59375	0.236 %	4.96e-7	4.97e-7	0.172 %
7	3.71816	3.73321	0.405 %	8.41e-7	8.54e-7	1.58 %
32	9.11531	9.13915	0.262 %	6.13e-5	6.25e-5	1.91 %
33	9.38093	9.41333	0.345 %	6.54e-5	6.68e-5	2.19 %
34	9.70218	9.76138	0.610 %	7.83e-5	7.95e-5	1.53 %
35	9.91657	9.97539	0.593 %	8.50e-4	8.63e-5	1.54 %
36	10.2474	10.2879	0.395 %	9.21e-5	9.32e-5	1.25 %
37	10.5504	10.5354	0.142 %	9.84e-5	9.87e-5	0.257 %
38	10.8113	10.8707	0.550 %	1.06e-4	1.06e-4	0.252 %
39	11.0926	11.1483	0.502 %	1.17e-4	1.19e-4	0.986 %
	X error	maximum	0.593 %	Y error	maximum	2.29 %
		minimum	0.004 %		minimum	0.06 %
		average	0.325 %		average	1.23 %
		standard deviation	0.187 %		standard deviation	0.67 %

different sources for use with the digitizer. For the most part, the source that the graph came from was not an original; this source probably copied the graph from another paper. There is no way of knowing how many times the graph has been reproduced, but the fact that the data are not first hand must be taken into account. To assess the effect of the copying of data, the test was run again with one variation. The original graph (Figure 9) was photocopied at 75% original size and then photocopied again at 133%. The graph is now approximately the original size. Figure 11 shows the re-plotted results of the photocopied data. The error analysis for the individual data points is presented in Table I.2.

The results in Tables I.1 and I.2 are similar when relating the errors on the X (ΔK) axis to errors on the Y (da/dN) axis. In both cases, the X axis errors are negligible. The largest error in either graph is less than 1% for the X value of the digitized point. The Y average error in Table I.1 is 1.23%, and it increases to almost twice that value in Table I.2. This suggests that Y axis errors are larger than X axis errors, and that photocopying magnifies the errors that result.

Two questions must be addressed with respect to the errors presented in Tables I.1 and I.2. First, why are there errors? Second, why are there larger errors for the Y axis values than the X axis values?

The answer to the first question goes back to the manual functions that are performed when digitizing the graphs. The Numonics 2400 Digitablet has a fixed coordinate system; when a graph is digitized, the axes of the graph must be aligned with the internal axes of the Digitablet. This requires patience since small movements create

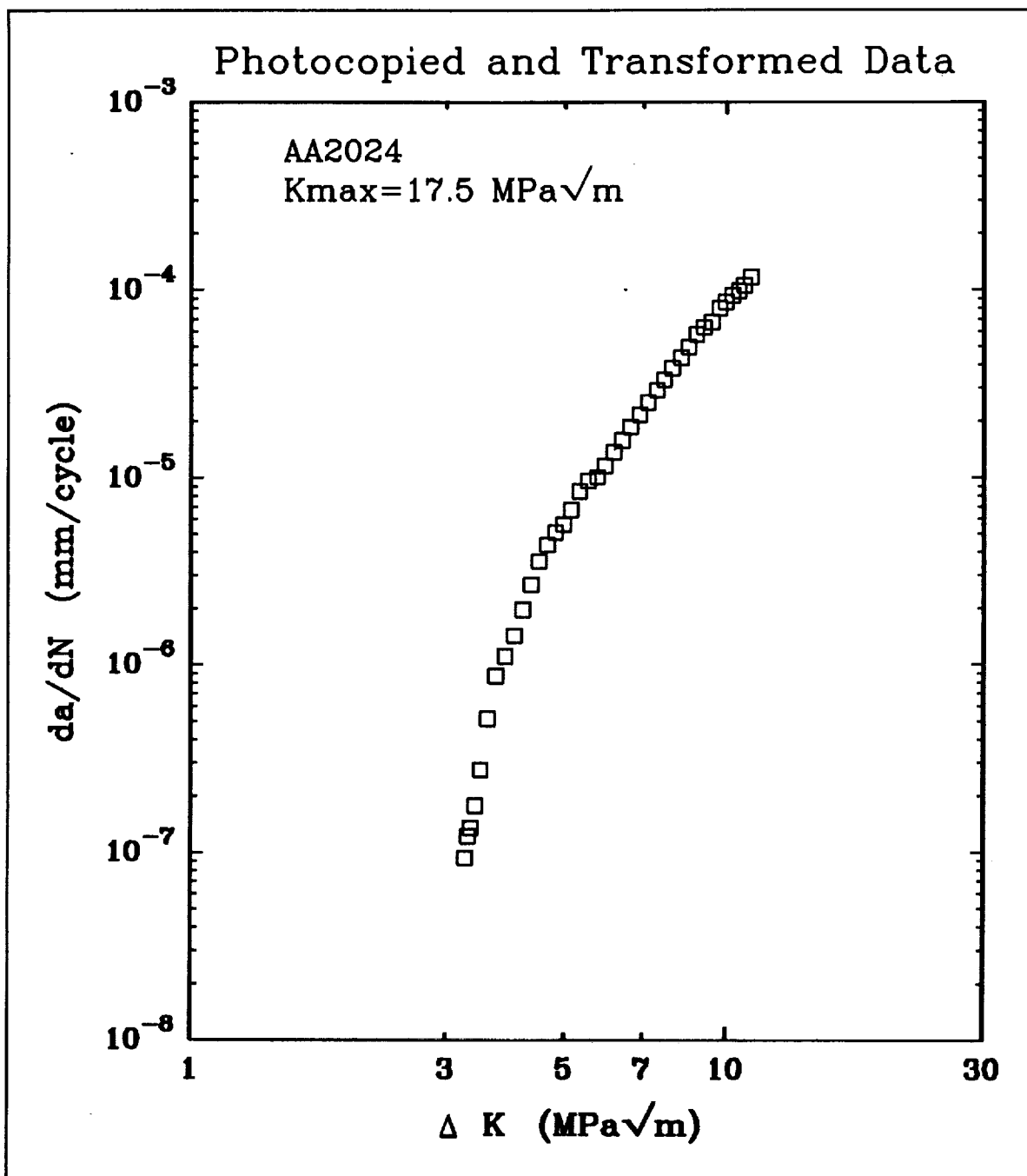


Figure 11: Plot of data that were photocopied numerous times.

Table I.2: Error analysis for photocopied graph (Figure 11)

	X original MPa√m	X measured MPa√m	% error	Y original mm/cycle	Y measured mm/cycle	% error
1	3.26197	3.25497	0.214 %	9.77e-8	9.30e-8	2.081 %
2	3.29374	3.29016	0.109 %	1.19e-7	1.22e-7	2.178 %
3	3.32718	3.33587	0.261 %	1.31e-7	1.35e-7	2.700 %
4	3.39286	3.39618	0.098 %	1.71e-7	1.77e-7	3.382 %
5	3.47126	3.47622	0.143 %	2.65e-7	2.74e-7	3.457 %
6	3.58530	3.58054	0.132 %	4.96e-7	5.14e-7	3.586 %
7	3.71816	3.71651	0.044 %	8.41e-7	8.69e-7	3.280 %
32	9.11531	9.06185	0.590 %	6.13e-5	6.29e-5	2.610 %
33	9.38093	9.37736	0.038 %	6.54e-5	6.71e-5	2.654 %
34	9.70218	9.70212	0.001 %	7.83e-5	7.94e-5	1.384 %
35	9.91657	9.96108	0.447 %	8.50e-4	8.58e-5	0.926 %
36	10.2474	10.2471	0.002 %	9.21e-5	9.28e-5	0.785 %
37	10.5504	10.5244	0.247 %	9.84e-5	9.83e-5	0.062 %
38	10.8113	10.7782	0.306 %	1.06e-4	1.05e-4	0.981 %
39	11.0926	11.0858	0.062 %	1.17e-4	1.16e-4	0.617 %
	X error	maximum	0.615 %	Y error	maximum	4.412 %
		minimum	0.001 %		minimum	0.062 %
		average	0.240 %		average	1.968 %
		standard deviation	0.168 %		standard deviation	1.104 %

noticeable errors in the digitized points. The user must continually adjust the graph until each axis strays no more than 0.01 to 0.02 centimeters in the perpendicular direction from the origin to the endpoint.

Another manual error occurs when selecting points with the digitablet cursor. Points may be close together, or they may have odd shapes that make it difficult to find the center. It is easier to digitize a '+' or an 'x' than it is to digitize a 'v' or a '□'. Finally, there is a tendency to move the cursor (mouse) when the enter button is pushed. Therefore, both axis alignment and the graph point marking suffer from human incapacibilities.

The next link in the chain is the transformation process. The mathematics of the program DIGITIZE.EXE are sound, but the input may be imprecise. A reference point on each axis is chosen, and the distance from the Digitablet origin to the reference point is recorded in order to scale the Digitablet output. Originally, the reference points were one cycle higher than the origin on logarithmic scales. This method proved to be ineffective when there were five full cycles present on the Y axis (da/dN data). Typical errors were 4 to 5%, but when the reference point was chosen to be as far from the origin as possible, errors in the Y axis values decreased to about 1 to 2%. Improvements were noted for the X axis as well. Errors of 0.6 to 0.8% dropped to between 0.1 and 0.3%

There is no exact answer as to why the Y axis errors are larger than the X axis errors, but several possible explanations exist. The user is required to line up the axes with the Digitablet coordinate system. After photocopying a graph, the axes are often no

longer perpendicular, making it impossible to have both the X and Y axes correctly aligned. Often one axis is either consciously or subconsciously chosen to be more correctly aligned. Horizontal markings on the Digitablet surface coax the user to be more careful with the X axis than the Y axis.

Another possible cause for greater accuracy in X values than in Y values is the structure of the data. The stress intensity on the X axis rarely varies more than one cycle on a logarithmic plot while the crack growth rate data on the Y axis may span two to six cycles. This wide range of values may degrade accuracy, since small errors will be magnified by the large scale. This theory and the axis alignment theory were tested, both generating inconclusive results.

The X and Y axes were switched in several tests to determine if axis alignment produced a noticeable difference in digitization errors. A sample of data was then retrieved from a file and plotted with just one cycle on the Y axis. The results suggest that the configuration of the da/dN data is more significant than axis alignment. The results of these tests along with operator bias tests are presented in Table I.3. More photocopying examples are also included.

All three operators achieved similar degrees of accuracy in digitizing the graph displayed in Figure 7. There was little variation in the average error for both the X and Y axes. Most users should be able to digitize graphs with accuracy comparable to the data presented in this table.

The photocopying of the graphs presents another problem, distortion. The axes of a plot may not be perpendicular due to inadequacies in the copier, presenting an error

Table I.3: Summary of test results

Type of Graph	Description	avg. error in X value	avg. error in Y value
Log-log scale	laser printer quality**	0.209 %	0.709 %
	laser printer quality	0.325 %	1.225 %
	X and Y axes reversed	2.13 %	0.235 %
	(ΔK on Y and da/dN on X)		
	data in one cycle on Y axis	0.184 %	0.294 %
	and one cycle on X axis		
Semi-log	photocopied twice	0.240 %	1.97 %
	(133 % then 75 %)		
	photocopied once (100 %)	0.128 %	1.087 %
	photocopied once (100 %)	0.100 %	1.412 %
	X and Y axes reversed	0.290 %	0.291 %
	one cycle on Y axis	0.516 %	0.418 %
User bias test	same graph for all three		
Log-log scale	user 1	0.325 %	1.23 %
	user 2	0.272 %	1.17 %
	user 3	0.541 %	1.30 %

source that can not be controlled. When this occurs, it is impossible to align both axes correctly at the beginning of the digitization process. The user must try to minimize these unavoidable errors on each axis.

** Plot went directly from graphics package to Hewlett Packard Laser Jet.

Based on the tests in Table I.3, a conservative estimate of the errors involved with the data files is $\pm 1\%$ on the X axis and $\pm 3\%$ on the Y axis. The standard range of variation during laboratory tests can be much larger than these error estimates. A difference of 50% in da/dN for two specimens tested under the same conditions would not be unheard of. A 40% uncertainty band is presented for the test data in Figure 12. This estimate was created on the basis of other scatter bands presented for crack growth rate tests.⁷ All digitized data from Figures 10 and 11 easily fit in this band. Since the experimental data have a large uncertainty associated with fatigue crack growth rates in corrosive environments, the data that were supplied to the programmers should be sufficiently accurate to conduct realistic tests of the computer models.

I.6: Conclusions for Data Collection and Preparation

One purpose of this project was to create a database of crack growth rate data for use in two computer modelling programs. In creating this database, several techniques were developed to convert a graph with data points into an accurate file of digital data. The results may be useful to anyone interested in the process of digitization and transformation, as well as the programmers who will test their work here.

1. A database of forty-six crack growth rate data files was created. The database includes static load environmental crack growth rate data

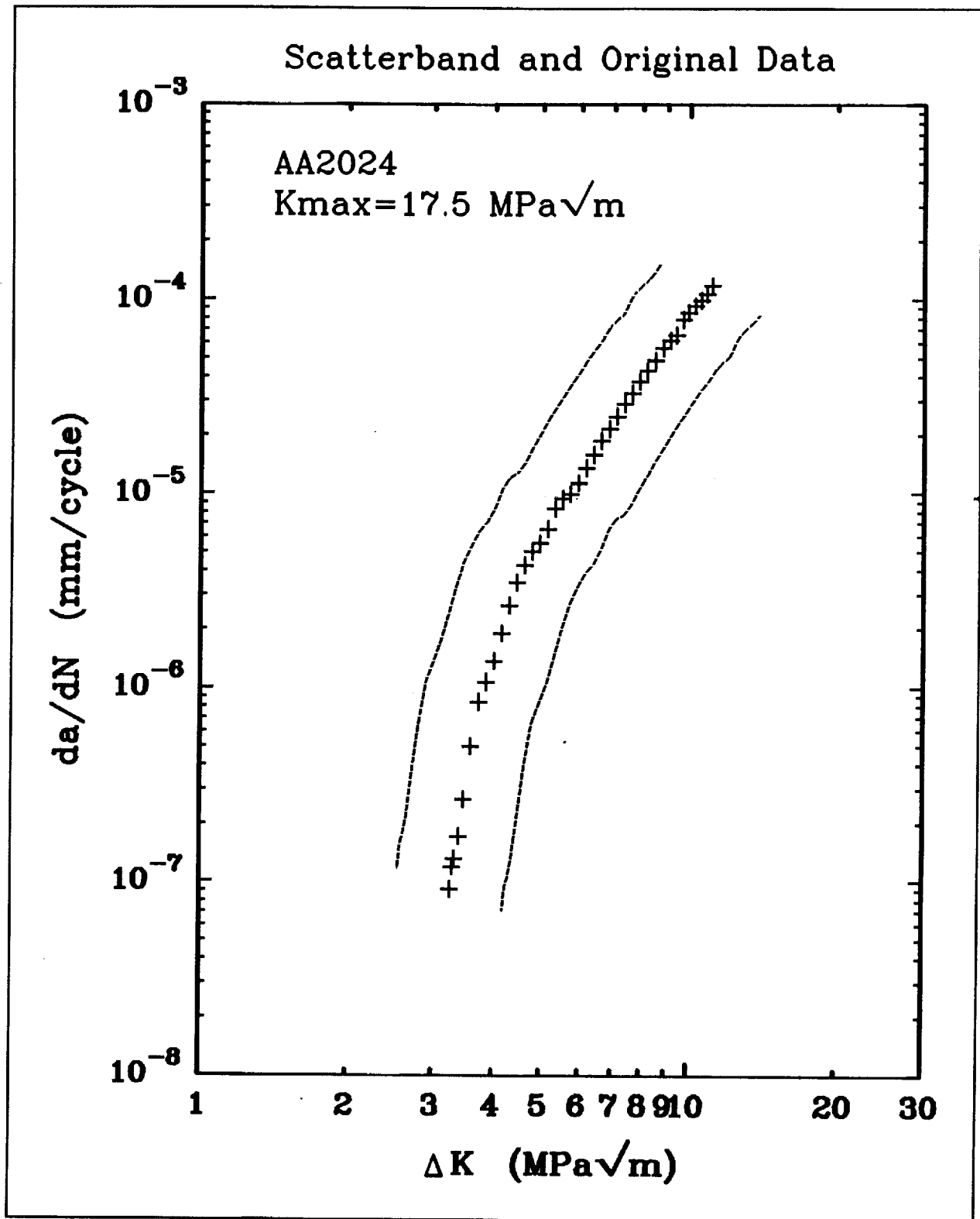


Figure 12: 40% uncertainty band for test data.

$((da/dt)_{\text{environment}}-K)$, inert environment fatigue crack growth rate data $((da/dN)_{\text{fatigue}}-\Delta K)$, and crack growth rate data for fatigue in a corrosive environment $((da/dN)_{\text{total}}-\Delta K)$. Three alloys are included in the database which focuses on variations in environment, loading frequency, and stress ratio.

2. A method for digitizing the points on a literature graph and transforming them to correct da/dN versus ΔK values was developed. Using the Numonics 2400 Digitab, a data file is created by electronically reading graph points. The file is transferred to DOS and processed with a transformation program called DIGITIZE.EXE. The program converts the data to numerical values referenced to the axes of the original graph, for either linear or logarithmic scales.
3. An error analysis was performed on the complete process of photocopying a graph, enlargement, digitization, and transformation. Photocopying increased errors, and human errors are unavoidable during digitization, but these effects were small. All errors are negligible when compared to the typical uncertainty associated with laboratory testing. The largest average error in any test was 2.1% while the smallest was 0.10%. The accuracy of the method is acceptable for supplying data for the computer models.

Section II: Interpolative Model

II.1: Crack Growth Rate Equations

The interpolative computer model has the capability to fit a set of $(da/dN)_{total}$ versus ΔK data to either the Forman Equation (with or without closure), the Hyperbolic Sine Equation (SINH), the Sigmoidal Equation, or the Paris Equation. The program allows the user to select the form of the crack growth rate equation, as well as which equation constants are to be optimized and which are to be fixed. The applicability of these equations to time dependent environmental FCP is assessed for Ti-6Al-4V in an aqueous chloride environment.

Forman Equation (closure included)

The Forman Equation including closure, developed by R.G. Forman, is discussed in detail in the NASA FLAGRO (Version 2.0)¹⁶ user's manual, and is of the general form:

$$\frac{da}{dN} = \frac{C (1-f)^n \Delta K^n \left(1 - \frac{\Delta K_{th}}{\Delta K}\right)^p}{(1-R)^n \left(1 - \frac{\Delta K}{(1-R) K_C}\right)^q} \quad (II.1)$$

where N is the number of load cycles, a the is crack length, R the is stress ratio, and ΔK is the stress intensity factor range. The coefficient C, and the exponents n, p, and q, are

empirical constants which depend on material and environment. The parameter K_C is the critical value of the stress intensity factor for unstable fracture, while ΔK_{th} is the threshold value of the stress intensity factor range.

The crack opening function, f , is used to calculate the effect of stress ratio on crack growth for a constant amplitude load. The function was defined by Newman¹⁶ from crack closure considerations as:

$$f = \frac{K_{op}}{K_{max}} = \begin{cases} \max(R, A_o + A_1 R + A_2 R^2 + A_3 R^3) & R \geq 0 \\ A_o + A_1 R & -2 \leq R < 0 \end{cases} \quad (II.2)$$

where:

$$A_o = (0.825 - 0.34\alpha + 0.05\alpha^2) \left[\cos\left(\frac{\pi}{2} \frac{S_{max}}{\sigma_o}\right) \right]^{\frac{1}{\alpha}} \quad (II.3a)$$

$$A_1 = (0.415 - 0.071\alpha) \frac{S_{max}}{\sigma_o} \quad (II.3b)$$

$$A_2 = 1 - A_o - A_1 - A_3 \quad (II.3c)$$

$$A_3 = 2A_o + A_1 - 1 \quad (II.3d)$$

and K_{op} is the opening stress intensity factor, below which the crack is closed. The parameter α describes the condition of plane stress or plane strain, and S_{max}/σ_o is the ratio of the maximum applied stress to the flow stress, where the flow stress is the stress required to produce plastic deformation in a solid. The parameter α is a material constant with values ranging from 1 for plane stress to 3 for plane strain. S_{max}/σ_o varies from experiment to experiment and is not a material constant, however, the value is

taken as 0.3 for most materials which were incorporated in the NASA FLAGRO program. Certain materials do not exhibit a large effect of stress ratio on da/dN , and the effects of crack closure do not need to be considered. For these materials α is set to 5.845 and S_{\max}/σ_o to 1.0. The parameter f is then equal to zero for $R \leq 0$ and becomes R for $0 \leq R < 1$. For positive stress ratios, the Forman Equation with closure then reduces to:

$$\frac{da}{dN} = \frac{C \Delta K^n \left(1 - \frac{\Delta K_{th}}{\Delta K}\right)^p}{\left(1 - \frac{\Delta K}{(1-R) K_c}\right)^q} \quad (\text{II.4})$$

For negative stress ratios, ΔK is replaced by K_{\max} , since only the positive part of a loading wave contributes to crack growth. Figure 13 shows a plot of f as a function of R for the cases represented by Equations II.1 and II.4.

Original Forman Equation

The original form of the Forman Equation, without an explicit treatment of crack closure (taken from NASA FLAGRO Version August 1986)¹⁷, is:

$$\frac{da}{dN} = \frac{C \Delta K^n (1-R)^m \left(1 - \frac{\Delta K_{th}}{\Delta K}\right)^p}{\left(1 - R - \frac{\Delta K}{K_c}\right)^q} \quad (\text{II.5})$$

The coefficient C , and the exponents m , n , p , and q are all empirical constants. C , m , n , p , and q will not have the same values as in Equation II.1 for a given set of data.

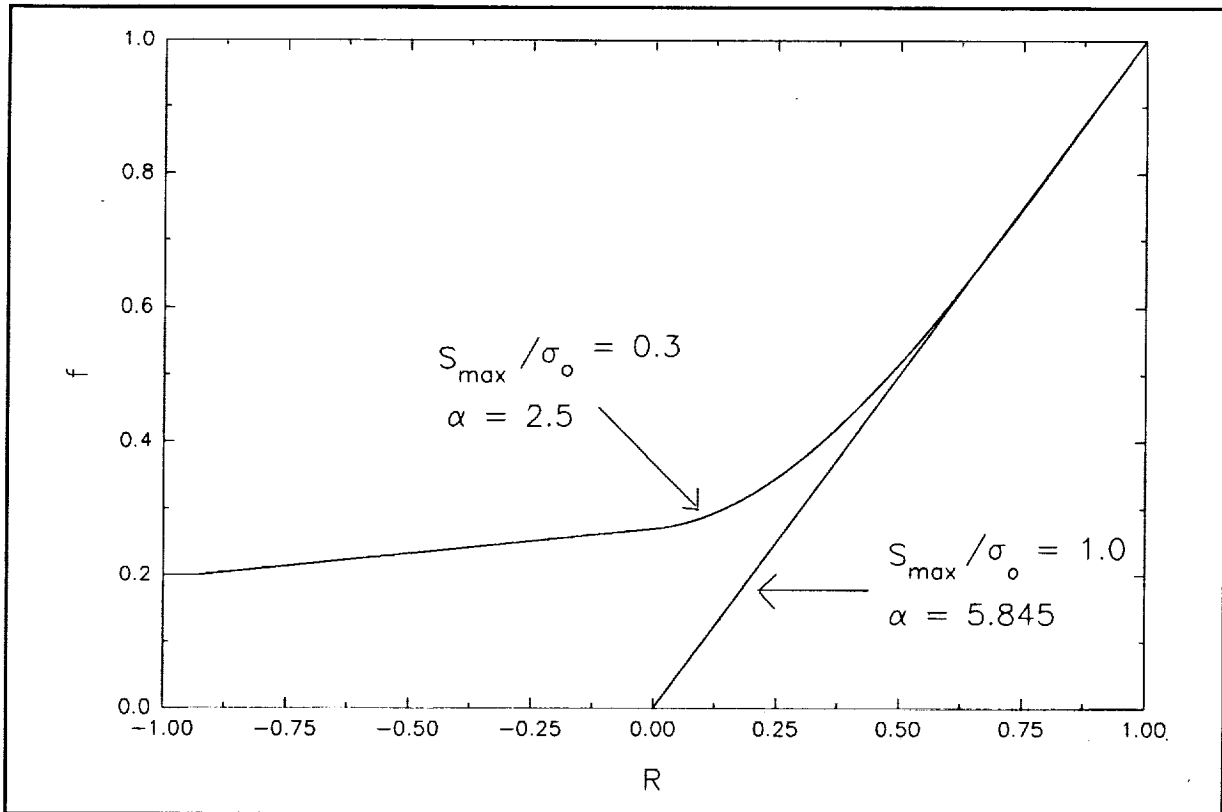


Figure 13: Crack closure function, f , as a function of stress ratio. From NASA FLAGRO User's Manual¹⁶.

Paris Equation

The Paris Equation is a power law equation of the form:

$$\frac{da}{dN} = C \Delta K^n \quad (\text{II.6})$$

where C and n are empirical constants. This equation effectively describes the FCP behavior in Region II, but since growth rates in Regions I and III are asymptotic to characteristic stress intensity ranges, this equation may not accurately model broad range da/dN versus ΔK data.

SINH Equation

The Hyperbolic Sine (SINH) Equation was originally developed by Pratt & Whitney, and is discussed by Haritos¹⁸ and Van Stone¹⁹. The basic equation is of the form:

$$\log \frac{da}{dN} = C_1 \sinh(C_2 [\log(\Delta K) + C_3]) + C_4 \quad (\text{II.7})$$

where $\Delta K = K_{\max} - K_{\min}$ and da/dN is the rate of crack growth per unit cycle. The parameters C_3 and C_4 are the horizontal and vertical locations of the inflection point respectively. The parameter C_1 is a constant with a value of 0.5. The slope at the inflection point is defined to be $C_1 C_2$. The SINH equation is symmetric about the inflection point, there is no mathematical definition of K_C or ΔK_{th} . The curvature is identical in both the near toughness and near threshold regimes¹⁹. The SINH Equation is schematically shown in Figure 14.

The parameters C_2 through C_4 are material-environment properties. To determine the values of the coefficients in the SINH equation, nonlinear regression must be used. This is done using an algorithm from Kuester²⁰. The algorithm uses a procedure proposed by Marquardt²¹ to determine the parameters in a non-linear equation using the method of least squares.

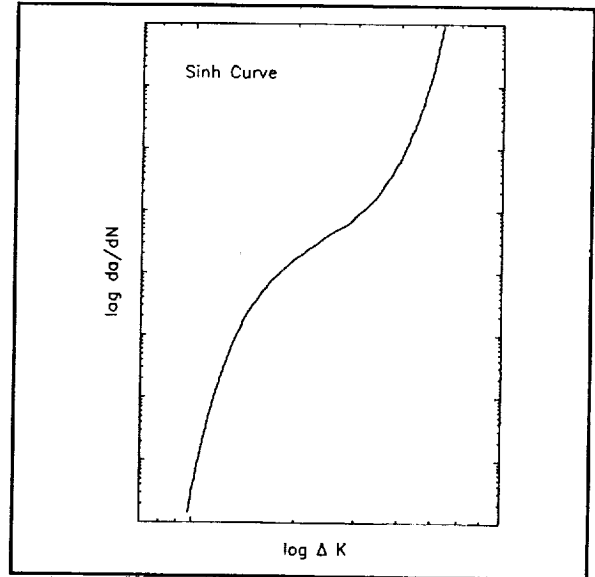


Figure 14: Schematic drawing of a SINH curve.

The procedure requires the user to input initial estimates for the parameters C_2 , C_3 , and C_4 . These estimates can be determined from a graph of the data. Upper and lower bounds are then selected for each coefficient. Since the algorithm uses a least-squares objective function, the best value for each parameter is found by minimizing the sum of the squared errors for each data set. The sum of the squared errors, SSE, is defined as:

$$SSE = \sum (Y_{Pred} - Y_{actual})^2 \quad (II.8)$$

where Y_{Pred} is the predicted value of da/dN and Y_{actual} is the actual value of da/dN at a given ΔK . The algorithm determines the parameters by iteratively solving the following partial differential equations:

$$\frac{\partial SSE}{\partial C_2} = -2 \sum [\beta] [C_1 \cosh(C_2 (\log \Delta K + C_3)) (\log \Delta K + C_3)] = 0 \quad (II.9a)$$

$$\frac{\partial SSE}{\partial C_3} = -2 \sum [\beta] [C_1 \cosh(C_2 (\log \Delta K + C_3))] C_2 = 0 \quad (II.9b)$$

$$\frac{\partial SSE}{\partial C_4} = -2 \sum [\beta] = 0 \quad (II.9c)$$

$$\beta = [y - C_1 \sinh(C_2 (\log \Delta K + C_3)) - C_4] \quad (II.9d)$$

where y refers to the actual value of da/dN .

Sigmoidal Equation

The Sigmoidal Equation was originally developed by GE Aircraft Engines, and is discussed by Van Stone¹⁹ and Haritos¹⁸. The equation is of the form:

$$\frac{da}{dN} = e^B \left(\frac{\Delta K}{\Delta K_{th}} \right)^P \left[\ln \left(\frac{\Delta K}{\Delta K_{th}} \right) \right]^Q \left[\ln \left(\frac{\Delta K_C}{\Delta K} \right) \right]^D \quad (II.10)$$

$$\Delta K_C = (1 - R) K_C$$

where ΔK_C is the critical value of the stress intensity factor range, and ΔK_{th} is the threshold value of the stress intensity factor range. A schematic of a sigmoidal curve is shown in Figure 15. The curve fitting

parameters $B, P, Q, D, \Delta K_{th}$ and ΔK_C are material-environment properties.

The Sigmoidal Equation has an advantage over the SINH Equation because of defined values for both ΔK_{th} and K_C . The Sigmoidal Equation is not identical in the near threshold and near toughness domains. Also, the Sigmoidal Equation defines the curvature in the transitions from Regions I and II, and

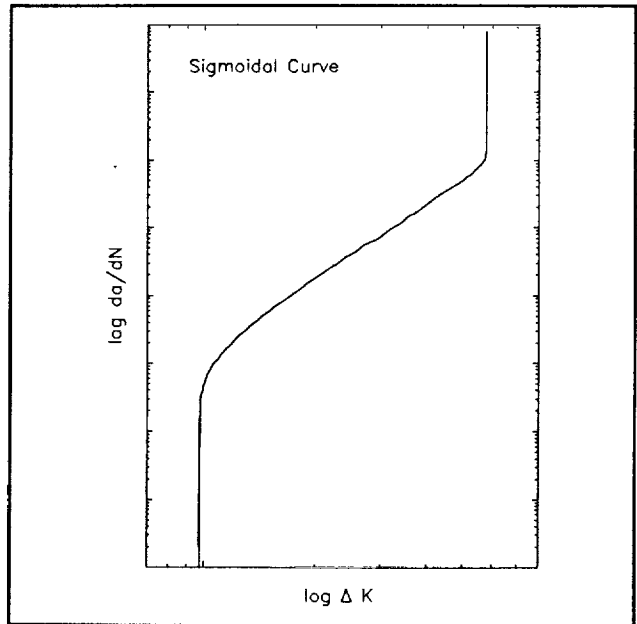


Figure 15: Schematic drawing of a sigmoidal curve.

Regions II and III. The main reason for this increased accuracy is the fact that the SINH Equation only has four curve fitting parameters, while the Sigmoidal Equation has six¹⁹. The Sigmoidal Equation can also be rewritten in linear form, and the equation parameters determined using the least squares methods discussed below.

To determine the equation parameters for the Forman, Paris and Sigmoidal Equations, the equations are first rewritten in linear form using logarithms. Using ΔK

and da/dN data, a set of simultaneous linear equations is constructed involving da/dN , ΔK , and the equation parameters. These simultaneous equations are solved using Gaussian Elimination and matrix algebra to determine the equation parameters. For example, the Forman Equation without closure (Equation II.5) is rewritten as

$$Y = A_1 X_1 + A_2 X_2 + A_3 X_3 + A_4 X_4 + A_5 X_5 \quad (\text{II.11})$$

where :

$$Y = \log \left(\frac{da}{dN} \right) \quad (\text{II.12a})$$

$$X_1 = \log (1 - R) \quad (\text{II.12b})$$

$$X_2 = \log (\Delta K) \quad (\text{II.12c})$$

$$X_3 = \log \left(1 - \frac{\Delta K_{th}}{\Delta K} \right) \quad (\text{II.12d})$$

$$X_4 = - \log \left(1 - R - \frac{\Delta K}{K_c} \right) \quad (\text{II.12e})$$

$$X_5 = 1.0 \quad (\text{II.12f})$$

and $A_1 = m$, $A_2 = n$, $A_3 = p$, $A_4 = q$, and $A_5 = \log C$. Similarly, the Forman Equation with closure, the Paris Equation and the Sigmoidal Equation can be rewritten in linear form.

The Forman Equation (with and without closure), the Paris Equation, and the

Sigmoidal Equation can be written in matrix form as:

$$[A] [X] = [Y] \quad (II.13)$$

where the A matrix contains the equation parameters such as C, n, p, q, and m, the X matrix contains the values of X_1 through X_5 , and the Y matrix contains the values of $\log (da/dN)$. This equation can be rewritten as:

$$[A] = [X]^{-1} [Y] \quad (II.14)$$

The equation parameters can then be determined by Gaussian Elimination. As stated earlier, the SINH Equation can not be written in linear form, thus Gaussian Elimination can not be used for the SINH Equation. Instead, a non-linear least-squares algorithm must be used.

Equation Parameters

The FCP laws used in the interpolation model all change with stress ratio, frequency, and hold time variations. The interpolative model can be used to empirically describe such changes within the data range, but will not likely provide accurate predictions outside of the bounds of the experimental values. As a first approximation, the equation parameters, such as C, n, p, and q are set equal to linear relationships involving assumed logarithmic functions of the stress ratio, frequency and hold time of the applied load. The form of the relationship depends on the number of data sets available to the program and the form of the crack growth rate equation. The number of loading variables (R, hold time, frequency, K_{max} , and K_{min}) that the equation

parameters are related to is equal to the number of data sets entered. If only one da/dN versus ΔK data set is entered the crack growth rate equation parameters for a given frequency are set equal to the following relationship:

$$\eta = a_1 \log \left[\left(\frac{1}{f} \right) + 1 \right] \quad (\text{II.15})$$

f = frequency of the applied load

where η is an equation parameter such as C or n, and a_1 is constant fit by the computer. The user has the option of deciding which parameters to fit and which to fix. The accuracy of the fitted equation increases as the number of the parameters fitted increases. The form of the relationship was selected so that at low frequencies (higher corrosion effects), the log value increases for a fixed frequency. If two data sets are entered, and the user has selected the Forman Equation as the crack growth rate model, the relationship is:

$$\eta = a_1 \log \left[\left(\frac{1}{f} \right) + 1 \right] + a_2 \log \left[\frac{\tau + 1}{0.1} \right] \quad (\text{II.16})$$

f = frequency of the applied load

τ = hold time of the applied load

If the user selects the Paris Equation, the SINH Equation, or the Sigmoidal Equation and enters two data sets, the relationship is:

$$\eta = a_1 \log \left[\left(\frac{1}{f} \right) + 1 \right] + a_2 \log \left[\frac{1 - 0.1R}{0.1} \right] \quad (\text{II.17})$$

f = frequency of the applied load

R = stress ratio

if the stress ratio is held constant. If K_{\max} is held constant for the data set then the relationship is:

$$\eta = a_1 \log \left[\left(\frac{1}{f} \right) + 1 \right] + a_2 \log (K_{\max}) \quad (\text{II.18})$$

If K_{\min} is held constant, K_{\max} in Equation II.18 is replaced by K_{\min} . The form of the relationship was selected so that a dependency on the stress ratio could be introduced into the Paris, SINH and Sigmoidal Equations. The Forman Equation already describes the effect of stress ratio based on a crack closure strategy; that is why a hold time effect and not a stress ratio effect was included in Equation II.16.

The effects of hold time are not accounted for in the Paris, SINH or Sigmoidal Equations if two data sets are used. To take into account the hold time for the Paris, Sigmoidal or SINH Equations, three data sets must be used. If three data sets are entered, the following relationship is used for all of the crack growth rate equations:

$$\eta = a_1 \log \left[\left(\frac{1}{f} \right) + 1 \right] + a_2 \log \left[\frac{1 - 0.1R}{0.1} \right] + a_3 \log \left[\frac{\tau + 1}{0.1} \right] \quad (\text{II.19})$$

f = frequency of the applied load

τ = hold time of the applied load

R = stress ratio

if the stress ratio is constant. If K_{\max} is held constant the relationship is :

$$\eta = a_1 \log \left[\left(\frac{1}{f} \right) + 1 \right] + a_2 \log (K_{\max}) + a_3 \log \left[\frac{\tau + 1}{0.1} \right] \quad (\text{II.20})$$

If K_{\min} is held constant, then K_{\max} in Equation II.20 is replaced by K_{\min} . These equations allow the user to determine the equation parameters for a particular data set if the load characteristics are known. The assumed logarithmic functions of f , R , K_{\max} , K_{\min} , and τ must be tested with experimental data. These functions should only be used for interpolation, not prediction of the effects of variables outside the range of the curve-fit data. The logarithmic forms of the relationships were selected so that the relationships were defined for the allowable ranges of frequency, hold time, K_{\max} , K_{\min} , and stress ratio. For example, the expression involving the hold time is always defined unless $\tau = -1.0$, which is not physically permissible. For all $\tau \geq 0$ the expression does not tend toward infinity.

To determine the values of a_1 , a_2 , and a_3 , the equation parameters are determined for each data set entered. A set of simultaneous equations is then developed for each parameter which relates the parameter values to the given load characteristics. Matrix algebra and Gaussian Elimination are then used to solve these equations and determine the coefficients.

Using Equations II.15 through II.20, the program allows the user to interpolate da/dN data given the stress ratio (or K_{\max} or K_{\min}), frequency, hold time, and ΔK . This is done by first selecting the form of the crack growth rate equation, entering ΔK and da/dN data, and determining the values of the coefficients a_1 , a_2 , and a_3 in Equations

II.15 through II.20 for selected equation parameters. Given the value of the frequency, hold time, and stress ratio (or K_{\max} or K_{\min}), appropriate values for the crack growth rate equation parameters can be determined for any set of load conditions for the same material-environment system. Given a value of ΔK , da/dN can then be calculated.

II.2: Interpolative Computer Modeling Program

Computer Program Development

The first step in developing the computer modeling program was to obtain a copy of the FLAGRO source code from R.G. Forman at the NASA-Johnson Space Flight Center. Many of the subroutines in the interpolative model were taken directly from FLAGRO. The next step was to locate the sections of the program that were essential. This was necessary because the FLAGRO program is too large to run on the FORTRAN compilers available at the University of Virginia. The sections that were removed to be used in the final program were the subroutines which loaded the material properties from a library data file for use in the crack growth rate equations, and the subroutines which controlled the entering of ΔK and da/dN data.

The subroutines in FLAGRO which controlled the linear regression analysis used to determine the equation parameters offered the user a choice between the Forman Equation with closure or the Paris Equation. Also, the user was only given the choice of determining C , n , or both C and n in Equations II.1 and II.6. The code was first

modified so that the Forman Equation without closure, the SINH Equation, and the Sigmoidal Equation could be used to model da/dN data, as well as the existing Forman Equation with closure and the Paris Equation. The user is thus allowed to choose from five crack growth rate equations. The program was then altered so that the user could optimize any combination of the equation parameters, including the parameters C , n , p , q , and m . Next, subroutines which used least squares regression and Gaussian elimination to solve for the equation parameters were added to the program. The subroutines used to perform the least squares analysis and Gaussian Elimination were based upon FORTRAN programs written by Scott²² and Ellis²³. Subroutines to perform non-linear least squares regression were also added²⁰.

Subroutines to plot the actual and predicted da/dN data were also added to the program. These subroutines were based upon the Watcom Graphical Kernel System (WGKS) package. The actual input data were plotted as points, while the fitted crack growth rate equation was plotted as a smooth curve. This allows the user to judge how well the curve fit equation correlates with the input data. Finally, the program was modified so that the parameters which were optimized were set equal to the linear relationships (Equations II.15 through II.20) involving the stress ratio (or K_{max} or K_{min}), frequency and hold time of the applied load.

Comparison to NASA FLAGRO

The stand alone interpolative computer program developed to model fatigue behavior contains many of the useful features found in the FLAGRO program. As

mentioned earlier, the materials files used in the FLAGRO program are incorporated into the stand alone program. When the FLAGRO program is used, however, the user is required to enter the material properties manually when fitting data to a crack growth rate equation. The option to fit data to an equation does not utilize the material files that are available. The stand alone program does utilize these files when the user so desires, and allows the user to enter the material properties from a material file. The material properties that are necessary are the yield strength, K_{IC} , A_K , B_K , S_{max}/σ_o , ΔK_o , and α used in Equations II.2, II.3, II.23, and II.24. These material properties are used when calculating ΔK_{th} , K_C , and the crack opening function f . The equation parameters C , n , p , and q in the Forman Equation with closure are also loaded. These parameters are only loaded so that the user can see the values for these constants determined by NASA.

Another difference between the stand alone program and the NASA FLAGRO program is the option to hold K_{max} or K_{min} constant for a set of data. The NASA FLAGRO program assumes that the stress ratio, R , is constant for the data entered. This assumption is not always valid since experiments are conducted with K_{max} (or K_{min}) being constant. If the user wishes to hold K_{max} or K_{min} constant, the program calculates the stress ratio for every point in the data set using one of the following equations:

$$R = \frac{K_{max} - \Delta K}{K_{max}} \quad (II.21)$$

$$R = \frac{K_{min}}{K_{min} + \Delta K} \quad (II.22)$$

This array of stress ratios is then used in the least squares regression used to determine

the equation parameters, and is also used when calculating the crack closure function, f , when necessary. The values of K_C and ΔK_{th} are constant for a given material data set.

The values for K_C and ΔK_{th} calculated by the NASA FLAGRO program are primarily accurate for fatigue in moist air. Since the stand-alone program was developed to model fatigue behavior in embrittling environments, these values are not always acceptable. An option to optimize K_C and ΔK_{th} has been incorporated into the stand-alone program in order to address this problem. The user presently has the option of entering K_C and ΔK_{th} manually, calculating the values from the equations contained in the NASA FLAGRO program using the material properties discussed earlier, or optimizing the values based on input da/dN versus ΔK data. If the user decides to calculate the value using the NASA FLAGRO equations, the following relationships are used:¹⁶

$$\Delta K_{th} = \Delta K_o \left(\frac{4}{\pi} \right) \tan^{-1} (1 - R) \quad (II.23)$$

$$K_C = K_{IC} \left(1 + B_k e^{-\left[\frac{A_k t}{t_o} \right]^2} \right) \quad (II.24)$$

$$t_o = 2.0 \left(\frac{K_{IC}}{\sigma_{YS}} \right)^2$$

where t is the thickness, ΔK_o is the fatigue threshold at $R = 0$, A_k and B_k are material constants, and σ_{YS} is the yield strength. If the user decides to optimize the values for K_C or ΔK_{th} , the program fits the data set to a cubic equation using least squares regression. The cubic equation contains an upper and lower asymptote, and these asymptotes

correspond to the value of K_C and ΔK_{th} . These two parameters are then used in subsequent interpolative modeling using the Forman or Sigmoidal Equations.

Several statistical parameters were also added to the stand alone program. First, the coefficient of determination, r^2 , is calculated for each data set fit to a crack growth rate equation. The coefficient of determination is the percentage of variation in the dependent variable, da/dN , which is accounted for by the relationship between da/dN and ΔK represented by the fitted crack growth rate equation. Mathematically the coefficient of determination is calculated as:

$$r^2 = 1 - \frac{\sum (Y_{actual} - Y_{pred})^2}{\sum (Y_{actual} - Y_{average})^2} \quad (II.25)$$

where Y_{actual} is the actual value of da/dN and Y_{pred} is the equation predicted value of da/dN at a given ΔK . $Y_{average}$ is the average value of the actual da/dN values. The coefficient of determination will range between 0 and 1.0. The closer the value is to 1.0, the better the fit of the crack growth rate equation.²⁴

Confidence interval estimates for each fitted equation parameter were also added to the program. A $100(1-\alpha)$ percent confidence interval for the equation parameter β_j is defined as:

$$\beta_j - t_{\alpha/2, n-p} \sqrt{\sigma^2 C_{jj}} \leq \beta_j \leq \beta_j + t_{\alpha/2, n-p} \sqrt{\sigma^2 C_{jj}} \quad (II.26)$$

where t is the student's t distribution with $n-p$ degrees of freedom. The quantity σ^2 is given by:

$$\sigma^2 = \frac{SSE}{n-p} \quad (II.27)$$

and C_{jj} is the jj th element of the $([X]'[X])^{-1}$ matrix. The $[X]$ matrix is defined as before, there are n data points in the data set, and p equation parameters are fitted.²⁴

II.3: Data Testing and Results for the Interpolative Model

Data Testing

The first criteria used to test the interpolative computer model was to benchmark the programs' linear least squares regression subroutines against the FLAGRO program. To do this, data set TT1B was curve fit to the Forman Equation with closure using the stand alone program and the FLAGRO program. The data was taken from an article by Dawson and Pelloux¹⁴. The value for K_C was entered as 69 ksi \sqrt{in} , ΔK_{th} was 7.27 ksi \sqrt{in} , α was 2.5, and S_{max}/σ_o was 0.3 for each program. The parameters C and n were fit, while p was 0.25 and q was 0.75 for each program. Results are shown in Table II.1.

Table II.1: Bench marking of linear regression algorithm*

Parameter	FLAGRO	Stand Alone	Difference	% Difference
C	0.5759×10^{-7}	0.5673×10^{-7}	8.6×10^{-10}	1.49
n	2.271	2.271	0.0	0.0

*The units for the equation constants depend on the units of the fitted $da/dN-\Delta K$ data. The fitted constants can only be used with data that have units consistent with the data used to determine the constants.

The results were identical for the parameter n , and varied only slightly for parameter C . Thus, the linear least squares regression analysis contained in the stand alone program is acceptable.

The algorithm used to determine the parameters in the Hyperbolic Sine Equation was also bench marked using results from Haritos¹⁸ for $R = 0.1$, $f = 1$ Hz, and $\tau = 0.0$ seconds. The values selected by Haritos¹⁸ and the interpolative model are shown in Table II.2. The values selected by the interpolative model did vary from those selected by Haritos¹⁸, however, the values determined by the interpolative model yielded an r^2 of 0.996, while Haritos' values yielded an r^2 of 0.992. Results are shown in Figure 16.

Table II.2: Bench marking of non-linear regression algorithm.

Parameter	Haritos	Interpolative Model	% Difference
C_2	3.197	3.896	21.9
C_3	-1.762	-1.6167	8.2
C_4	-2.530	-2.8080	11.0

The second criteria used to test the accuracy of the computer model was to determine how well the program fit fatigue data to the various crack growth rate equations. The data used were for titanium alloy Ti-6Al-4V in both an air environment and a 1.0% NaCl solution. The data were taken from a NASA-UVA Light Aerospace Alloy and Structures Technology Progress Report²⁵. The frequency was constant at 5 Hz, the hold time was constant at 0.0 seconds for all of the data, and α was entered as 2.5.

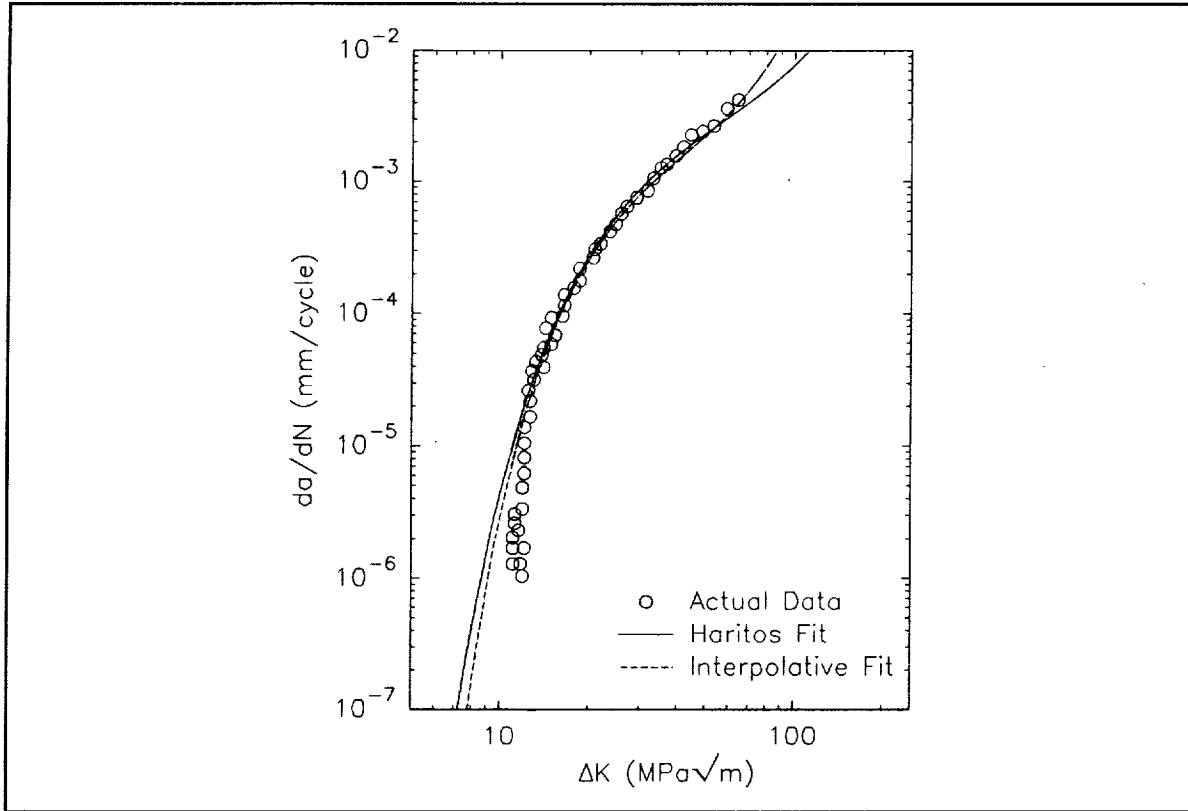


Figure 16: Comparison of curves fit by Haritos¹⁸ and the interpolative model.

The first equation tested was the Forman Equation with closure. Two tests were conducted for each data set. In the first test, only C and n were fit, while p and q were entered manually. The parameter p was set equal to 0.25 and q was 0.75. These values were taken from the NASA FLAGRO materials file. The values calculated by the program are shown in Table II.3. In the second test, all of the equation parameters were optimized. The values selected by the program are shown in Table II.4. In both tests, the values for ΔK_{th} were determined from ΔK_o , and the value of K_C was held constant at 3953 MPa√mm for air and 4270 MPa√mm for 1.0% NaCl. The value of ΔK_o was taken from the FLAGRO material files as 121.6 MPa√mm for Ti-6Al-4V (MA).

The same tests were then conducted for the Forman Equation without closure, holding the parameter m constant at 1. The results for fitting only C and n are shown in Table II.5, and the results for fitting C, n, p , and q are shown in Table II.6. Finally, the data were fit to the SINH Equation and the Sigmoidal Equation; results are shown in Tables II.7 and II.8. Results are shown graphically in Figures 17 through 22.

Notice that when fitting C, n, p , and q in the Forman Equation (with and without closure), as well as when fitting B, P, Q , and D in the Sigmoidal Equation, the equation is not always accurate outside of the fitted data range. The equation often becomes sinusoidal in nature when all four parameters are fit. This means that near the threshold, as ΔK decreases, da/dN increases. Also, as ΔK approaches ΔK_C , da/dN decreases as ΔK increases. This is not physically permissible, thus when all four parameters are fit, the parameter values often cannot be used for ΔK values outside of the fitted data range. This problem can be corrected by fitting a larger range of data to the equations. If data from all three regions of crack growth are fit to the equation, from ΔK_{th} to ΔK_C , this problem will be eliminated. Unfortunately, the data used in this study did not encompass all three regions of crack growth.

Recently, Newman** suggested setting p and q equal to 2.0 when values are not definable from wide-range da/dN - ΔK data. The data for titanium alloy Ti-6Al-4V in

** Pages 54 through 68 have been revised at the request of Dr. Robert S. Piascik, Mechanics of Materials Branch, NASA Langley Research Center, in order to include a third analysis case where $p = q = 2.0$. These values for p and q were selected by Dr. James C. Newman, Mechanics of Materials Branch, NASA Langley Research Center. This case was not included in analysis of model capability to interpolate trends in fatigue behavior.

both the air and 1.0% NaCl environments were fit to the Forman Equation with and without crack closure. K_C was held constant at 3953 MPa $\sqrt{\text{mm}}$ for the air environment, and at 4270 MPa $\sqrt{\text{mm}}$ for the 1.0% NaCl solution. S_{max}/σ_o was entered as 0.3, α was 2.5, and ΔK_{th} was calculated from ΔK_o . ΔK_o was taken from the FLAGRO materials files as 121.6 MPa $\sqrt{\text{mm}}$ for Ti-6Al-4V (MA). The values determined for C and n are shown in Tables II.8a and II.8b. Results are shown graphically in Figures 22a through 22f.

Notice in Figures 22a through 22f, that setting p and q equal to 2.0 alleviates the problem encountered when fitting all four equation parameters in the Forman Equation. When holding p and q constant at 2.0, the equation does not tend to become sinusoidal, and the crack growth rates predicted by the equation are physically permissible, even outside the data range. The instability problem encountered with the Sigmoidal Equation has yet to be addressed.

Table II.3: Forman Equation (Equation II.1) with closure (C,n Fit)

Parameter	Environment	R = 0.1	R = 0.4	R = 0.7
C	Air	0.6032×10^{-17}	0.8089×10^{-15}	0.1210×10^{-13}
n	Air	5.036	4.200	3.762
C	1.0% NaCl	0.1727×10^{-16}	0.3308×10^{-15}	0.3554×10^{-14}
n	1.0% NaCl	5.028	4.532	4.095

Table II.4: Forman Equation (Equation II.1) with closure (C,n,p,q Fit)

Parameter	Environment	R = 0.1	R = 0.4	R = 0.7
C	Air	0.1510×10^{-57}	0.2404×10^{-23}	0.2829×10^{-24}
n	Air	22.07	8.020	8.129
p	Air	-14.71	-1.395	-9.469
q	Air	-78.72	-16.43	-6.056
C	1.0% NaCl	0.4368×10^{-34}	0.2289×10^{17}	0.3345×10^{15}
n	1.0% NaCl	12.33	-10.21	-9.031
p	1.0% NaCl	-6.494	8.012	16.43
q	1.0% NaCl	-33.84	99.19	41.21

Table II.5: Forman Equation (Equation II.5) without closure (C,n Fit)

Parameter	Environment	R = 0.1	R = 0.4	R = 0.7
C	Air	0.1917×10^{-17}	0.6918×10^{-15}	0.1673×10^{-13}
n	Air	5.036	4.200	3.762
C	1.0% NaCl	0.5500×10^{-17}	0.2766×10^{-15}	0.4921×10^{-14}
n	1.0% NaCl	5.028	4.532	4.095

Table II.6: Forman Equation (Equation II.5) without closure (C,n,p,q Fit)

Parameter	Environment	R = 0.1	R = 0.4	R = 0.7
C	Air	0.3942×10^{-56}	0.1029×10^{-19}	0.1453×10^{-20}
n	Air	22.07	8.020	8.129
p	Air	-14.71	-1.395	-9.469
q	Air	-78.72	-16.43	-6.056
C	1.0% NaCl	0.9722×10^{-34}	0.7540×10^{-5}	0.2978×10^{-6}
n	1.0% NaCl	12.33	-10.21	-9.031
p	1.0% NaCl	-6.494	8.012	16.43
q	1.0% NaCl	-33.84	99.19	41.21

Table II.7: Hyperbolic Sine Equation (Equation II.7), $C_1 = 0.5$

Parameter	Environment	R = 0.1	R = 0.4	R = 0.7
C_2	Air	2.8560	1.4889	1.0491
C_3	Air	-3.3127	-4.1999	-4.9851
C_4	Air	-2.6468	-1.5061	-1.0000
C_2	1.0% NaCl	1.4749	1.7548	2.1795
C_3	1.0% NaCl	-4.3175	-1.0000	-1.3854
C_4	1.0% NaCl	-1.0000	-7.6946	-6.8909

Table II.8: Sigmoidal Equation (Equation II.10)

Parameter	Environment	R = 0.1	R = 0.4	R = 0.7
B	Air	-118.60	-38.07	-32.34
P	Air	48.71	13.60	13.60
D	Air	64.59	14.15	6.150
Q	Air	-16.23	-2.097	-8.944
B	1.0% NaCl	-56.96	87.05	46.99
P	1.0% NaCl	22.31	-34.64	-28.53
D	1.0% NaCl	25.40	-72.27	-37.41
Q	1.0% NaCl	-6.652	8.918	17.51

Table II.8a: Forman Equation (Equation II.1) with closure for $p = q = 2$

Parameter	Environment	R = 0.1	R = 0.4	R = 0.7
C	Air	0.1642×10^{-14}	0.1317×10^{-12}	0.1029×10^{-11}
n	Air	4.144	3.374	2.968
C	1.0% NaCl	0.1272×10^{-13}	0.6862×10^{-12}	0.2976×10^{-12}
n	1.0% NaCl	3.970	3.247	3.310

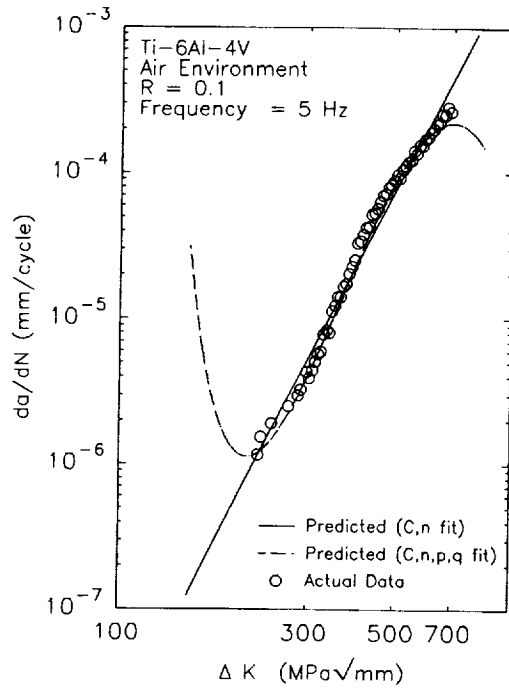
Table II.8b: Forman Equation (Equation II.5) without closure for $p = q = 2.0$

Parameter	Environment	$R = 0.1$	$R = 0.4$	$R = 0.7$
C	Air	0.5630×10^{-15}	0.6290×10^{-13}	0.3141×10^{-12}
n	Air	4.144	3.374	2.968
C	1.0% NaCl	0.4544×10^{-14}	0.3305×10^{-12}	0.9106×10^{-13}
n	1.0% NaCl	3.970	3.247	3.310

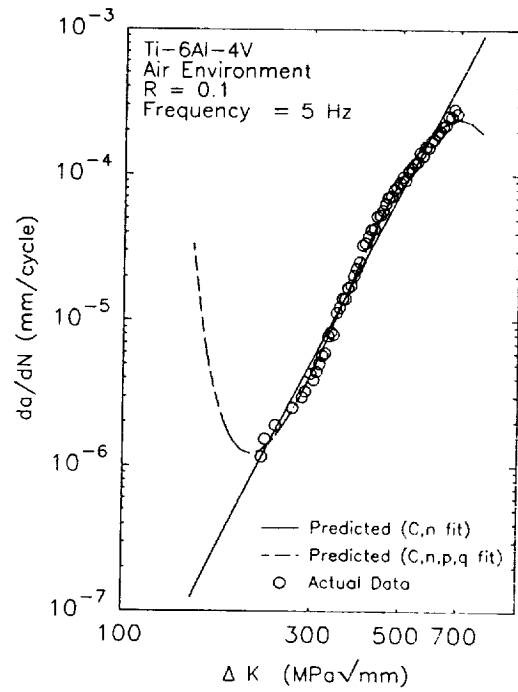
In order to quantitatively determine how well the crack growth rate equations fit the data sets, the coefficient of determination was calculated for each equation and data set. These values are shown in Tables II.9 and II.10 for the original two tests conducted. Results for the case recommended by Newman of $p = q = 2$ in the Forman Equation (with and without closure) are shown in Tables II.10a and II.10b.

The third criteria used to test the computer program was to see how well the program could interpolate trends in da/dN behavior. To accomplish this task, three sets of data for titanium alloy Ti-6Al-4V in 3.5% NaCl solution were used; conditions were constant except for the loading frequency, thus all of the equation parameters had to be expressed as a function of frequency. The data were taken from a study by Dawson and Pelloux¹⁴. To test the model, data for 1 Hz and 10 Hz were fit to the Forman Equation (with and without closure), the SINH Equation, and the Sigmoidal Equation, and the

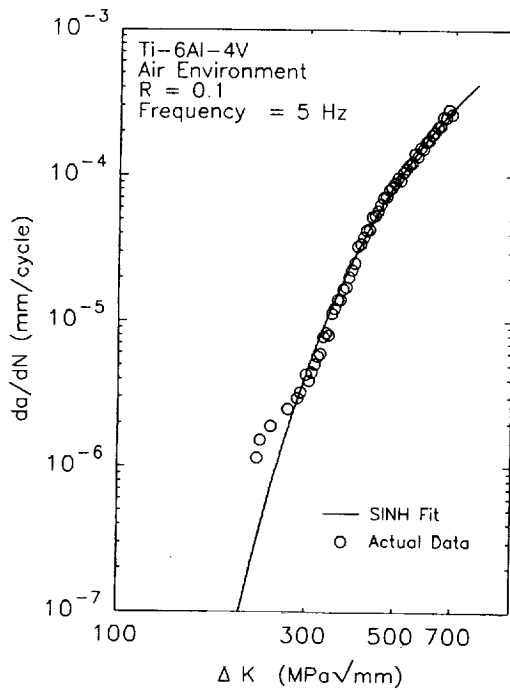
1. The first part of the document is a list of the names of the persons who have been appointed to the various positions of the Board of Directors of the Corporation.



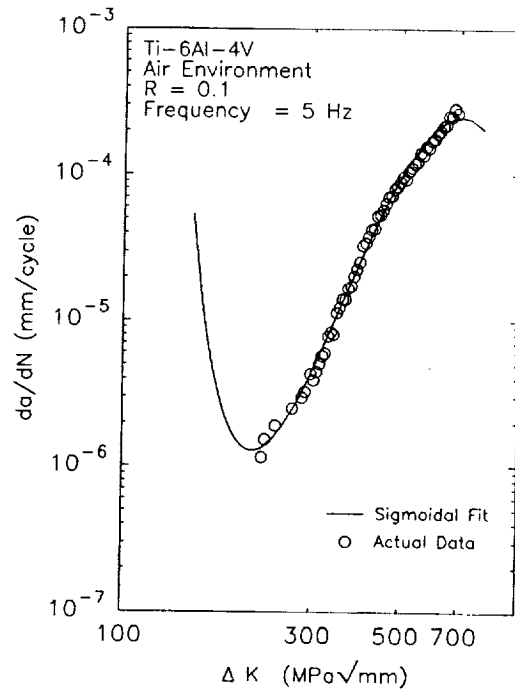
A) Forman Equation (closure).



B) Forman Equation (no closure).

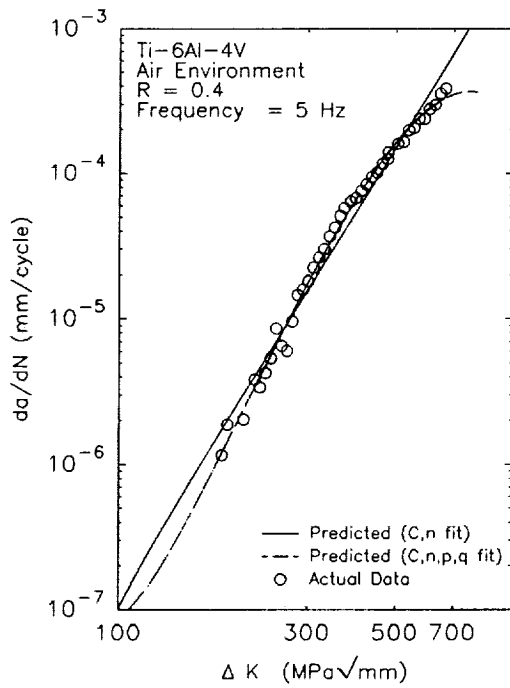


C) SINH Equation.

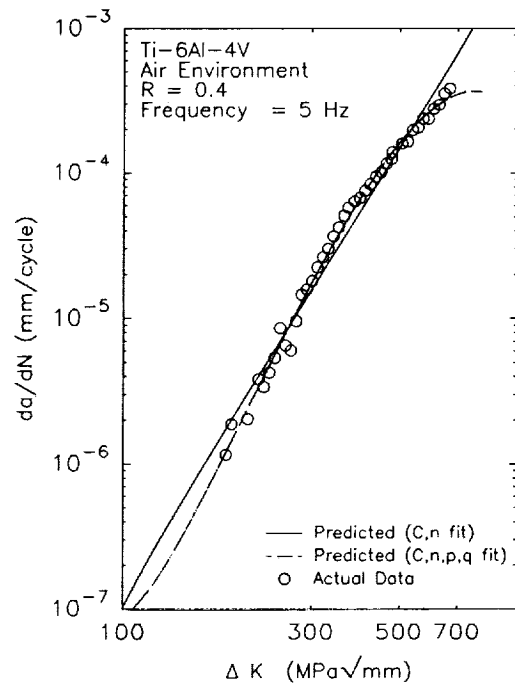


D) Sigmoidal Equation.

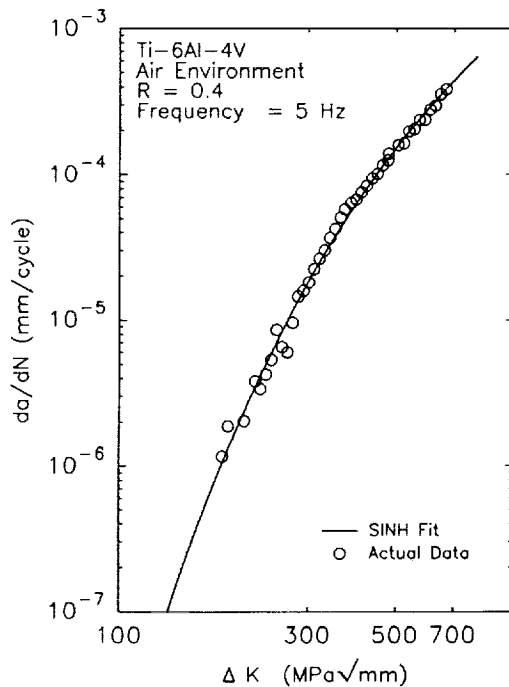
Figure 17: Fit of fatigue data for Ti-6Al-4V in air with $R = 0.1$ at 5 Hz.



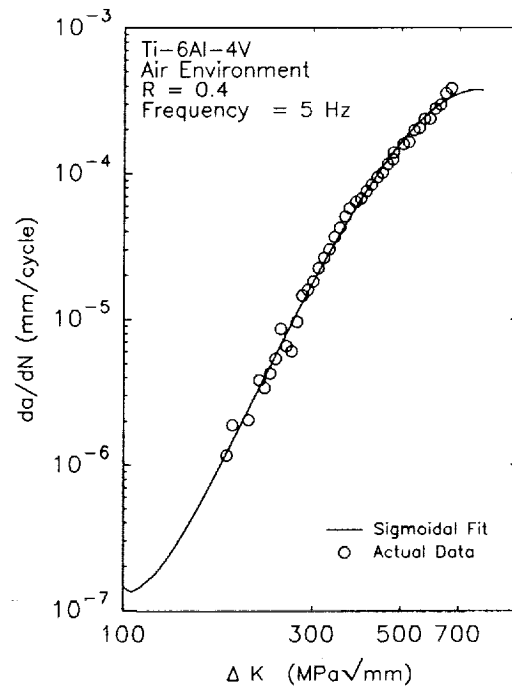
A) Forman Equation (closure).



B) Forman Equation (no closure).

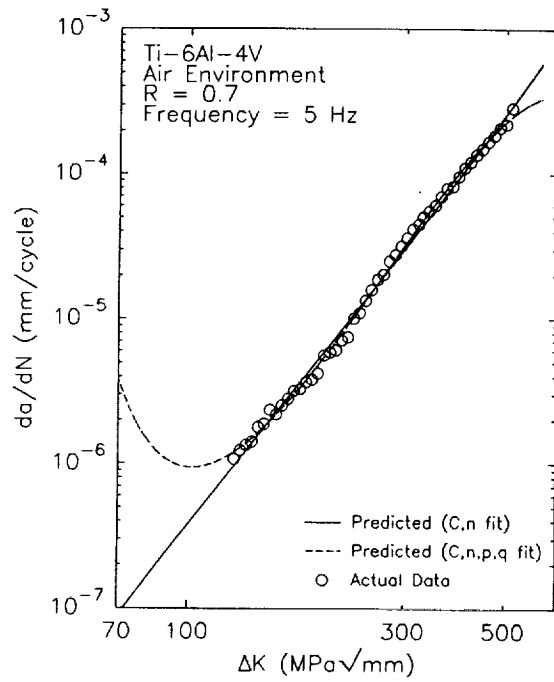


C) SINH Equation.

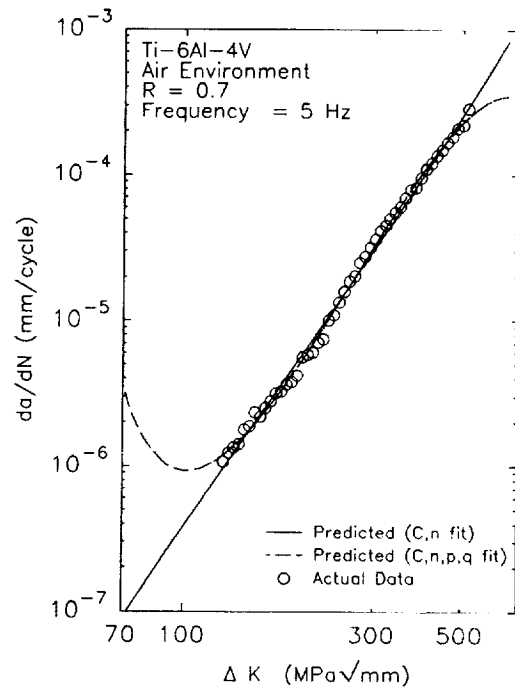


D) Sigmoidal Equation.

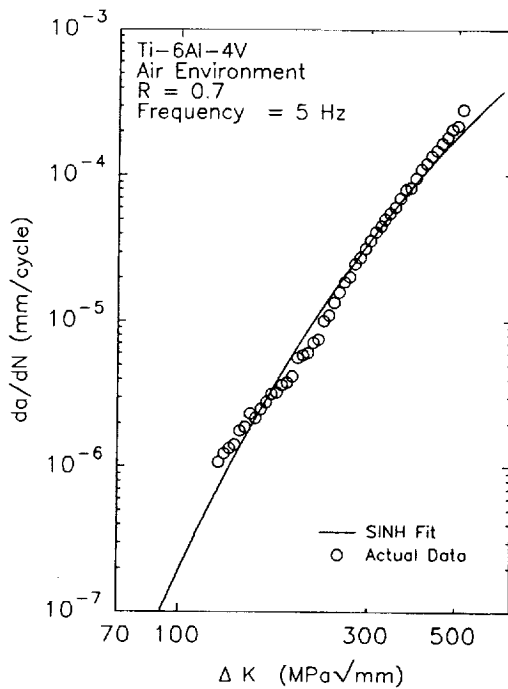
Figure 18: Fit of fatigue data for Ti-6Al-4V in air with R = 0.4 at 5 Hz.



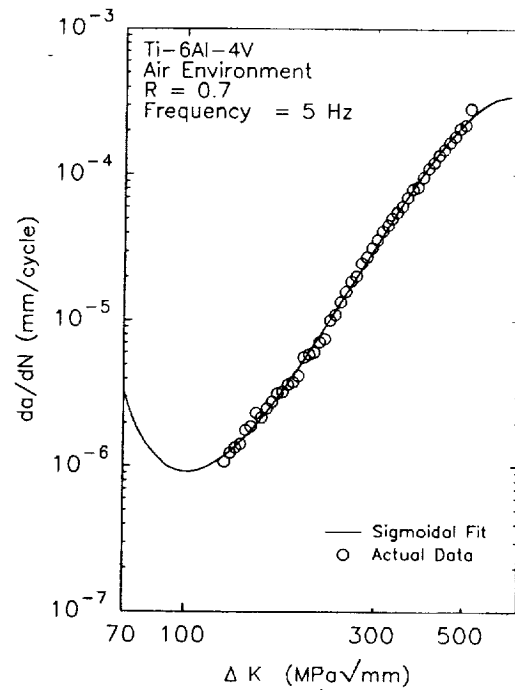
A) Forman Equation (closure).



B) Forman Equation (no closure).

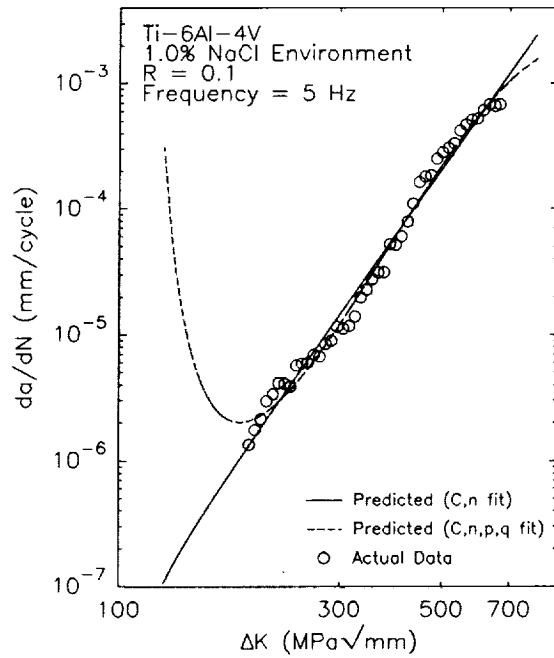


C) SINH Equation.

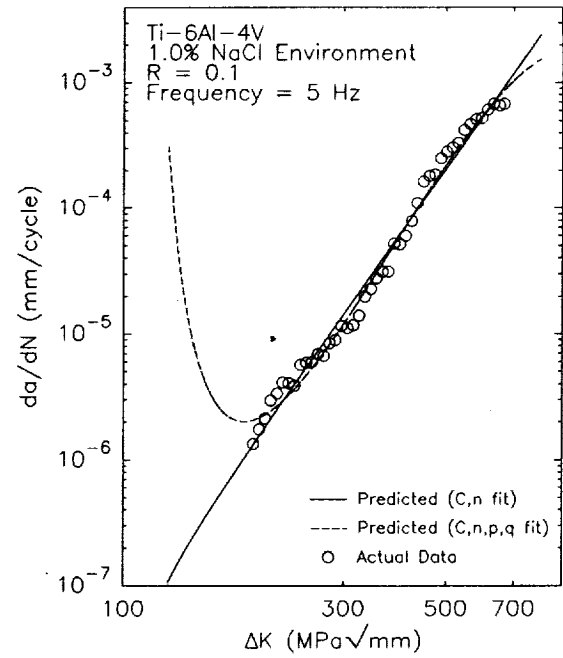


D) Sigmoidal Equation.

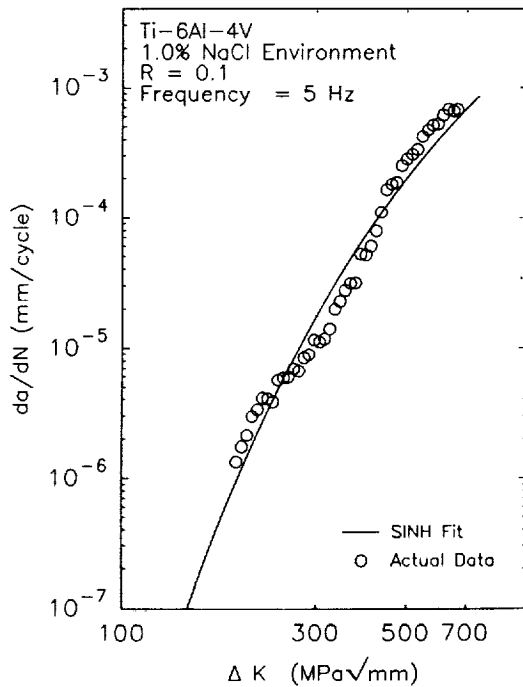
Figure 19: Fit of fatigue data for Ti-6Al-4V in air with R = 0.7 at 5 Hz.



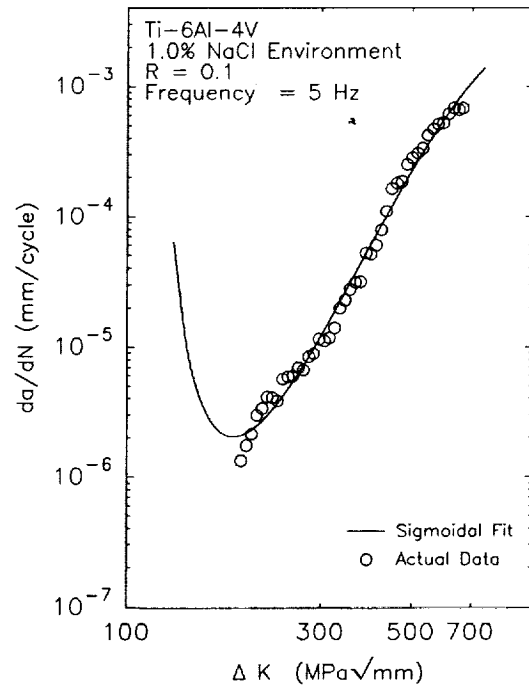
A) Forman Equation (closure).



B) Forman Equation (no closure).

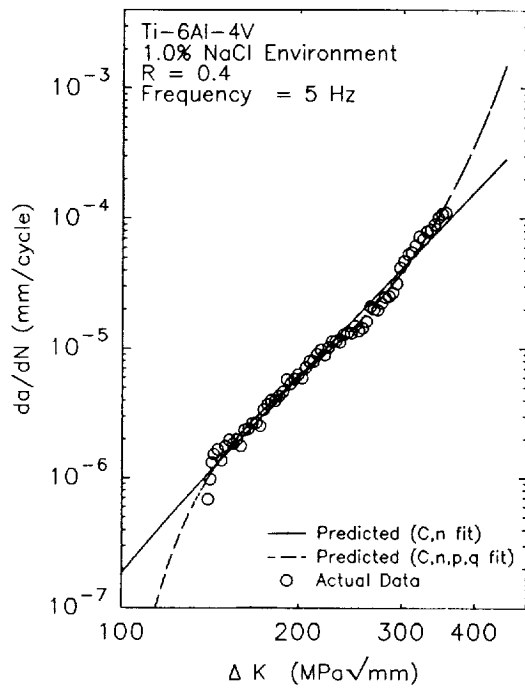


C) SINH Equation.

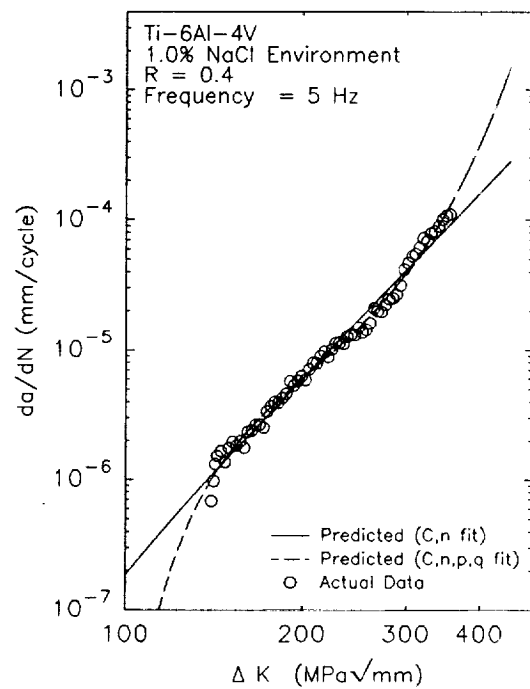


D) Sigmoidal Equation.

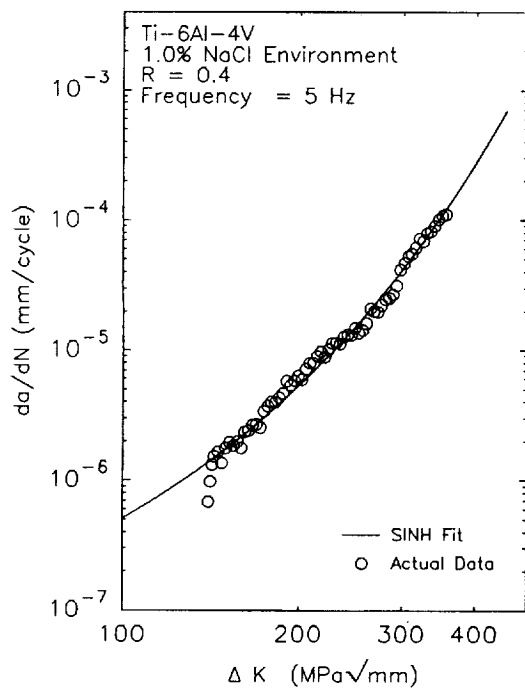
Figure 20: Fit of fatigue data for Ti-6Al-4V in 1.0% NaCl with R = 0.1 at 5 Hz.



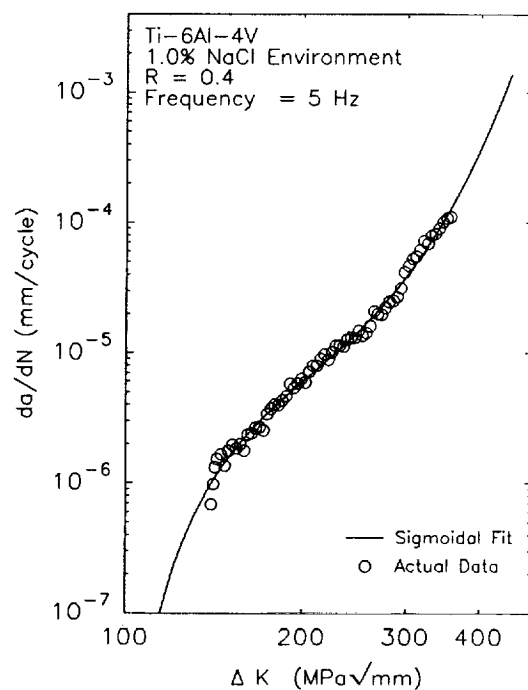
A) Forman Equation (closure).



B) Forman Equation (no closure).

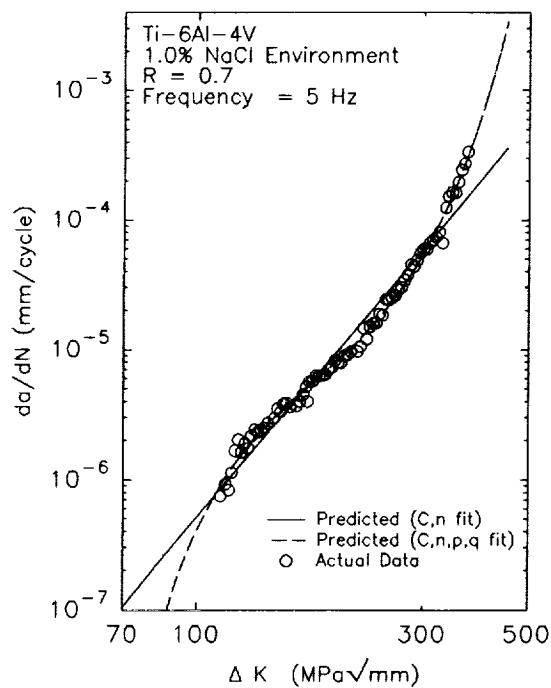


C) SINH Equation.

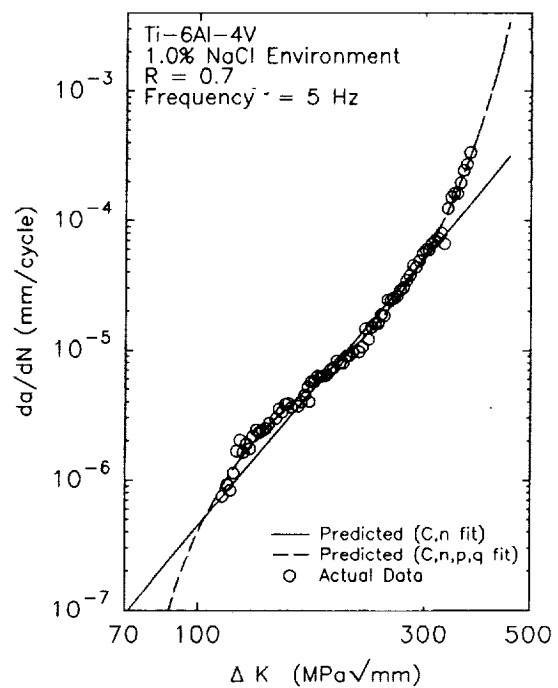


D) Sigmoidal Equation.

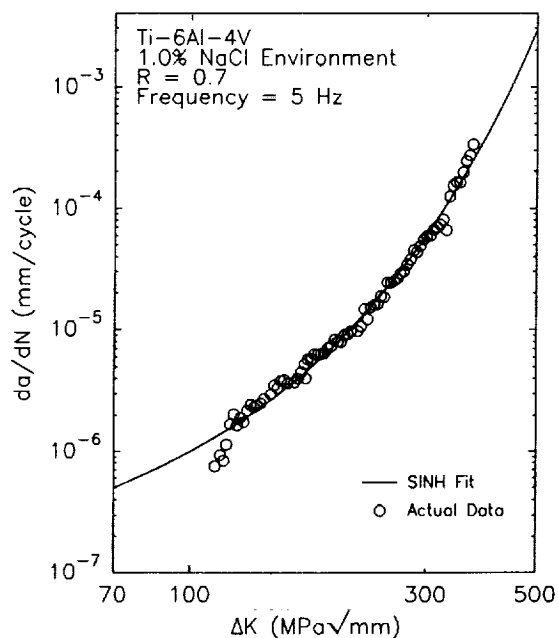
Figure 21: Fit of fatigue data for Ti-6Al-4V in 1.0% NaCl with $R = 0.4$ at 5 Hz.



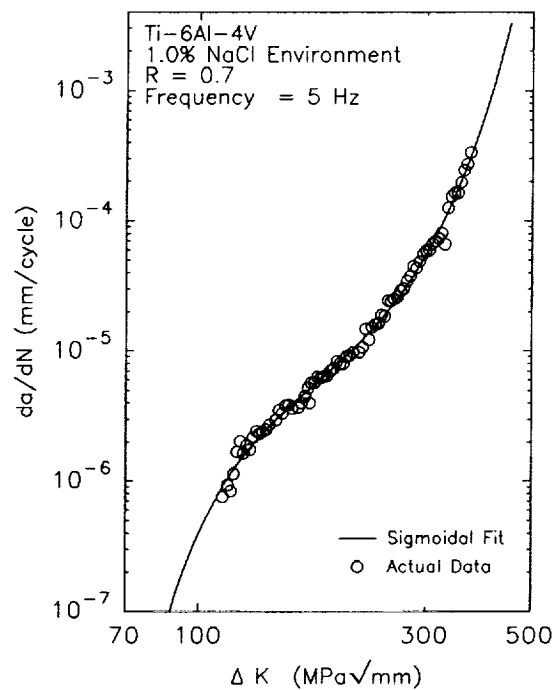
A) Forman Equation (closure).



B) Forman Equation (no closure).

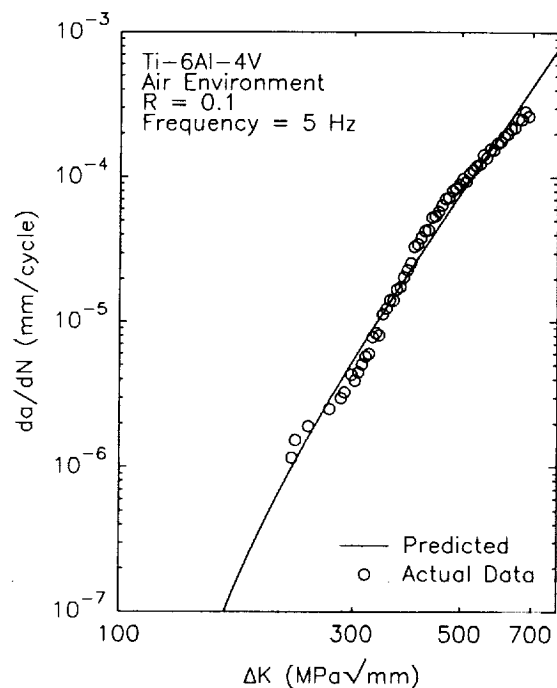


C) SINH Equation.

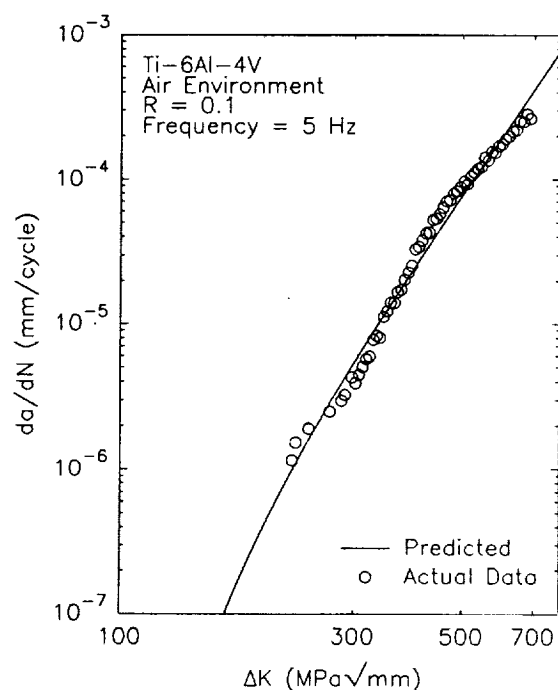


D) Sigmoidal Equation.

Figure 22: Fit of fatigue data for Ti-6Al-4V in 1.0% NaCl with $R = 0.7$ at 5 Hz.

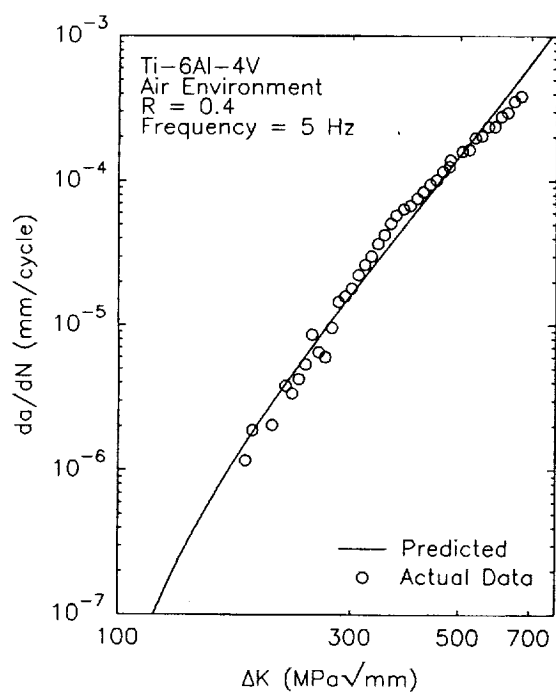


A) Forman Equation (closure).

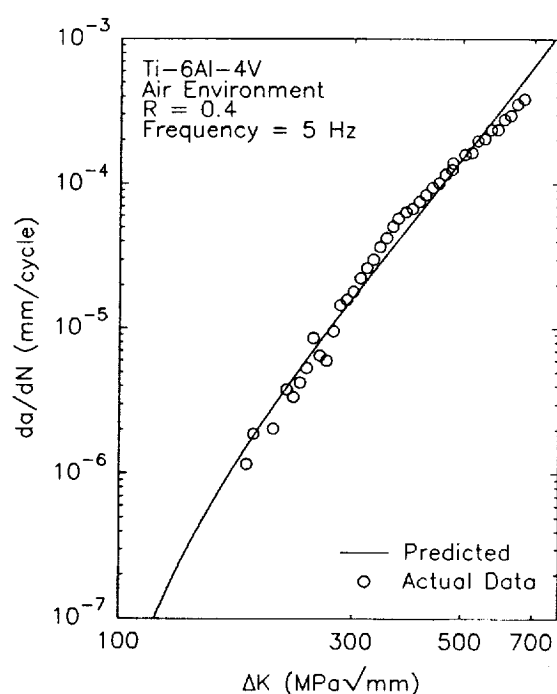


B) Forman Equation (no closure).

Figure 22a: Fit of fatigue data for Ti-6Al-4V in air with $R = 0.1$ at 5 Hz for $p = q = 2$.

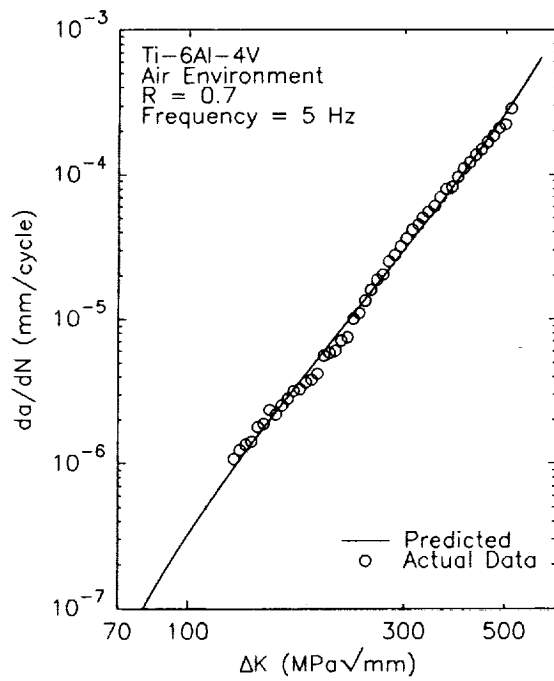


A) Forman Equation (closure).

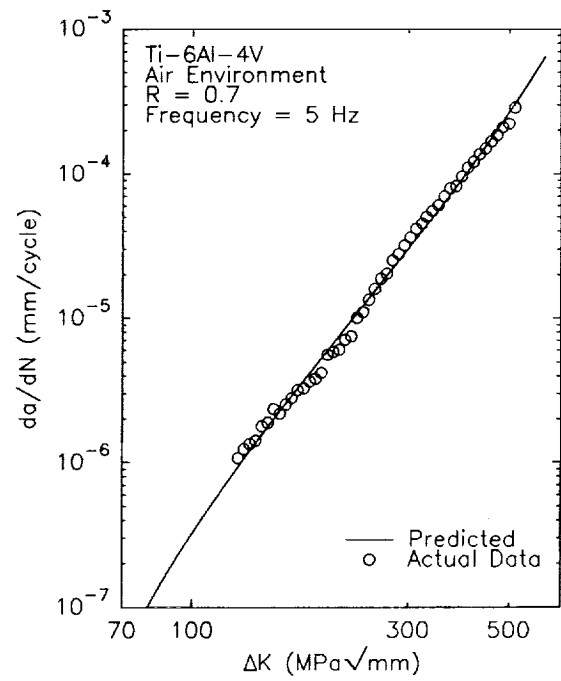


B) Forman Equation (no closure).

Figure 22b: Fit of fatigue data for Ti-6Al-4V in air with $R = 0.4$ at 5 Hz for $p = q = 2$.

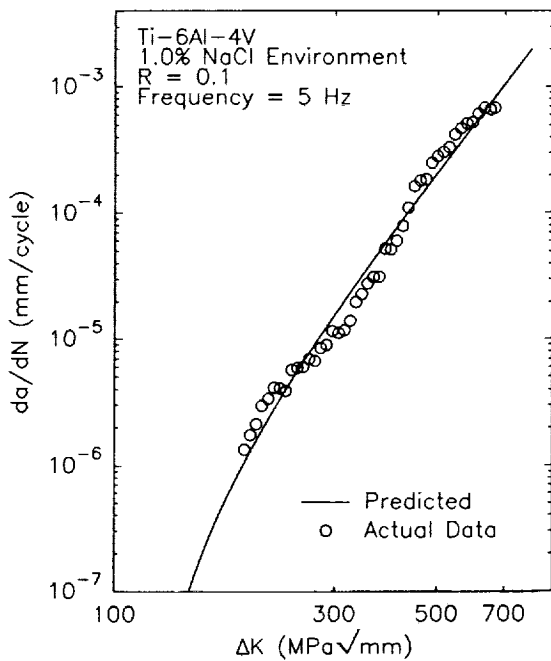


A) Forman Equation (closure).

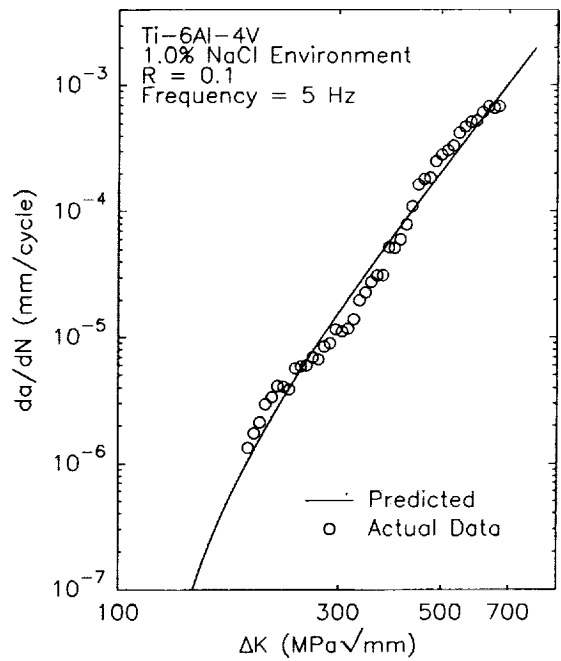


B) Forman Equation (no closure).

Figure 22c: Fit of fatigue data for Ti-6Al-4V in air with $R = 0.7$ at 5 Hz for $p = q = 2$.

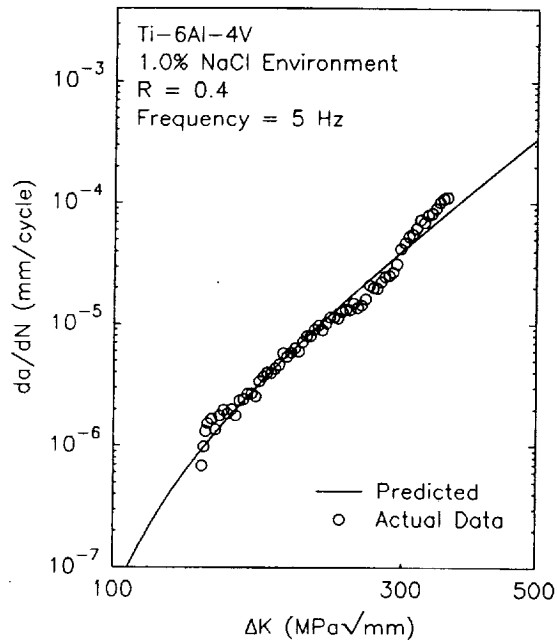


A) Forman Equation (closure).

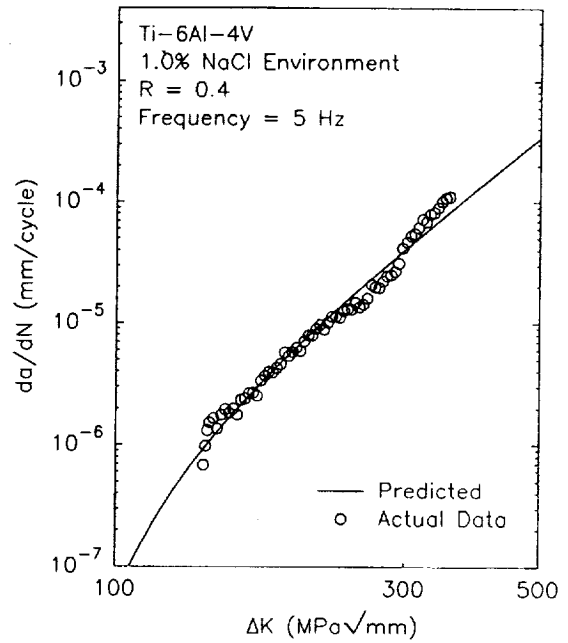


B) Forman Equation (no closure).

Figure 22d: Fit of fatigue data for Ti-6Al-4V in 1.0% NaCl with $R = 0.1$ at 5 Hz for $p = q = 2$.

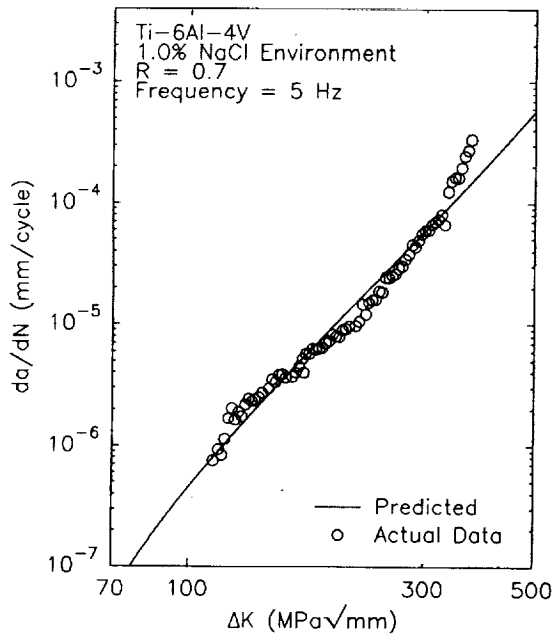


A) Forman Equation (closure).

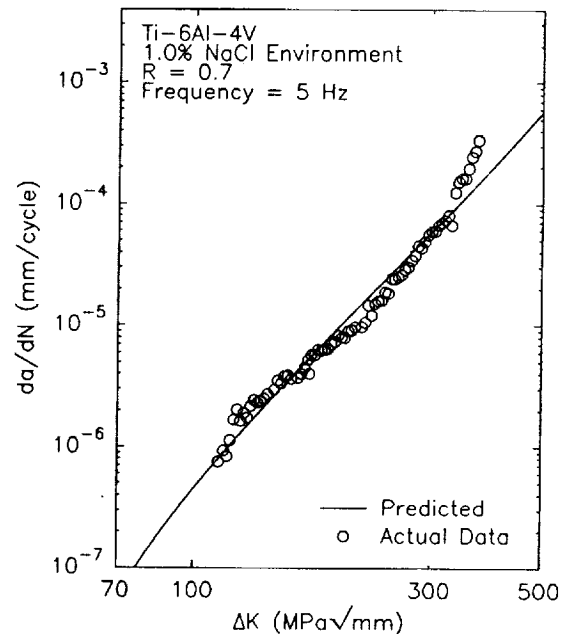


B) Forman Equation (no closure).

Figure 22e: Fit of fatigue data for Ti-6Al-4V in 1.0% NaCl with R = 0.4 at 5 Hz for p = q = 2.



A) Forman Equation (closure).



B) Forman Equation (no closure).

Figure 22f: Fit of fatigue data for Ti-6Al-4V in 1.0% NaCl with R = 0.7 at 5 Hz for p = q = 2.

Table II.9: Coefficients of determination

Environment	R	Forman Closure: C, n $p = 0.25, q = 0.75$	Forman Closure: C, n, p, q	Forman No Closure: C, n $p = 0.25, q = 0.75$	Forman No Closure: C, n, p, q	Sigmoidal	SINH
Air	0.1	0.8569	0.9809	0.8569	0.9809	0.9816	0.9964*
Air	0.4	0.8391	0.9843	0.8391	0.9843	0.9846	0.9945*
Air	0.7	0.9893	0.9919*	0.9893	0.9919*	0.9917	0.9453
1.0% NaCl	0.1	0.9371	0.9608*	0.9371	0.9608*	0.9567	0.8976
1.0% NaCl	0.4	0.9500	0.9829	0.9500	0.9829	0.9836	0.9902*
1.0% NaCl	0.7	0.7578	0.9894*	0.7578	0.9894*	0.9891	0.9500

* denotes equation which displayed the highest coefficient of determination for each data set

Table II.10 : Average coefficients of determination.

Equation Type	Parameters Fit	Environment	Coefficient
Forman (with closure)	C, n (p = 0.25, q = 0.75)	Air	0.8951
		1.0% NaCl	0.8816
Forman (with closure)	C, n, p, q	Air	0.9857
		1.0% NaCl	0.9777
Forman (no closure)	C, n (p = 0.25, q = 0.75)	Air	0.8951
		1.0% NaCl	0.8816
Forman (no closure)	C, n, p, q	Air	0.9857
		1.0% NaCl	0.9777
Sigmoidal	B, P, Q, D	Air	0.9857
		1.0% NaCl	0.9765
Hyperbolic Sine	C ₂ , C ₃ , C ₄ (C ₁ = 0.5)	Air	0.9787
		1.0% NaCl	0.9459

Table II.10a: Coefficients of determination for $p = q = 2.0$

Environment	R	Forman Closure C, n ($p = q = 2.0$)	Forman No Closure: C, n ($p = q = 2.0$)
Air	0.1	0.9034	0.9034
Air	0.4	0.8801	0.8801
Air	0.7	0.9846	0.9846
1.0% NaCl	0.1	0.9573	0.9573
1.0% NaCl	0.4	0.9128	0.9128
1.0% NaCl	0.7	0.7445	0.7445

Table II.10b: Average coefficients of determination for $p = q = 2.0$

Equation Type	Parameters Fit	Environment	Coefficient
Forman (with closure)	C,n ($p = q = 2.0$)	Air	0.9227
		1.0% NaCl	0.8715
Forman (no closure)	C,n ($p = q = 2.0$)	Air	0.9227
		1.0% NaCl	0.8715

parameters were set equal to the appropriate linear relationship. In reality, only one data set is needed to determine the effect of frequency, however, data for 1 Hz and 10 Hz were used so that the relationships determined would be accurate over a wider range of data than if only one data set was used. (If only one data set was used, the relationships determined would only be accurate for frequencies very near the frequency for which data were entered.) Since two data sets were used, the equation parameters were set equal to relationships involving two loading variables, frequency and either the hold time or the stress ratio, even though the hold time and stress ratio are constant. Using these relationships, the equation parameters were interpolated for a frequency of 5 Hz. The fatigue crack growth was then calculated for a range of ΔK values using the resultant equation, and the interpolated growth rates were compared to actual data.

The Forman Equation with closure was tested first, fitting only the parameters C and n ; p was entered as 0.25 and q was 0.75. The fitted values are listed in Table II.11.

Table II.11: Forman Equation with closure (C,n Fit)

Parameter	Environment	1 Hz	10 Hz
C	3.5% NaCl	0.4398×10^{-8}	0.4007×10^{-7}
n	3.5% NaCl	3.481	2.432

The parameters were set equal to the following linear relationships:

$$C = -0.13741 \times 10^{-6} \log\left[\left(\frac{1}{f}\right) + 1\right] + 0.45761 \times 10^{-7} \log\left[\frac{\tau + 1}{0.1}\right] \quad (\text{II.28})$$

$$n = 4.040 \log \left[\left(\frac{1}{f} \right) + 1 \right] + 2.265 \log \left[\frac{\tau + 1}{0.1} \right] \quad (\text{II.29})$$

$$\Delta K_{ch} = 13.648 \log \left[\left(\frac{1}{f} \right) + 1 \right] + 6.708 \log \left[\frac{\tau + 1}{0.1} \right] \quad (\text{II.30})$$

These results are graphically shown graphically in Figure 23. Next, the parameters C,n,p, and q were fit, and the resulting values are shown in Table II.12.

Table II.12 Forman Equation with closure (C,n,p,q Fit)

Parameter	Environment	1 Hz	10 Hz
C	3.5% NaCl	0.5994 X 10 ⁻⁴	0.3430 X 10 ⁻⁴
n	3.5% NaCl	0.9971	0.2544
p	3.5% NaCl	2.971	2.253
q	3.5% NaCl	0.4662	2.075

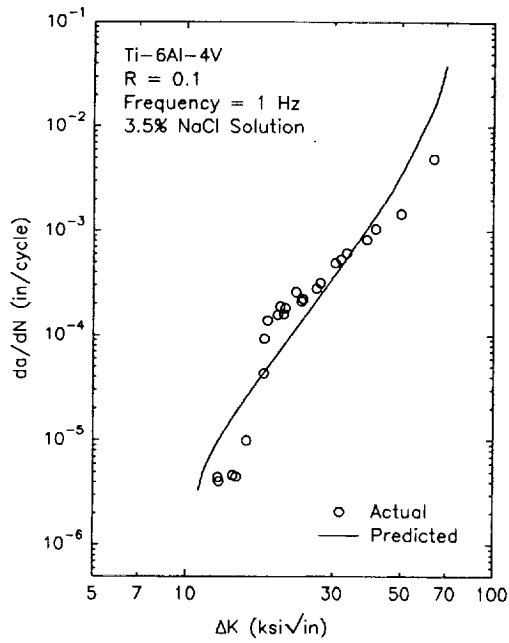
The following relationships were determined:

$$C = 0.9877 \times 10^{-4} \log \left[\left(\frac{1}{f} \right) + 1 \right] + 0.30212 \times 10^{-4} \log \left[\frac{\tau + 1}{0.1} \right] \quad (\text{II.31})$$

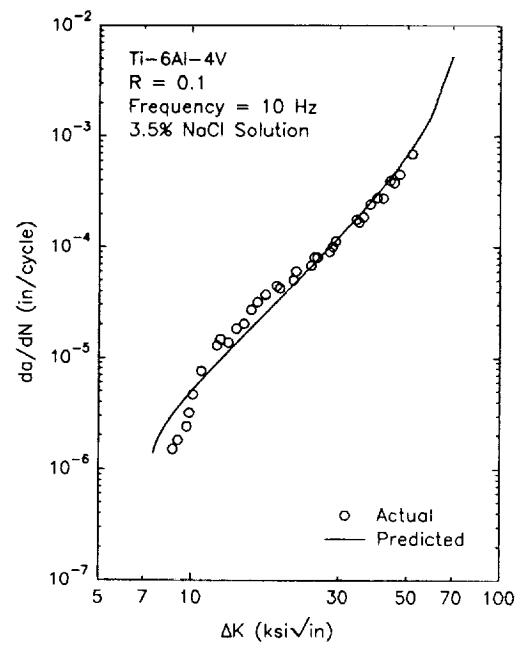
$$n = 2.861 \log \left[\left(\frac{1}{f} \right) + 1 \right] + 0.1360 \log \left[\frac{\tau + 1}{0.1} \right] \quad (\text{II.32})$$

$$p = 2.765 \log \left[\left(\frac{1}{f} \right) + 1 \right] + 2.138 \log \left[\frac{\tau + 1}{0.1} \right] \quad (\text{II.33})$$

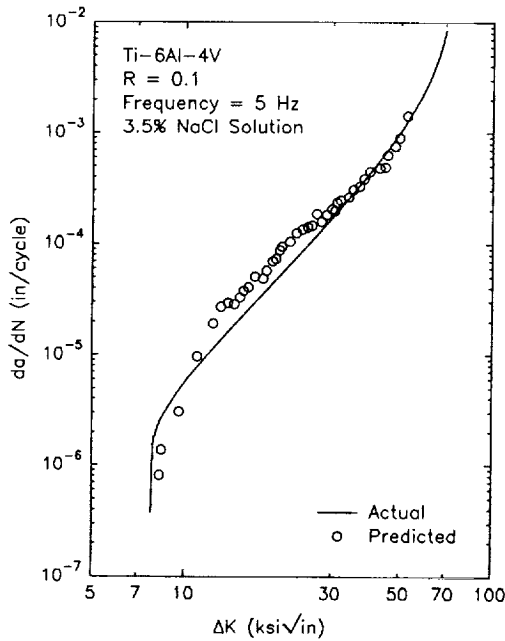
$$q = -6.197 \log \left[\left(\frac{1}{f} \right) + 1 \right] + 2.332 \log \left[\frac{\tau + 1}{0.1} \right] \quad (\text{II.34})$$



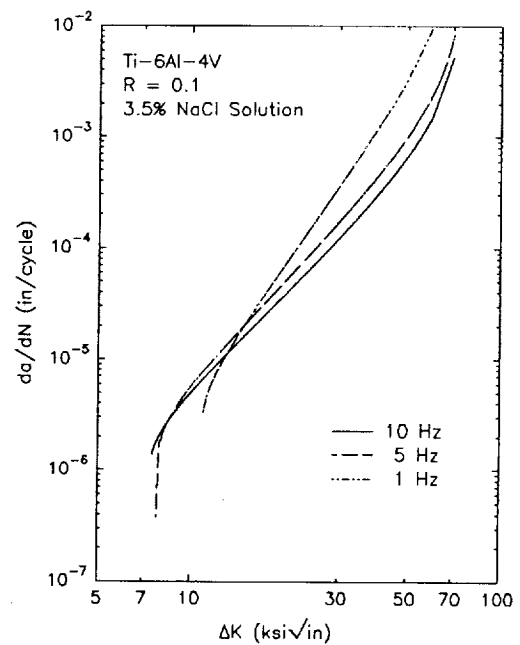
A) Fitted data for 1 Hz.



B) Fitted data for 10 Hz.



C) Interpolated data for 5 Hz.



D) Effect of frequency on equation.

Figure 23: Fitted and interpolated data using Forman Equation with closure (C,n fit)

$$\Delta K_{th} = 13.648 \log \left[\left(\frac{1}{f} \right) + 1 \right] + 6.708 \log \left[\frac{\tau + 1}{0.1} \right] \quad (\text{II.35})$$

These results are shown graphically in Figure 24.

The second equation tested was the Forman Equation without closure. Originally, only the parameters C and n were fit. The parameter m was held constant at 1.0, p was constant at 0.25, and q was constant at 0.75. The fitted parameters are listed in Table II.13.

Table II.13: Forman Equation without closure (C,n Fit)

Parameter	Environment	1 Hz	10 Hz
C	3.5% NaCl	0.2008×10^{-8}	0.2335×10^{-7}
n	3.5% NaCl	3.481	2.432

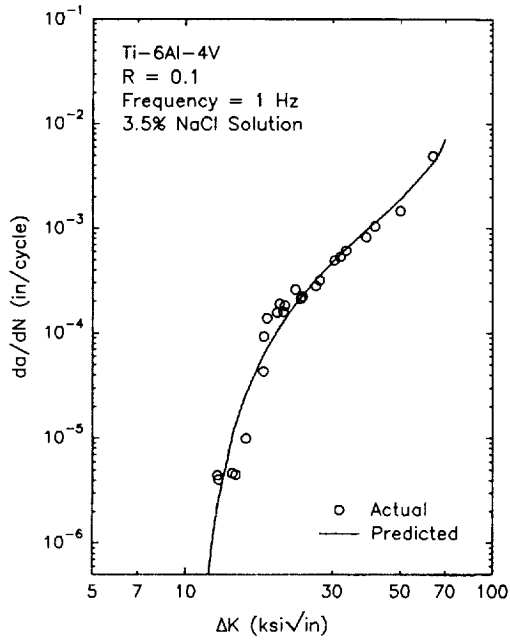
The parameters were set equal to the following linear relationships:

$$C = -0.82216 \times 10^{-7} \log \left[\left(\frac{1}{f} \right) + 1 \right] + 0.26757 \times 10^{-7} \log \left[\frac{\tau + 1}{0.1} \right] \quad (\text{II.36})$$

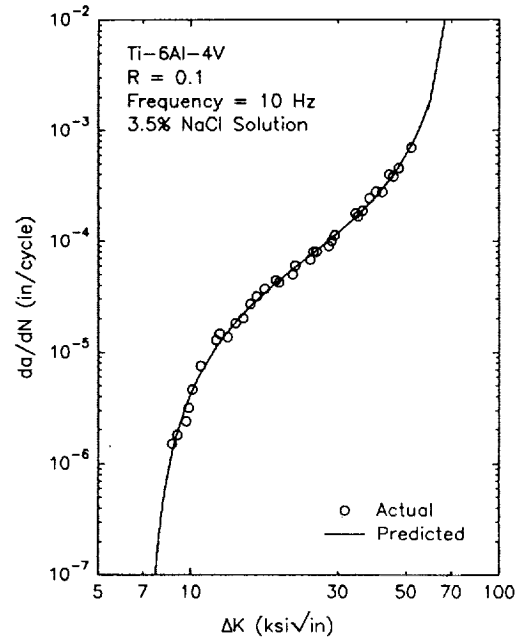
$$n = 4.040 \log \left[\left(\frac{1}{f} \right) + 1 \right] + 2.265 \log \left[\frac{\tau + 1}{0.1} \right] \quad (\text{II.37})$$

$$\Delta K_{th} = 13.648 \log \left[\left(\frac{1}{f} \right) + 1 \right] + 6.708 \log \left[\frac{\tau + 1}{0.1} \right] \quad (\text{II.38})$$

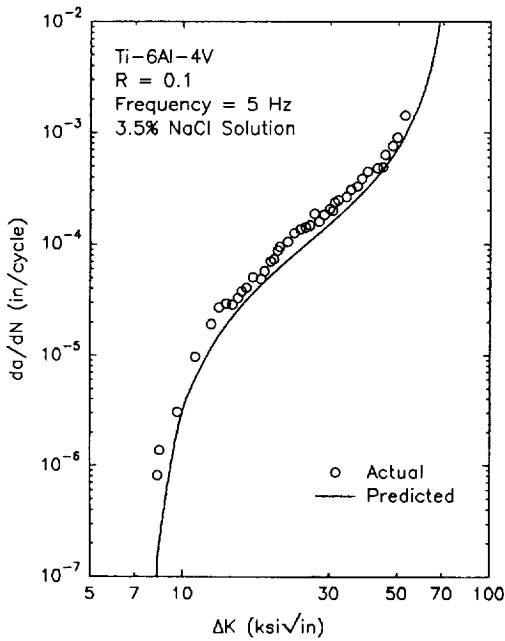
These results are graphically shown in Figure 25. Next, the parameters C, n, p, and q were fit, and the selected values are shown in Table II.14. Again the parameter m was



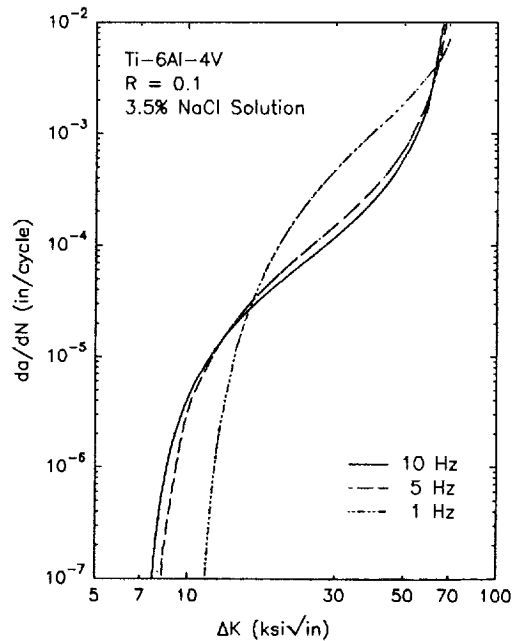
A) Fitted data for 1 Hz.



B) Fitted data for 10 Hz.

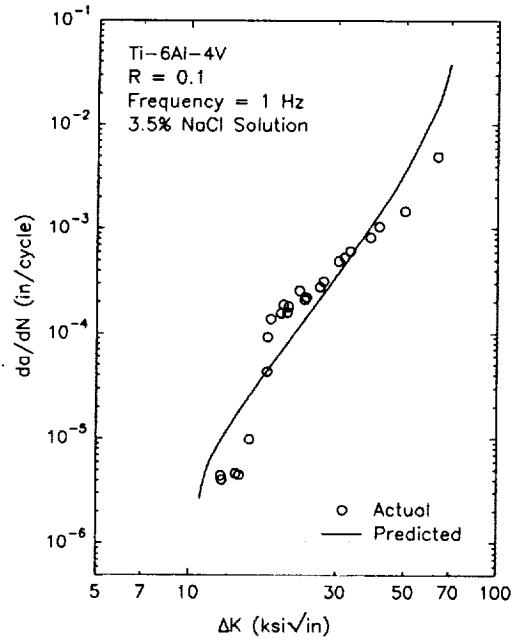


C) Interpolated data for 5 Hz.

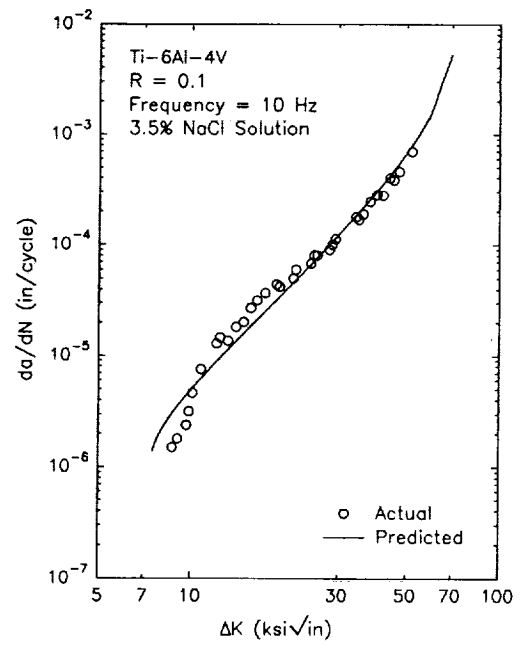


D) Effect of frequency on equation.

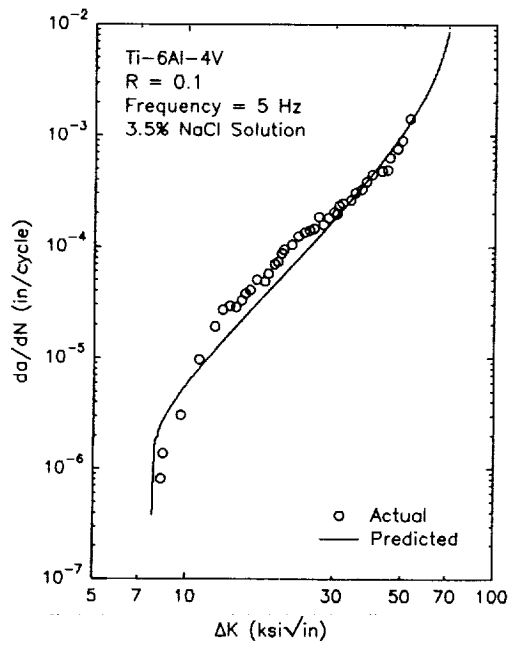
Figure 24: Fitted and interpolated data using Forman Equation with closure (C,n,p,q fit)



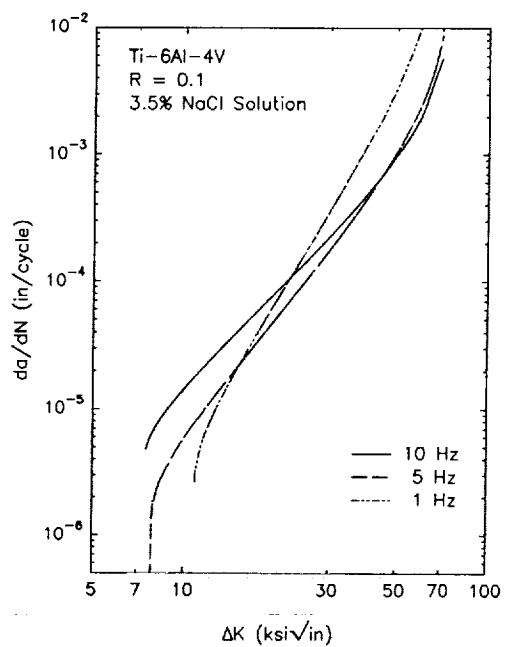
A) Fitted data for 1 Hz.



B) Fitted data for 10 Hz.



C) Interpolated data for 5 Hz.



D) Effect of frequency on equation.

Figure 25: Fitted and interpolated data using Forman Equation without closure (C,n fit)

held constant at 1.0.

Table II.14: Forman Equation without Closure (C,n,p,q Fit)

Parameter	Environment	1 Hz	10 Hz
C	3.5% NaCl	0.5028×10^{-4}	0.2887×10^{-4}
n	3.5% NaCl	0.9971	0.2544
p	3.5% NaCl	2.971	2.253
q	3.5% NaCl	0.4662	2.075

The following relationships were determined:

$$C = 0.82467 \times 10^{-4} \log \left[\left(\frac{1}{f} \right) + 1 \right] + 0.25452 \times 10^{-4} \log \left[\frac{\tau + 1}{0.1} \right] \quad (\text{II.39})$$

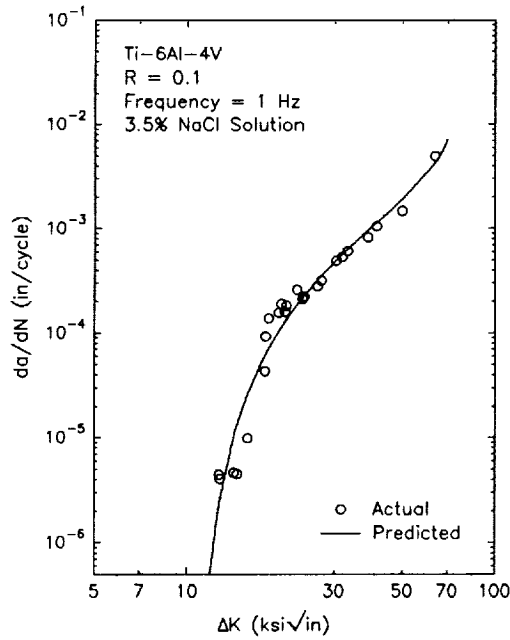
$$n = 2.861 \log \left[\left(\frac{1}{f} \right) + 1 \right] + 0.1360 \log \left[\frac{\tau + 1}{0.1} \right] \quad (\text{II.40})$$

$$p = 2.765 \log \left[\left(\frac{1}{f} \right) + 1 \right] + 2.138 \log \left[\frac{\tau + 1}{0.1} \right] \quad (\text{II.41})$$

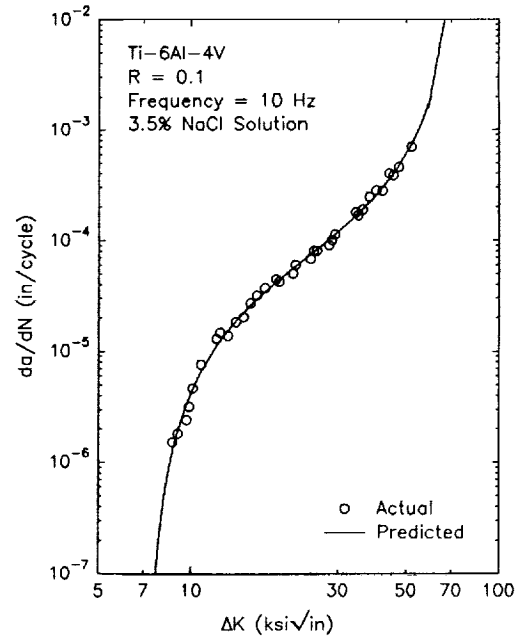
$$q = -6.197 \log \left[\left(\frac{1}{f} \right) + 1 \right] + 2.332 \log \left[\frac{\tau + 1}{0.1} \right] \quad (\text{II.42})$$

$$\Delta K_{th} = 13.648 \log \left[\left(\frac{1}{f} \right) + 1 \right] + 6.708 \log \left[\frac{\tau + 1}{0.1} \right] \quad (\text{II.43})$$

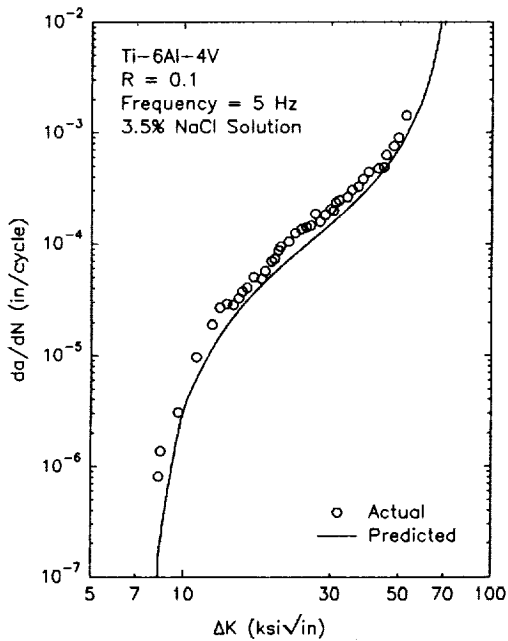
The results are depicted in Figure 26.



A) Fitted data for 1 Hz.



B) Fitted data for 10 Hz.



C) Interpolated data for 5 Hz.

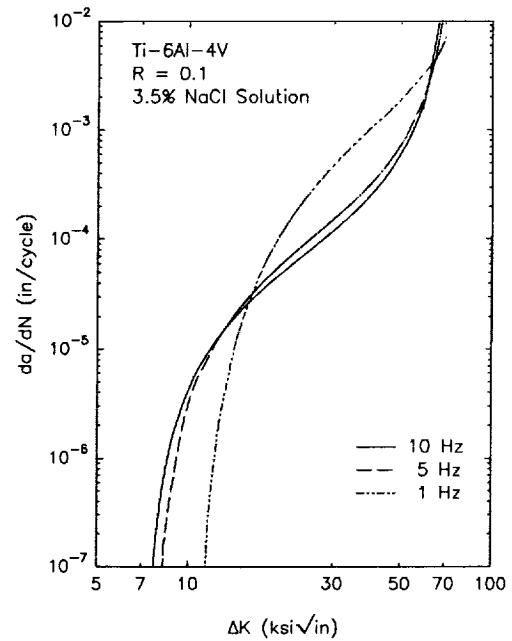


Figure 26: Fitted and interpolated data using Forman Equation without closure (C,n,p,q fit).

The third equation tested was the Hyperbolic Sine Equation (SINH Equation). The values selected by the program are listed in Table II.15, and results are graphically shown in Figure 27.

Table II.15: SINH Equation Parameters

Parameter	Environment	1 Hz	10 Hz
C_2	3.5% NaCl	4.9126	4.3797
C_3	3.5% NaCl	-1.5793	-1.4022
C_4	3.5% NaCl	-3.0435	-4.0799

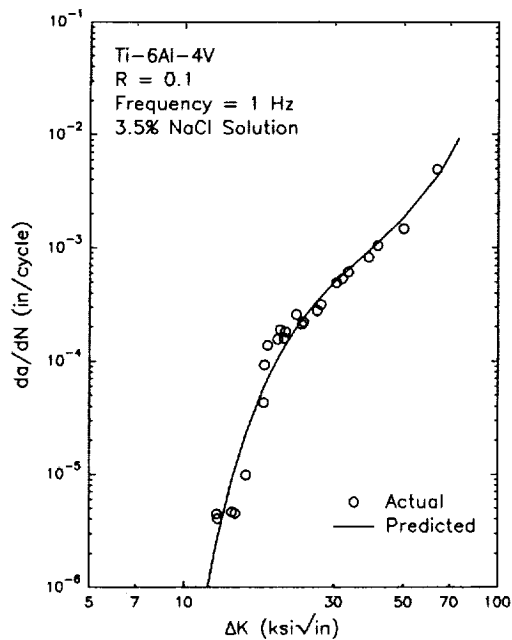
The parameter C_1 was held constant at 0.5. The following relationships were determined:

$$C_2 = 2.0527 \log \left[\left(\frac{1}{f} \right) + 1 \right] + 4.3135 \log \left[\frac{1 - 0.1R}{0.1} \right] \quad (\text{II.44})$$

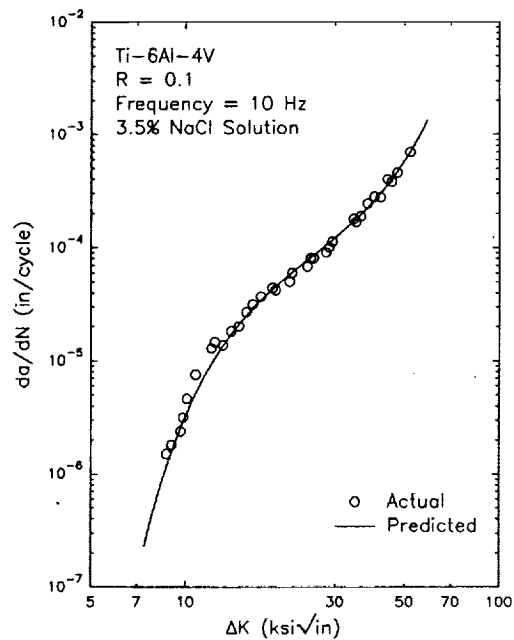
$$C_3 = -0.6824 \log \left[\left(\frac{1}{f} \right) + 1 \right] - 1.3800 \log \left[\frac{1 - 0.1R}{0.1} \right] \quad (\text{II.45})$$

$$C_4 = 3.9917 \log \left[\left(\frac{1}{f} \right) + 1 \right] - 4.2637 \log \left[\frac{1 - 0.1R}{0.1} \right] \quad (\text{II.46})$$

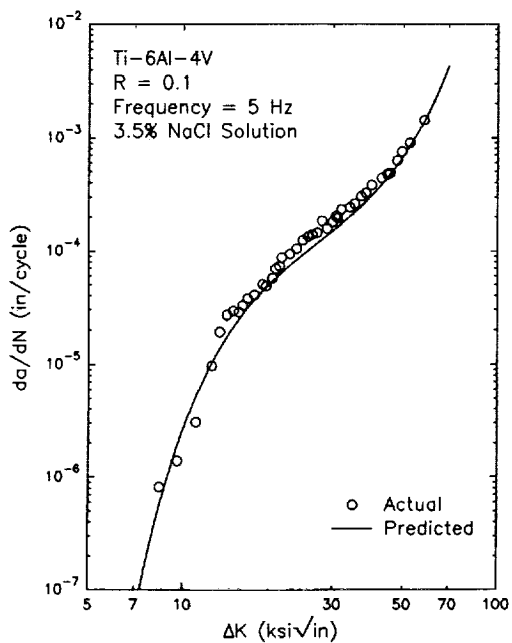
The final equation tested was the Sigmoidal Equation. The values calculated by the program are listed in Table II.16, and the results are graphically shown in Figure 28.



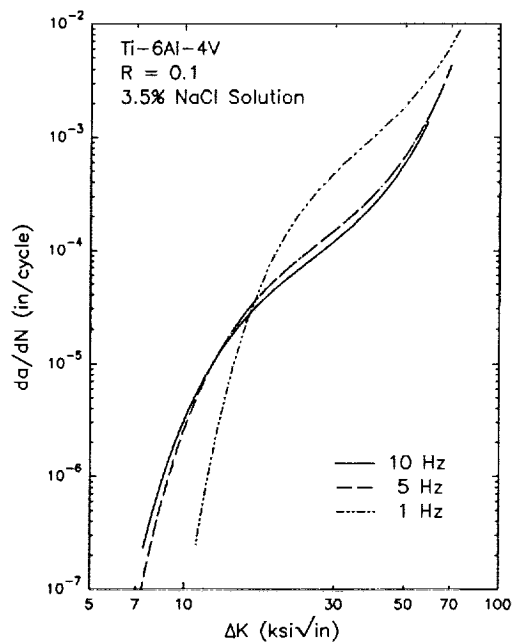
A) Fitted data for 1 Hz.



B) Fitted data for 10 Hz.



C) Interpolated data for 5 Hz.



D) Effect of frequency on equation.

Figure 27: Fitted and interpolated data using Hyperbolic Sine (SINH) Equation.

Table II.16: Sigmoidal Equation Parameters

Parameter	Environment	1 Hz	10 Hz
B	3.5% NaCl	-7.290	-7.888
P	3.5% NaCl	-0.453	-1.493
Q	3.5% NaCl	2.920	2.242
D	3.5% NaCl	-0.516	-2.078

The following relationships were determined:

$$B = 2.3025 \log \left[\left(\frac{1}{f} \right) + 1 \right] - 8.0183 \log \left[\frac{1 - 0.1R}{0.1} \right] \quad (\text{II.47})$$

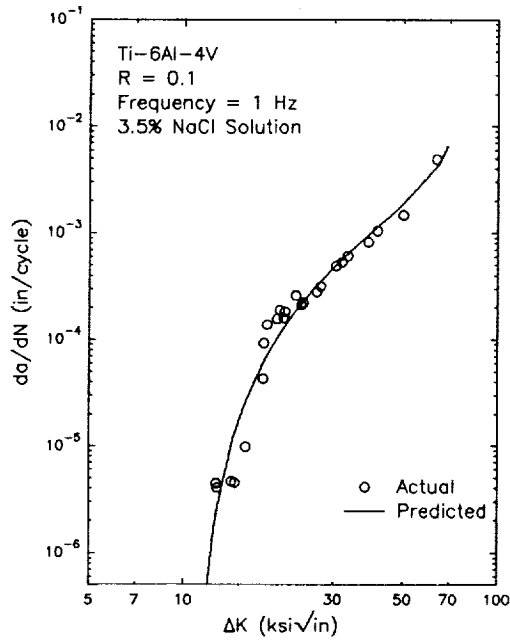
$$P = 4.0048 \log \left[\left(\frac{1}{f} \right) + 1 \right] - 1.6660 \log \left[\frac{1 - 0.1R}{0.1} \right] \quad (\text{II.48})$$

$$Q = 2.6135 \log \left[\left(\frac{1}{f} \right) + 1 \right] + 2.1430 \log \left[\frac{1 - 0.1R}{0.1} \right] \quad (\text{II.49})$$

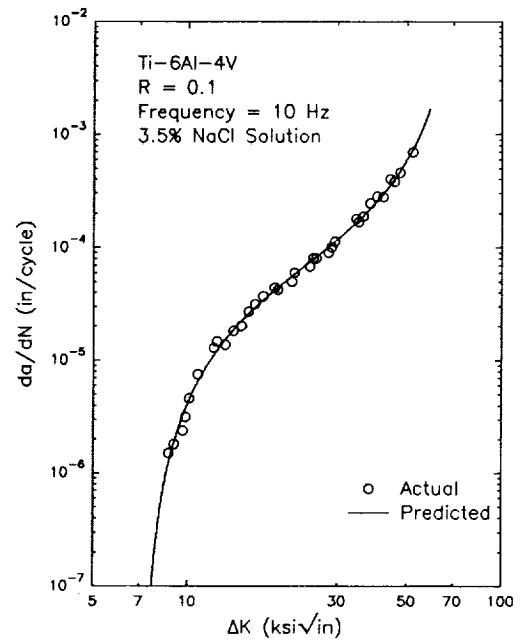
$$D = 6.0157 \log \left[\left(\frac{1}{f} \right) + 1 \right] - 2.3375 \log \left[\frac{1 - 0.1R}{0.1} \right] \quad (\text{II.50})$$

$$\Delta K_{th} = 13.648 \log \left[\left(\frac{1}{f} \right) + 1 \right] - 6.738 \log \left[\frac{1 - 0.1R}{0.1} \right] \quad (\text{II.51})$$

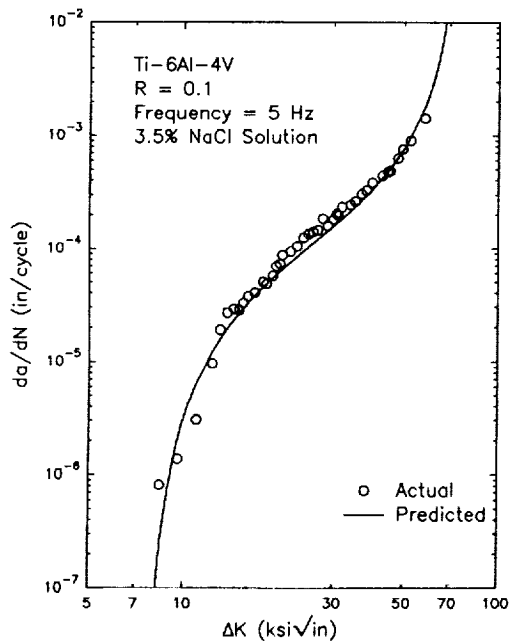
In all of the tests, the value of K_C was 83.27 ksi $\sqrt{\text{in}}$. The values of ΔK_{th} were entered as



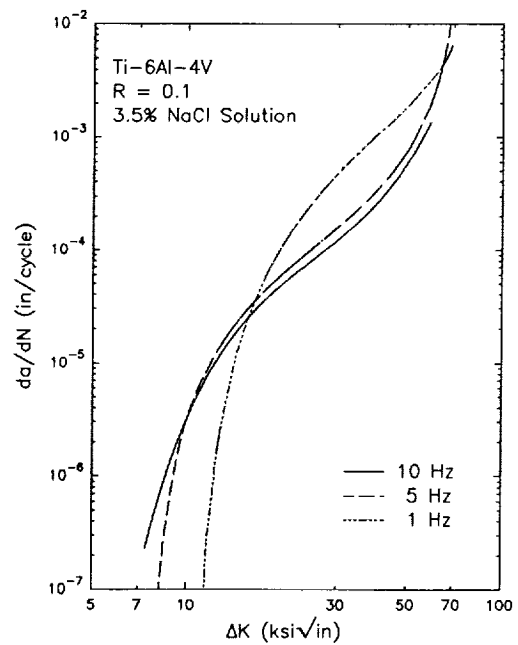
A) Fitted data for 1 Hz.



B) Fitted data for 10 Hz.



C) Interpolated data for 5 Hz.



D) Effect of frequency on equation.

Figure 28: Fitted and interpolated data using Sigmoidal Equation.

10.82 ksi $\sqrt{\text{in}}$ for 1 Hz and 7.27 ksi $\sqrt{\text{in}}$ for 10 Hz. The value of ΔK_{th} was interpolated for 5 Hz.

As seen in Figures 23-28, the actual data for Ti-6Al-4V in 3.5% NaCl solution display the frequency "crossover" effect first reported in $\alpha + \beta$ titanium alloys by Dawson and Pelloux¹⁴, and later by Dawson²⁶ and Yoder and coworkers²⁷. The "crossover" effect is a change in the ordering of da/dN values as a function of frequency at a transition ΔK value associated with the onset of "cyclic" stress corrosion cracking (SCC)¹⁴. Dawson and Pelloux called this transition level ΔK_{SCC} , a frequency dependent parameter lower than K_{ISCC} . Below the transition ΔK level, da/dN decreases with decreasing frequency due to passive film formation at the crack tip¹⁴. Above ΔK_{SCC} , da/dN is controlled by hydrogen embrittlement mechanisms, thus da/dN increases as frequency decreases and more time is allowed for hydrogen embrittlement to occur²⁷. The interpolated data also displayed this "crossover" effect.

Tests were also conducted in which the data for 1 Hz and 5 Hz were entered, and data for 10 Hz were interpolated, as well as tests where the data for 5 Hz and 10 Hz were entered, and data for 1 Hz were interpolated. Thus, three cases were analyzed:

- 1) Case 1: the frequency at which data were interpolated was lower than the frequencies for which data were entered
- 2) Case 2: the frequency at which data were interpolated was between the frequencies at which data were entered
- 3) Case 3: the frequency at which data were interpolated was higher than the frequencies at which data were entered

The best results occurred for Case 2, where the frequency at which data were interpolated is between the range of frequencies for which data were entered. This is the case for which the results were presented in this report. When the frequency at which data were interpolated was higher than the frequencies at which data were entered, the results were less accurate. When the frequency at which data were interpolated was lower than the frequencies at which data were entered, the results were least accurate based upon the coefficients of determination.

It should be noted that the ability of the model to interpolate fatigue behavior in material-environment systems where the shape of the da/dN versus ΔK curve is strongly dependent on the environment has not been determined. Instead, the curves studied followed the commonly analyzed air case in shape.

II.4: Conclusions for the Interpolative Model

One aspect of this project was to develop an interpolative model for use by NASA in analyzing and predicting the fatigue behavior of metals in corrosive environments. A stand-alone computer program based on NASA FLAGRO was developed which can be used to curve fit da/dN versus ΔK data as well as interpolate trends in fatigue behavior.

1. The regression subroutines used in the linear least squares analysis of the Paris, Forman, and Sigmoidal Equations were bench marked against the

curve fitting subroutines contained in the FLAGRO program. Both the stand alone program and the FLAGRO program generated the same results for C and n when curve fitting a data set to the Forman Equation with closure.

2. The non-linear least squares algorithm was bench marked against results published by Haritos¹⁸. Using the baseline data from Haritos¹⁸, the values for the parameters in the SINH Equation were optimized. The values for the parameters determined by the interpolative program were different than the results published by Haritos¹⁸, however, the results generated by the stand-alone program yielded a slightly better fit based upon the coefficients of determination.
3. Based on the data for Ti-6Al-4V in air and a 1% NaCl solution, the Forman Equation (with and without closure) yielded the best results when fitting C, n, p, and q, with an average coefficient of determination of 0.9817 for all data tested. The Sigmoidal Equation displayed similar accuracy, with an average coefficient of determination of 0.9811 for all data tested. The SINH Equation also fit the data with accuracy, yielding an average coefficient of determination of 0.9623. The Forman Equation (with and without closure) was least accurate when the parameters C and n were fit; the coefficient of determination was 0.8884.
4. All of the crack growth rate equations were able to interpolate trends in da/dN versus ΔK behavior when the frequency at which data were

interpolated was within the range for which data were entered. The model was not able to accurately predict data when the frequency at which data were interpolated was outside the range at which data were entered.

5. The data for Ti-6Al-4V in 3.5% NaCl solution, used to test the model, displayed the frequency "crossover" effect. The interpolated data also displayed this effect. The model accurately shows that ΔK_{th} increases as frequency decreases.
6. Future work will concentrate on improving the logarithmic assumption which relates the equation parameters to the loading characteristics. This will be done by generating corrosion fatigue data for Ti-6Al-4V (ELI) in an aqueous chloride environment. These data will then be used to improve the relationships by analyzing the effects of frequency, hold time, and stress ratio on $(da/dN)_{total}$.

Section III: Linear Superposition Model

III.1: Introduction to the Linear Superposition Method

Although there are several methods of predicting environment-enhanced fatigue crack growth in materials, the simplest is linear superposition. This method predicts crack growth by summing the effects of mechanical fatigue and stress corrosion. Wei and Landes first proposed that the effect of an aggressive environment on fatigue crack propagation in high strength steels is independent of cyclic loading. Both effects can be added to give a first-order approximation of the total environment enhanced crack growth rate³. In equation form:

$$\frac{da}{dN}_{total} = \frac{da}{dN}_{fatigue} + \frac{da}{dN}_{stress\ corrosion} \quad (III.1)$$

Since stress corrosion crack growth is measured per unit time, it must be calculated for an entire cycle of fatigue loading. If the stress corrosion crack velocity, $(da/dt)_{environment}$, can be expressed as a function of stress intensity, K , this equation can be integrated over a cycle of loading to create $(da/dN)_{stress\ corrosion}$. In equation form:

$$\frac{da}{dN}_{stress\ corrosion} = \int_{\tau} \left[\frac{da}{dt}(K) \right] [K(t)] dt \quad (III.2)$$

where τ is the period of the fatigue load cycle. In actuality, environment may only affect cracking during a portion of this time; for example during loading but not unloading. As an example, if the crack growth velocity is a constant rate for the range of stress

intensities in a fatigue load cycle:

$$\frac{da}{dt} = C \quad \text{for all } K(t) \quad (\text{III.3})$$

then crack growth per cycle is given as:

$$\frac{da}{dN_{\text{stress corrosion}}} = \int_{\tau} C dt = C \tau \quad (\text{III.4})$$

and depends only on the period of the loading cycle, τ ($\tau = 1/f$), and the constant C .

For a more complex relationship between crack growth velocity and K such as:

$$\frac{da}{dt} = C K(t)^n \quad (\text{III.5})$$

the stress corrosion crack growth per cycle depends on the period and the loading function as well as the constants C and n . As shown in Appendix E, solving Equation III.2 in conjunction with Equation III.5 with $n = 2$ and sinusoidally varying stress intensity yields:

$$\frac{da}{dN_{\text{stress corrosion}}} = C \tau \left(\frac{\Delta K^2}{8} + K_{\text{avg}}^2 \right) \quad (\text{III.6})$$

where $K_{\text{avg}} = (K_{\text{max}} + K_{\text{min}}) / 2$. Additional solutions are derived in Appendix E for square wave and ramp loading coupled with a variety of n values.

The success of this method of prediction has been confirmed for various material-environment combinations^{3,28-29}. When Wei and Landes originally proposed the linear superposition method, they supported their work with fatigue crack growth rate predictions for 18Ni (250) maraging steel in gaseous hydrogen. The fatigue component

of the prediction used data for an argon environment which was frequency independent and representative of purely mechanical fatigue damage, as seen in Figure 29. Constant load time-based crack growth rate data for 18Ni steel in dehumidified hydrogen were integrated over a cycle of loading to create the stress corrosion component added to the baseline fatigue data³.

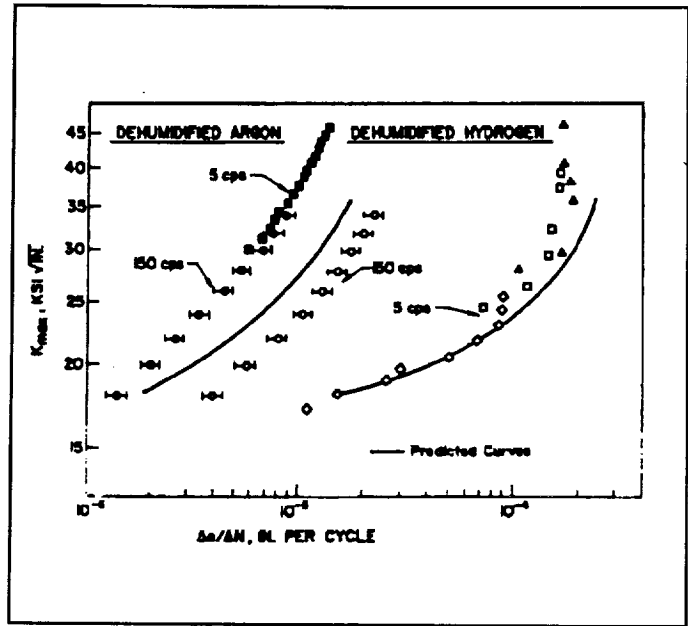


Figure 29: Measured and linear superposition predicted fatigue crack growth rates for maraging steel in H_2 . After Wei and Landes³.

The procedure reasonably predicted the absolute magnitude and frequency dependence of H_2 -enhanced fatigue crack propagation in 18Ni (250) maraging steel as shown in Figure 29.

The effects of ΔK and frequency on crack growth rates for AA 7079-T651 in saturated NaCl solution were predicted by Speidel using the method of superposition²⁸. His predictions, displayed in Figures 30 and 31, show the accuracy of the superposition model, especially at frequencies less than 1 Hz.

Harmon and coworkers²⁹ employed the linear superposition method to predict the effects of ΔK , hold time, and loading frequency on elevated temperature fatigue crack growth rates in nickel-base superalloys. This approach was added to an existing fatigue crack growth life prediction program, CRKGRO. To implement this approach, the Wei-

Landes model was used to predict fatigue crack growth in IN718 and AF115 at 1200° F. For both examples, shown in Figures 32 and 33, the effects of hold time are shown to be effectively modeled by superposition²⁹.

The preceding examples show the capability of the linear superposition method to predict fatigue crack growth rates for structural alloys in various gas and liquid environments, including elevated temperature. The superposition

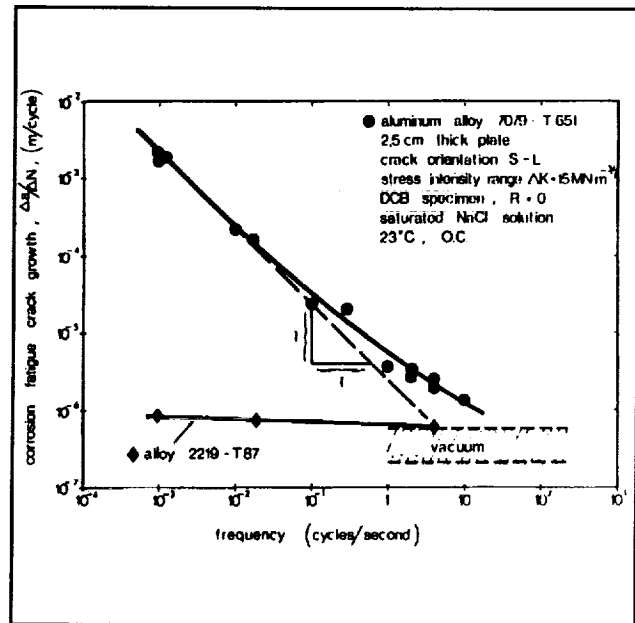


Figure 30: The measured and linear superposition predicted effect of loading frequency on NaCl enhanced da/dN_{total} for AA7079. After Speidel²⁸.

method is, however, only accurate and useful for limited cases. Specifically, the alloy must be extremely sensitive to stress corrosion cracking. The contribution of stress corrosion to crack growth must be significantly greater than that of inert environment mechanical fatigue. This condition is achieved when the loading frequency is low, the stress intensity is much higher than K_{ISCC} , and da/dt is relatively rapid. The predictions made by Speidel were for AA 7079-T651, a material which is affected strongly by environment compared to other 7xxx aluminum alloys, making it a good candidate for this model²⁸. The maraging steel is similarly sensitive to gaseous hydrogen embrittlement and nickel-based superalloys are prone to sustained load crack growth at relatively low applied K . Linear superposition is not likely to be useful for most structural alloy-

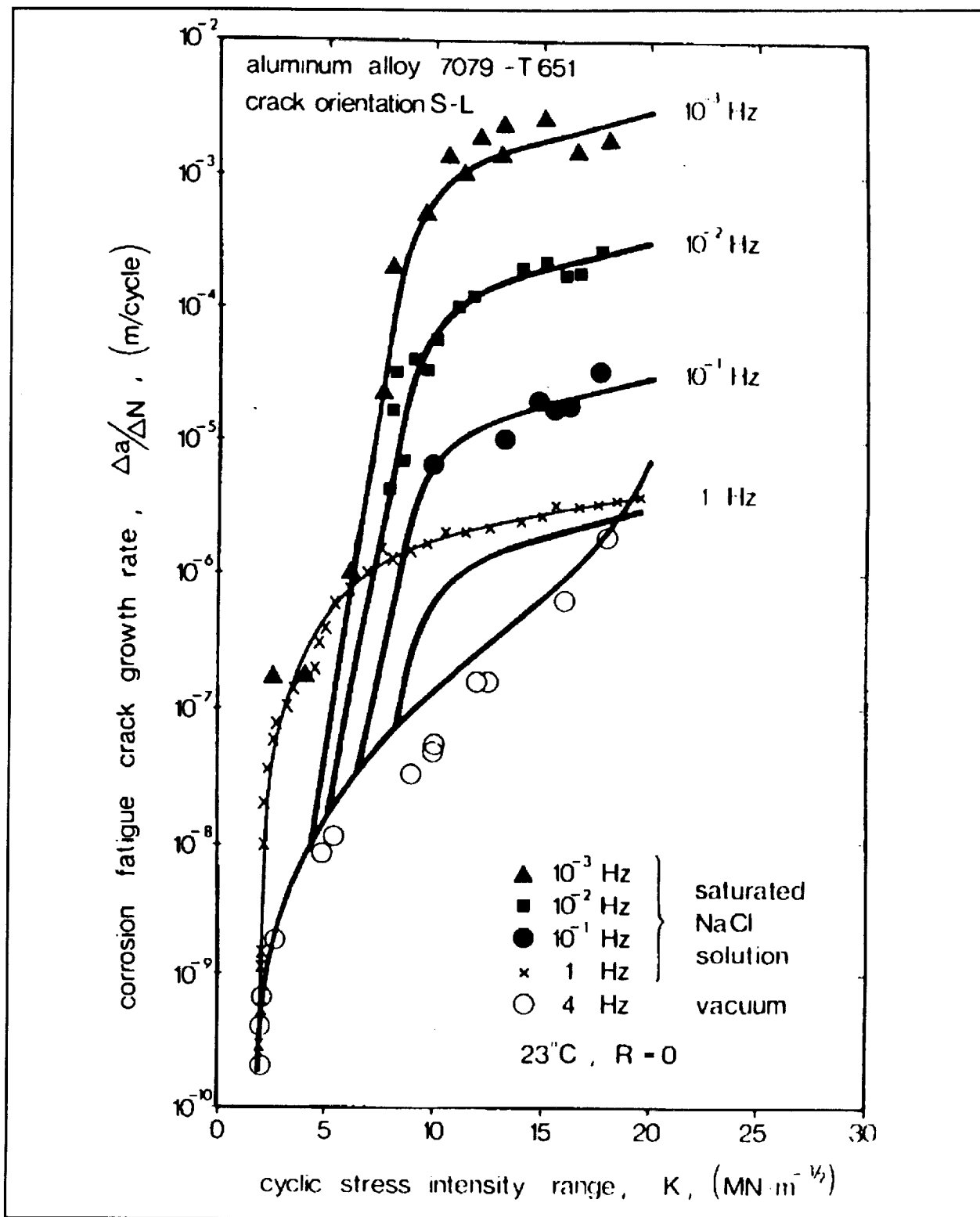


Figure 31: Linear superposition predicted (solid lines) and measured (data points) fatigue crack growth for stress corrosion cracking prone AA7079 in NaCl. After Speidel²⁸.

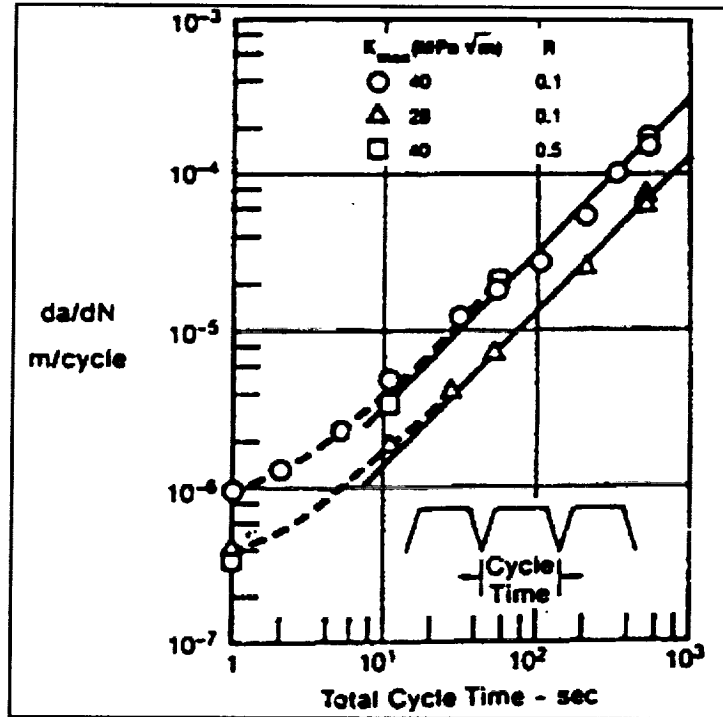


Figure 32 Application of Wei-Landes linear superposition model to fatigue crack propagation in IN718 at 1200° F with varying ΔK , R and τ . After Harmon²⁹.

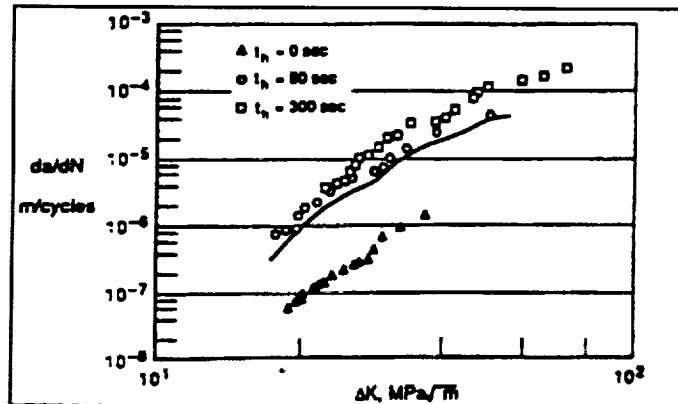


Figure 33: Application of linear superposition to predict the effect of hold time (τ) on da/dN for IN718 at 1200° F. After Harmon²⁹.

environment systems where the material is resistant to stress corrosion cracking.

III.2: Implementation of the Linear Superposition Model

The linear superposition method has been implemented in a FORTRAN program to predict corrosion fatigue crack propagation rates. The program offers the user options in determining the variables which affect crack growth rates. These options include: 1) the equations used to represent inert environment mechanical fatigue and stress corrosion crack growth rates, 2) the type of loading to which the cracked component is exposed, 3) the period of the loading cycle and the portion of this period over which environmental cracking occurs, 4) the range of output stress intensity factor ranges (ΔK), and 5) the number of output data points. With these inputs, the program predicts the total fatigue crack growth per cycle of loading for a given material-environment system. The method predicts the effects of ΔK , stress ratio (R), frequency (f), hold time (τ) and loading wave form.

Representing Crack Growth in Equation Form

The linear superposition method assumes that crack growth due to stress corrosion and inert environment mechanical fatigue are independent of one another. Both of these independent quantities are calculated over one cycle of loading and are added to give $(da/dN)_{total}$. The program allows for four different methods of

representing the crack growth rate laws.

- A) **Single Power Law** : The single power law, or Paris Equation, is the most common method of representing mechanically-based fatigue crack growth rates. This method assumes that a linear relationship exists between the logarithms of the growth rate and the stress intensity factor range. In equation form:

$$\frac{da}{dN} = A \Delta K^m \quad (\text{III.7})$$

An equation of this form can also be used for stress corrosion crack growth by interchanging da/dt for da/dN and replacing ΔK with K .

- B) **Double Power Law**: The double power law uses the same relation between stress intensity and crack growth as the single power law (Equation III.7) except the constants A and m change when the stress intensity reaches a certain level. By using two Paris Equations, the program can more accurately represent fatigue data near threshold. A two power-law approach is also useful for representing da/dt versus applied K .
- C) **Forman Equation**
- D) **Sigmoidal Equation**: To utilize either the Forman or the Sigmoidal Equations, which were discussed in the interpolative modeling section, the program must establish the equation constants for a specific material. The program allows the user the option of entering in the values of these

constants, or inputting a set of data and allowing the program to calculate the constants by linear regression analysis. When using the Forman Equation, the user is offered the option to read the constants from a library of materials that was extracted from the NASA-FLAGRO program.

For the program to function properly, the input da/dN and ΔK data must be in two columns. Whenever data are input from a file, the program assumes the first column contains the stress intensity factor range values, ΔK . The program allows the user to alter data files in three ways. An option is available to add an end of file (EOF) marker to the data. Most data files contain EOF markers when created, however this option insures that the program will not return an error while importing data from a file. The sorting option allows the user to order the data from smallest to largest stress intensity values. The conversion option allows the user to multiply each column of data by a constant factor as a method of converting units.

For any situation in which data are used to determine equation constants, the program allows the user to view a graph of the data along with the fitted equation. Each axis can either be spaced linearly or logarithmically. Points from the equation, generated in the plotting of the curve, can also be written to a file.

Representing the Load Wave Form

A wide variety of time dependent loading forms are important to components in service. For simplicity, only a few loading forms are typically employed in laboratory

characterization of corrosion fatigue. This program allows the user to choose from three different types of loading. Additional forms can be added if necessary.

- A) Sinusoidal Loading: This method of loading is a standard experimental practice, with the load constantly varying with no hold time. The stress intensity is modeled by:

$$K(t) = \frac{(K_{\max} - K_{\min})}{2} \left[\cos\left(\frac{2\pi t}{\tau} - \pi\right) + 1 \right] + K_{\min} \quad (\text{III.8})$$

where τ is the period of the load cycle. The load cycle begins at K_{\min} , the applied stress intensity increases to a maximum (K_{\max}) at $\tau/2$, then decreases to K_{\min} at the end of the period as seen in Figure 34.

- B) Ramp Loading: Ramp loading allows the user to control the percentages of the load cycle involved with increasing K from K_{\min} to K_{\max} , and with maintaining a constant K -hold period at K_{\max} . By default, the program assigns the remaining percentage to the unloading portion of the fatigue cycle, as seen in Figure 35. This function allows for no hold time, if requested, to simulate sawtooth or triangular loadings, as seen in Figure 36.
- C) Square Wave Loading: Square wave loading allows for periods of constant maximum and minimum stress intensities with negligible loading and unloading times. The program allows the user to select the percentage of the time spent at maximum stress intensity and allots the remaining time in the period to constant minimum stress intensity. A typical example is shown in Figure 37.

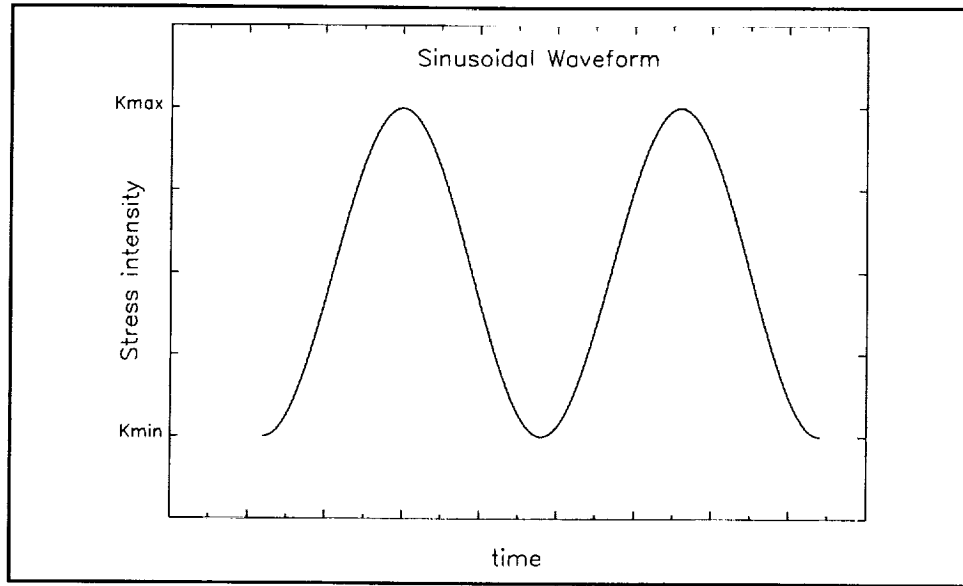


Figure 34: A typical sinusoidal loading function with respect to time.

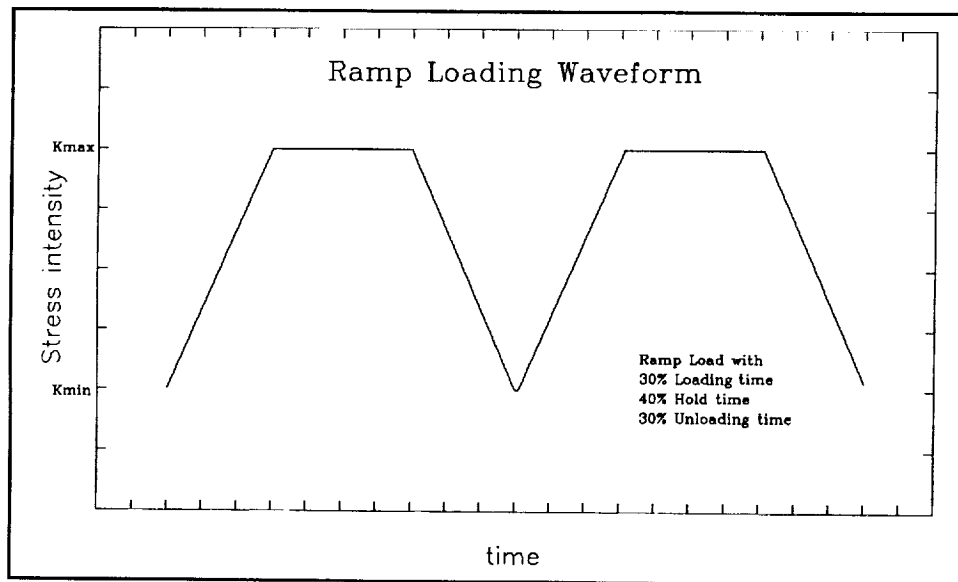


Figure 35: Ramp loading including a hold time at constant K_{max} .

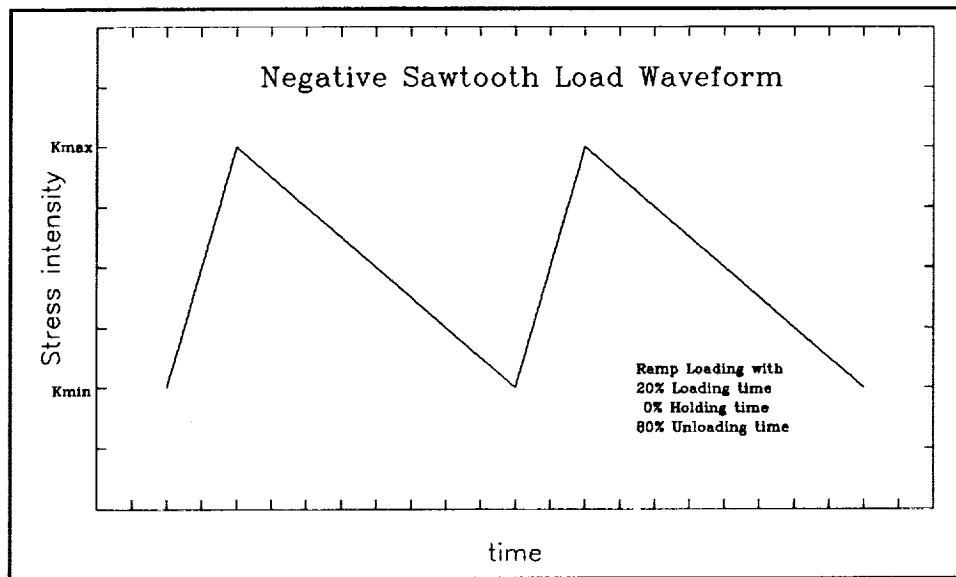


Figure 36: Ramp loading with no hold time.

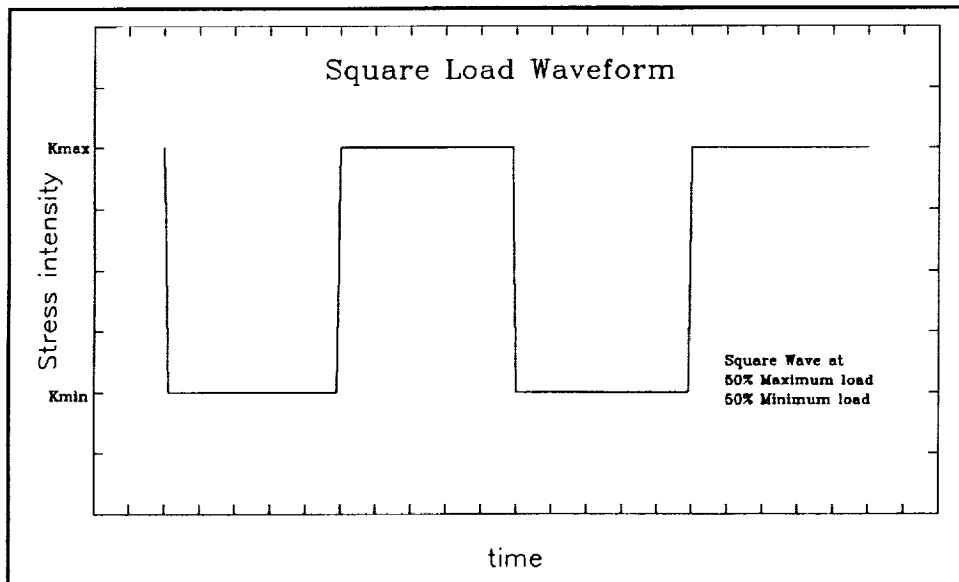


Figure 37: A typical square wave loading function.

Percent Reduction in Loading

While results are not conclusive and general for all material-environment systems, it is likely that stress corrosion cracking only contributes to the environmental da/dN during the loading and constant K hold-time portions of a load cycle³⁰. This notion is reasonable because initial unloading of a sharp crack causes a compressive stress singularity local to the tip. Environmental cracking is only operative under tensile stresses which are produced when the cycle again reverses to the loading mode. The program, therefore, allows the user to input a percent reduction on unloading crack growth. Initially, the program calculates the crack growth contribution from stress corrosion during unloading equivalent to that for loading. The input reduction is then taken into account by eliminating a percentage of the stress corrosion crack growth rate calculated for unloading.

Output Data Parameters

The program creates an output file which contains predicted corrosion fatigue, da/dN_{total} , versus ΔK values as well as additional information. The user has the following options in controlling the output data.

- A) Constant R , K_{max} , or K_{min} : The output data file contains two columns of data; the X column of stress intensity ranges, ΔK , and the corresponding Y column of corrosion fatigue crack growth rates, $(da/dN)_{total}$. Since fatigue crack growth rates are a function of the stress ratio, R , a ratio must be specified for each data point for the file to be useful. Most commonly, the

stress ratio is constant for a data set; however, if a constant K_{\max} or K_{\min} is specified, the stress ratio can be calculated for each ΔK and the input constant K_{\max} or K_{\min} .

- B) Maximum and minimum ΔK values.
- C) Number of data pairs.
- D) Spacing of ΔK values: This option allows the user, if predicting $(da/dN)_{\text{total}}$ over a large range of ΔK values, to space the ΔK data evenly on a linear or logarithmic scale.
- D) Frequency of loading: For all loading conditions, the program will ask for the frequency, f , of the loading cycle. The reciprocal of the frequency is the period, τ , therefore, the user must either know the loading frequency of interest, or know the time required to complete a cycle and take the reciprocal as the frequency.

The Calculation

Once the user has input the required parameters, the program calculates corrosion fatigue crack growth rates. For each ΔK specified by the user to be output, the program first calculates the crack growth rate due to fatigue. This is calculated using the equation chosen by the user to model fatigue. Next, the stress corrosion component is calculated by integrating the equation used to model time-based stress corrosion. For each loading condition, the integration is different. With sinusoidal loading, crack growth is integrated over the loading portion of the cycle (period = $1/2f$). The

unloading crack growth is initially equated to the loading portion, then adjusted for the input percent reduction. With ramp loading, crack growth during increased load is calculated first, followed by a calculation of crack growth due to the static load during the hold time. The unloading contribution is integrated, then adjusted for the percent reduction. For square loading, the calculation sums the stress corrosion for two different K values (K_{\max} and K_{\min}) over a period of loading. No reduction is calculated since the time period of unloading is zero. Once the crack growth rate due to stress corrosion for each portion of loading is calculated, the fatigue component is added to predict the corrosion fatigue crack propagation rate.

III.3: Data Testing and Results for the Linear Superposition Model

As shown earlier, the linear superposition method was used by Wei and Landes³, Speidel²⁸, and Harmon²⁹ to successfully predict fatigue crack growth rates in corrosive environments. To prove the capability for reliable predictions, the current program was first tested to insure that the integration method was accurate. The program was then employed for the same material-environment combinations tested by Wei and Landes³, Speidel²⁸, and Harmon²⁹ in an attempt to duplicate their results.

The effort to test the accuracy of the program focused on the numerical integration component. Since the superposition model works best when predicting crack growth rates with a majority contribution due to stress corrosion, inaccuracy in the

integration of stress corrosion over a loading cycle would cause significant errors in the final results. To test the integration, the exact solutions of hypothetical integrations were compared to program calculations. The exact solutions for all loading conditions were calculated for various models of stress corrosion crack growth. As shown in Appendix E, program results were completely accurate aside from round-off errors.

To obtain the baseline fatigue and stress corrosion models used in the original predictions, either the equation constants for one of the models or the original experimental data were required. In most cases only plots of data and modeled predictions were available from the original reports. To obtain the necessary information, graphs of data taken from the reports were digitized.

The computer program was first compared to the linear superposition calculations in the Wei and Landes paper³. The base fatigue data used were for 18Ni (250) maraging steel tested in argon. This was modeled by a two-slope Paris Equation. The stress corrosion data, also obtained from the Wei and Landes paper³, were modeled by a Sigmoidal Equation. As Figures 38 and 39 show, the program's models of the corrosion fatigue crack growth rates are consistent with the actual data, although the predictions do not coincide with the original predictions. Two differences in the calculations may explain this discrepancy. First, the program used Paris Equations to model the fatigue data and a Sigmoidal Equation to model stress corrosion kinetics. The original predictions made no transformation of data to an equation. Second, the original predictions were made by approximating the integral of stress corrosion over one cycle of loading³. Since Wei and Landes only meant for the superposition model to be a first-

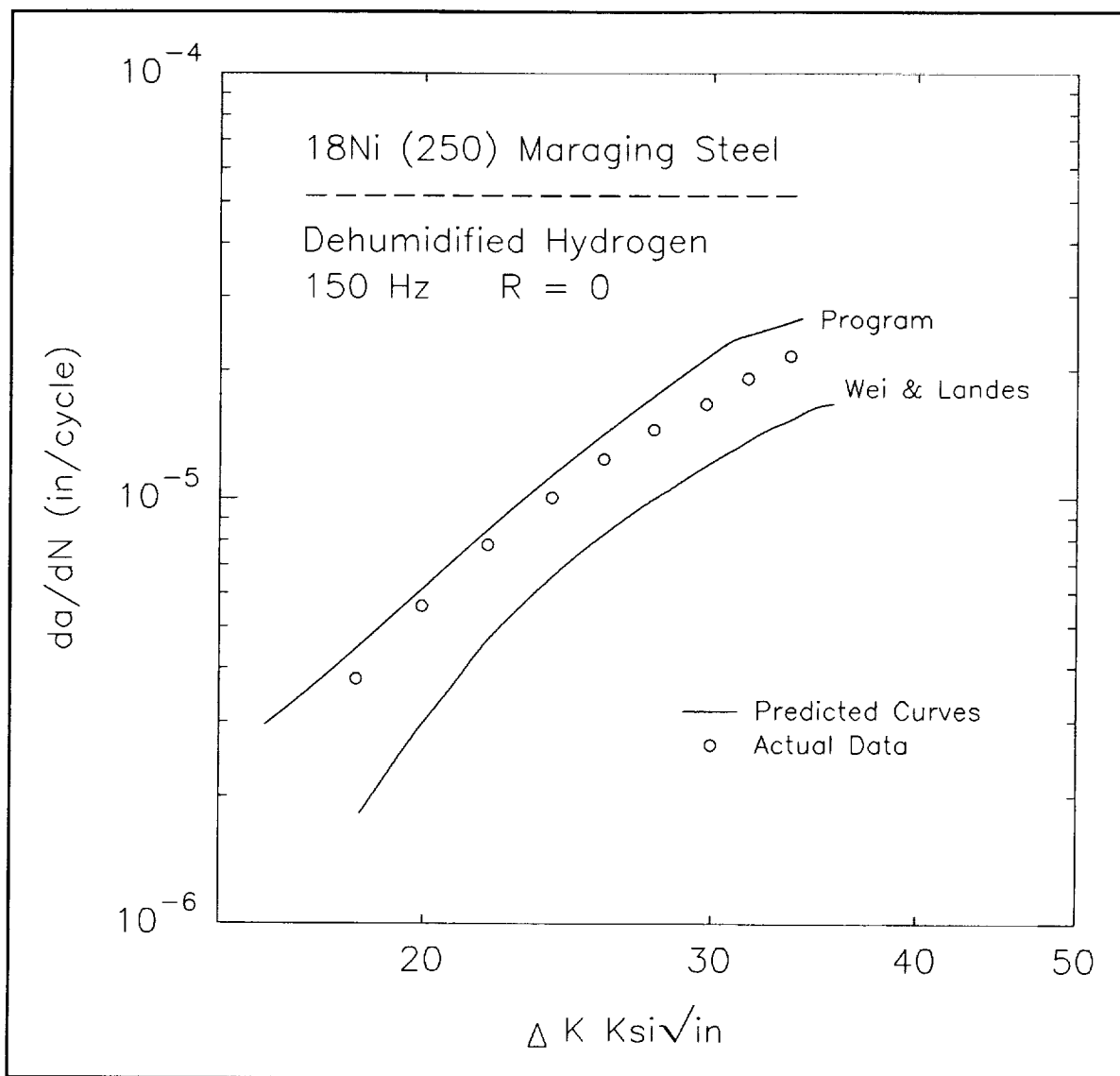


Figure 38: Linear superposition predictions, compared to measured $(da/dN)_{\text{total}}$, for 18Ni(250) maraging steel in gaseous hydrogen.

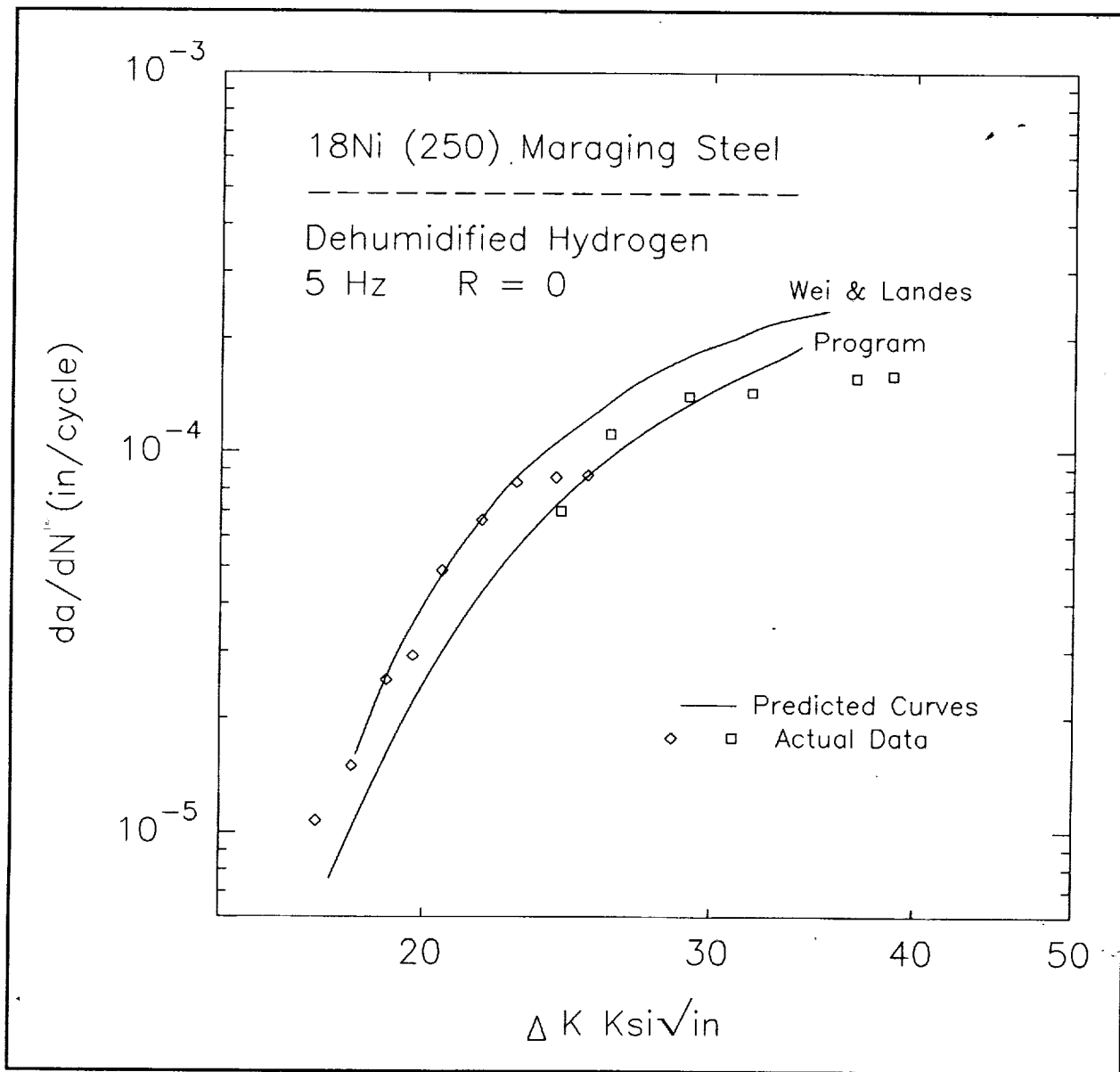


Figure 39: Linear superposition predictions, compared to measured $(da/dN)_{total}$, for 18Ni(250) maraging steel in H_2 at a lower loading frequency.

order approximation of crack growth rates, the need for precision was minimal. The current program uses Simpson's Rule to more accurately evaluate the integral.

The computer program results were then compared to predictions by Speidel, using the linear superposition model for AA7079-T651 in saturated NaCl solution, and focusing on the strong effect of loading frequency²⁸. To simulate Speidel's predictions, the stress corrosion data were approximated by a double power law. Speidel used a fatigue equation including the critical stress intensity value for unstable fracture, K_{IC} , and the threshold stress intensity range, ΔK_{th} , to model $(da/dN)_{fatigue}$. The program does not use this equation to model fatigue; however, the Forman Equation also incorporates the critical and threshold values for a material. Since the program will fit the Forman Equation to an input set of data, several points along the fatigue model Speidel used were calculated and fit to the Forman Equation. This approximation was sufficient since Speidel ignored the negligible fatigue contribution to crack growth at low frequencies²⁸.

The results from the program are comparable to those reported by Speidel as shown in Figures 40 and 41. The difference between the prediction and measured results at 1 to 10 Hz is attributed to the effect of time-cycle dependent corrosion fatigue which is not accounted for in the superposition model.

A third comparison was made to predictions published by Ashbaugh and Nicholas³¹. They observed the temperature dependence of sustained load cracking in IN718 at elevated temperature and proposed that the superposition model would work

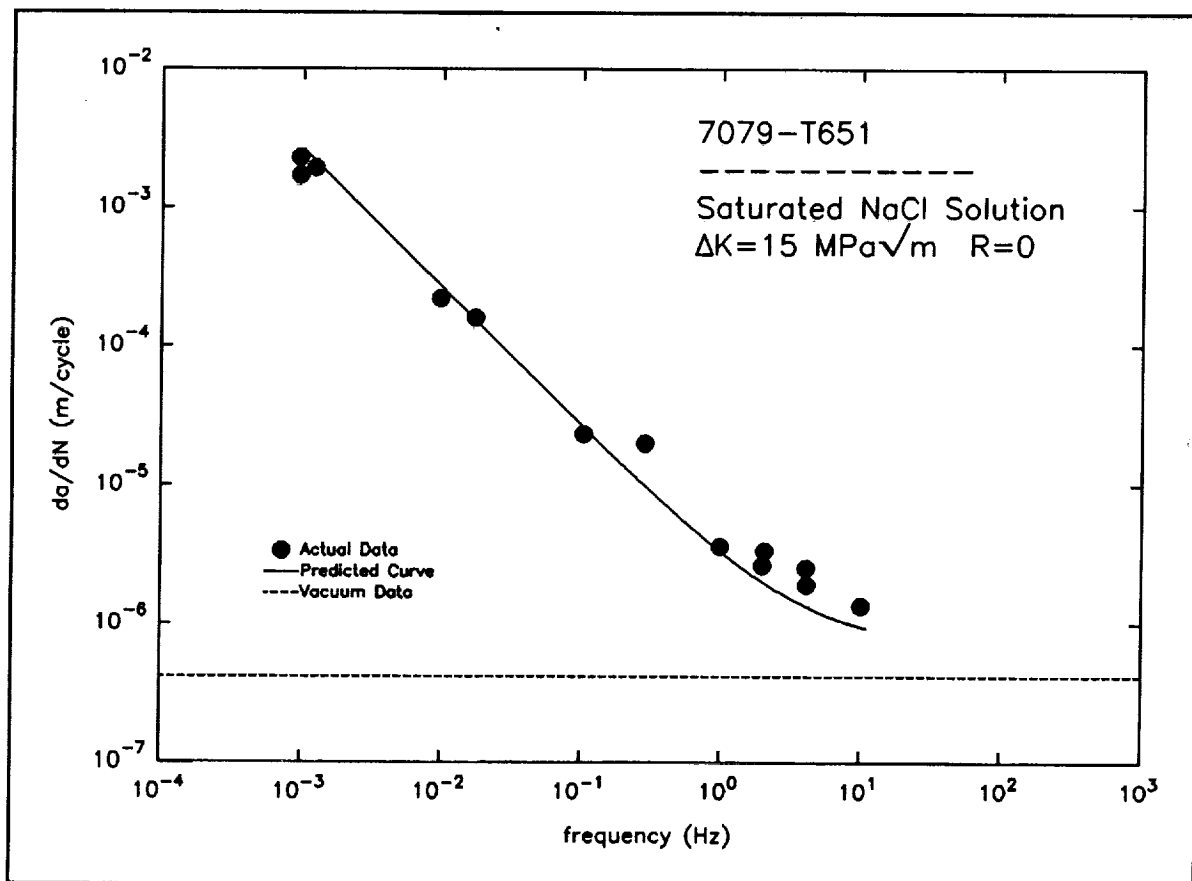


Figure 40: The loading frequency effect on the total environment-enhanced fatigue crack growth rate for AA7079 in aqueous chloride. Measurements reported by Speidel²⁸ are compared to the solid line predicted by the linear superposition model.

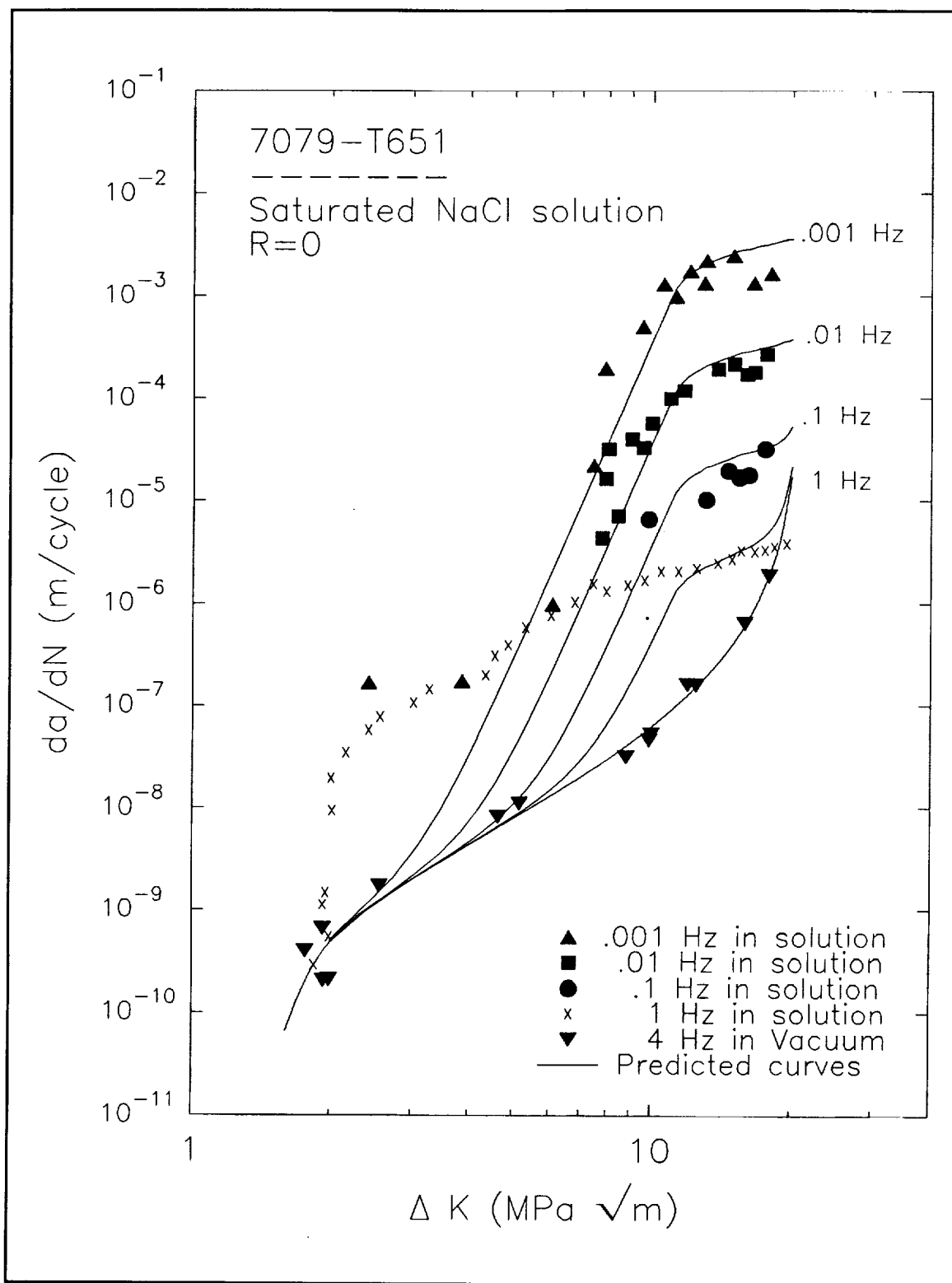


Figure 41: Linear superposition predictions of corrosion fatigue crack growth kinetics in a stress corrosion cracking susceptible aluminum alloy.

well in predicting the effect of temperature on fatigue crack growth rates. Ashbaugh and Nicholas³¹ modeled both the fatigue crack growth and stress corrosion with a Sigmoidal Equation. The predictions for FCP at two different temperatures were promising.

The program's predictions correspond well with those of Ashbaugh and Nicholas³¹, as seen in Figure 42. The loading frequency and wave form were duplicated from the experimental description. Sustained load cracking was not considered to occur during the unloading portion of the load cycle (crack growth period = $1/[2f]$). For stress ratios of 0.1 and 0.5 the predicted growth rates agreed with measured values.

III.4: Conclusions for the Linear Superposition Model

A computer program was created to predict corrosion fatigue crack propagation rates for materials in corrosive environments using the linear superposition method.

1. Although linear superposition is not accurate for all material-environment systems, this method has proven to be reliable in those limited cases where the environment has a strong effect on subcritical crack growth.
2. The program incorporates conditions which affect environmental fatigue cracking, including ΔK , R , f , τ , wave form and material fatigue and stress corrosion behavior.
3. The integration portion of the program was tested and proven to accurately

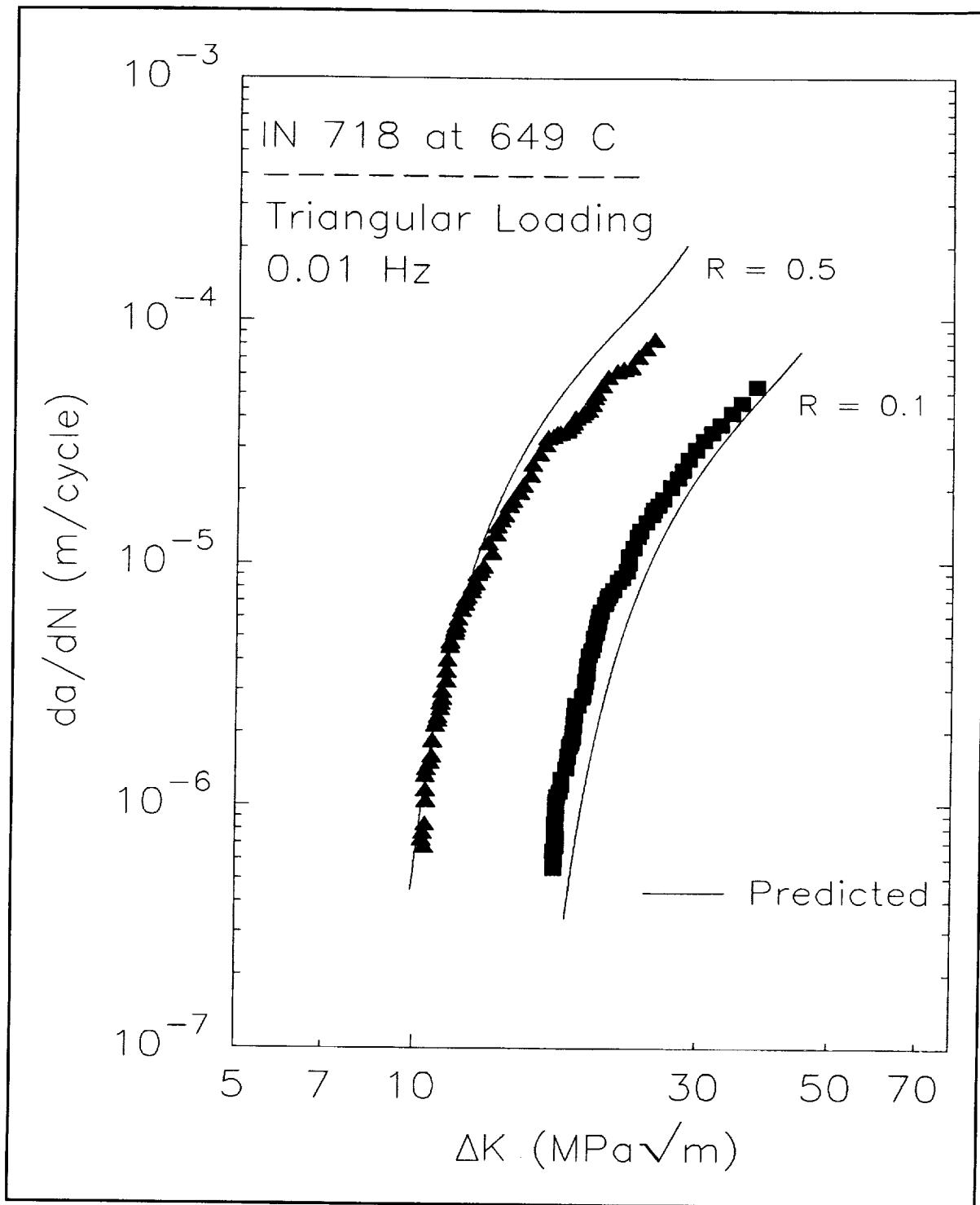


Figure 42: Linear superposition predictions of the effect of stress ratio on elevated temperature environmental fatigue cracking in IN718. Measured data were reported by Ashbaugh and Nicholas³¹.

calculate the total crack growth due to stress corrosion over a cycle of loading.

4. Comparisons to various applications of superposition verify the accuracy and capability of the current program to model experimental fatigue data.

References

1. R. W. Hertzberg Deformation and Fracture Mechanics of Engineering Materials. 3rd Ed. New York: John Wiley & Sons, Inc., 1989, pp. 517-604.
2. H. Logan. The Stress Corrosion Of Metals. New York: John Wiley and Sons, Inc., 1966.
3. R. P. Wei and J. D. Landes. "Correlation Between Sustained-Load and Fatigue Crack Growth in High-Strength Steels", Materials Research and Standards. MTRSA, Vol. 9, No. 7, 1969, pp. 25-27, 44-46.
4. J. P. Gallagher and R. P. Wei. "Corrosion Fatigue Crack Propagation in Steels", Corrosion Fatigue. O. Devereux, A. J. McEvily and R. W. Staehle, Eds., National Association of Corrosion Engineers, Houston, TX, 1972, pp. 409-423.
5. Atlas of Fatigue Curves. Howard Boyer, Ed., American Society for Metals, Metals Park, OH, 1986.
6. Aerospace Structural Metals Handbook. W. F. Brown et. al., Eds., Metals and Ceramic Information Center, Battelle Columbus Division, Columbus, OH, Vol.1, 1987.
7. Structural Alloys Handbook. J. M. Holt, H. Mindlin, and C. Y. Ho, Eds., CINDAS, Purdue University Research Foundation, West Lafayette, IN, Vol. 1-3, 1992.
8. M. O. Speidel. "Corrosion Fatigue in Fe-Ni-Cr Alloys", Stress Corrosion Cracking and Hydrogen Embrittlement of Iron Base Alloys. J. Hochmann, J. Slater and R. W. Staehle, Eds., National Association of Corrosion Engineers, Houston, TX, 1974, pp. 1071-1094.
9. "Introduction to Operating the Numonics Digitablt". University of Virginia. ACC Document No: TIB-151, Version 3, 1992.
10. "Introduction to the UNIX Operating System". University of Virginia. ACC Document No: U-002, Version 11, 1992.
11. "JOVE Text Editor on the RS/6000 or Sun Computer". University of Virginia. ACC Document No: U-003, Version 3, 1991.
12. "TCP/IP - A Primer of User Commands". University of Virginia. ACC Document

No: TIB-167, Version 5, 1992.

13. "UNIX Resource List". University of Virginia. ACC Document No: U-001, Version 4, 1992.
14. D. B. Dawson and R. M. Pelloux. "Corrosion Fatigue Crack Growth of Titanium Alloys in Aqueous Environments", Metallurgical Transactions. Vol. 5, March, 1974, pp. 723-731.
15. D. Slavik. Environmental Fatigue Crack Growth and Cracking Mechanisms in AA2090. Ph. D. dissertation, University of Virginia, Charlottesville, VA, 1993.
16. R. G. Forman et. al. NASA FLAGRO User's Manual (Version 2.0). Report No. JSC-22267, National Aeronautics and Space Administration, Lyndon B. Johnson Space Center, Houston, TX, 1992.
17. R. G. Forman et. al. NASA FLAGRO User's Manual (Version August 1986). Report No. JSC-22267A, National Aeronautics and Space Administration, Lyndon B. Johnson Space Center, Houston, TX, 1989.
18. G. Haritos, T. Nicholas, and G. O. Painter "Evaluation of Crack Growth Models for Elevated-Temperature Fatigue", Fracture Mechanics: Eighteenth Symposium, ASTM STP 945. D. T. Reed and R. P. Read, Eds., American Society for Testing and Materials, Philadelphia, PA, 1988, pp. 206-220.
19. R.H. Van Stone, O. C. Gooden and D. D. Krueger. "Advanced Cumulative Damage Modeling", Materials Laboratory, Air Force Wright Aeronautical Laboratories, Wright Patterson Air Force Base, OH, 1988, pp 10-14.
20. J. Kuester and J. Mize. Optimization Techniques with FORTRAN. New York: McGraw Hill Book Company, 1973. pp. 240-250.
21. D. M. Marquardt. "An Algorithm for Least Squares Estimation of Non-Linear Parameters", J. Soc. Indust. Appl. Math. Vol. 11, pp. 431-441, 1963.
22. T. C. Scott. ACLlib1: A Compilation of Basic Programs for Numerical Analysis. Air Conditioning Design and Development, Chrysler Corporation, Engineering and Research Office, Department 3860, 1973.
23. T. M. Ellis. Effective FORTRAN Programming. Workingham, England: Addison Wesley Publishing Company, 1990.
24. D. C. Montgomery and G. C. Runger. Applied Statistics and Probability for Engineers. New York: John Wiley and Sons, Inc., 1994, pp. 471-624.

25. R. P. Gangloff. "NASA-UVa Light Aerospace Alloy and Structures Technology Program", UVa Report No. UVA/528266/MSE94/114, March, 1994, p. 198.
26. D. B. Dawson. "Fatigue Crack Behavior of Ti-6Al-6V-2Sn in Methanol and Methanol Water Solutions", Metallurgical Transactions A. Vol 12, May, 1981, pp. 791-800.
27. G. R. Yoder, L. A Cooley, and T. W Crooker. "Effects of Microstructure and Frequency on Corrosion Fatigue Crack Growth in Ti-8Al-1Mo-1V and Ti-6Al-4V", Corrosion Fatigue: Mechanics, Metallurgy, Electrochemistry, and Engineering, ASTM STP 801. T. W Crooker and B. N. Leis, Eds., American Society for Testing and Materials, Philadelphia, PA, 1983, pp. 159-174.
28. M. O. Speidel. "Stress Corrosion and Corrosion Fatigue Crack Growth in Aluminum Alloys", Stress Corrosion Research. Hans Arup and R. N Perkins, Eds., Sijthoff & Noordhoff International Publishers, The Netherlands, 1979, pp. 117-176.
29. D. M. Harmon, C. R. Saff, and J. G. Burns. "Development of an Elevated Temperature Crack Growth Routine", AIAA paper 88-2387, American Institute of Aeronautics and Astronautics, 1988.
30. J. M. Barson and S. T. Rolfe. Fracture & Fatigue Control in Structures, 2nd Ed., New Jersey: Prentice Hall, Inc., 1987, p. 406.
31. N. E. Ashbaugh and T. Nicholas. "Fatigue Crack Growth at High Load Ratio in the Time-Dependent Regime", Fracture Mechanics: Nineteenth Symposium, ASTM STP 969. T.A. Cruse, Ed., American Society for Testing and Materials, Philadelphia, PA, 1988, pp. 800-817.

Appendix A: Data File Directory

4340 Steel

<u>File</u>	<u>R</u>	<u>Frequency (Hz)</u>	<u>Environment</u>	<u>Units</u>
T41A	0	0.1	Air	m/cyc, Pa√m
T41B	0	0.1	3.5% NaCl	m/cyc, Pa√m
T41C	0	0.1	Dist. water	m/cyc, Pa√m
T42A	0	0.001	Dist. water	m/cyc, MPa√m
T42B	0	0.01	Dist. water	m/cyc, MPa√m
T42C	0	0.1	Dist. water	m/cyc, MPa√m
T42D	0	1	Dist. water	m/cyc, MPa√m
T42E	0	4	Dist. water	m/cyc, MPa√m
T42F	0	4	Vacuum	m/cyc, MPa√m
T43A	0	0.4	Argon	m/cyc, MPa√m
T43B	0	0.4	Dist. water	m/cyc, MPa√m
T43C	0	0.2	Dist. water	m/cyc, MPa√m
T43D	0	0.04	Dist. water	m/cyc, MPa√m
T44A			3.5% NaCl	in/min, ksi√in

Ti - 6Al - 4V

<u>File</u>	<u>R</u>	<u>Frequency (Hz)</u>	<u>Environment</u>	<u>Units</u>
TT1A	0.1	10	Air	in/cyc, ksi√in
TT1B	0.1	10	3.5% NaCl	in/cyc, ksi√in
TT1C	0.1	5	3.5% NaCl	in/cyc, ksi√in
TT1D	0.1	1	3.5% NaCl	in/cyc, ksi√in
TT2A	0.5	2	3.5% NaCl	cm/cyc, ksi√in
TT2B	0.5	2	Dist. water	cm/cyc, ksi√in
TT2C	0.5	2	Argon	cm/cyc, ksi√in
TT2D			Dist. water	cm/sec, ksi√in
TT2E			3.5% NaCl	cm/sec, ksi√in
TT3A	0	4	Argon	cm/cyc, ksi√in
TT3B	0	4	Dist. water	cm/cyc, ksi√in
TT3C	0	4	3.5% NaCl	cm/cyc, ksi√in
TT4A			3.5% NaCl	cm/sec, ksi√in
TT5A	0.05	50	Argon	in/cyc, ksi√in
TT5B	0.05	50	Air	in/cyc, ksi√in
TT5C	0.05	50	Dist. water	in/cyc, ksi√in
TT5D	0.05	50	3.5% NaCl	in/cyc, ksi√in

7075 Aluminum

<u>File</u>	<u>R</u>	<u>Frequency (Hz)</u>	<u>Environment</u>	<u>Units</u>
T71A	0.1	5	Air	MPa√m, m/cycle
T71B	0.1	5	Argon	MPa√m, m/cycle
T72A	0		Air	MPa√m, mm/cycle
T72B	0.2		Air	MPa√m, mm/cycle
T72C	0.33		Air	MPa√m, mm/cycle
T72D	0.5		Air	MPa√m, mm/cycle
T72E	0.7		Air	MPa√m, mm/cycle
T72F	0.8		Air	MPa√m, mm/cycle
T73A	0.1	5	Dist. water	MPa√m, m/cycle
T73B	0.1	5	Air	MPa√m, m/cycle
T73C	0.1	5	H ₂ O vapor (67 Pa)	MPa√m, m/cycle
T73D	0.1	5	H ₂ O vapor (13 Pa)	MPa√m, m/cycle
T73E	0.1	5	H ₂ O vapor (4.7 Pa)	MPa√m, m/cycle
T73F	0.1	5	H ₂ O vapor (2.7 Pa)	MPa√m, m/cycle
T73G	0.1	5	H ₂ O vapor (2.0 Pa)	MPa√m, m/cycle

Appendix B: Procedure for Creating Data Files from Graphs

I. DIGITABLET USE

- A. Obtain a UNIX account from the ACC.
- B. In the basement of the Albert H. Small building, turn on the Numonics Digitablet. The control is located on the back side of the console used to display the digits.
- C. Reset the digitablet on the back right corner of the table top.
88888888 88888888 will appear on the console.
- D. Put the cross hair cursor over the cross hair at the bottom left corner of the menu and press MENU ORIGIN.
- E. Numerical values will now be shown on the console. Move the cursor and center the graph so that its axes are parallel to those on the digitablet (i.e. when the cursor is moved along the x-axis, a constant y value is shown on the console).
- F. Fasten the graph to the table top.
- G. If there are x and y values at the graph origin, place the cursor over the origin and press '0'. If there are no labeled x and y values at the origin, put the cross hair over the intersection of the first x and y values on each axis.
- H. Select ENGLISH or METRIC units on the menu by pressing the READ MENU key on the cursor.

- I. Record the characteristics of the graph on a reference sheet. The environment and any factors specific to the graph such as frequency, pressure, or stress ratio should be noted.
 1. Record the units on each axis.
 2. Record the x and y values at the origin (as entered by the cursor).
 3. Another reference point on each axis is needed. The highest labeled value on each axis should serve as the reference point. Improved accuracy is achieved by choosing the point as far away from the origin as possible. Record the graph value of each point.
 4. For each axis, the distance between the origin and the reference point should be recorded. The distance can be read from the digitablet console.
- J. Use the cursor and the READ MENU key to select DIGITIZING.
- K. Logon to a network computer (not the computer next to the digitablet). At the login prompt, type

"telnet" <cr> (carriage return)

Alt-A

"kelvin.seas" <cr>
- L. Enter your UNIX login ID and then your password. Type <cr> when prompted for the terminal type. Keep in mind that capital letters have different meanings than lower case letters.

- M. Turn on the computer next to the Digitablet and type
- `<cr>`
- `"connect telnet" <cr>`
- `"connect kelvin.seas" <cr>`
- N. Enter the login ID and password again.
- O. type `<cr>`
- `"export TERM" <cr>`
- P. Now invoke the Jove editor along with the name of the data file that you are about to create. Type
- `"jove Filename.DAT" <cr>`
- Q. On the digitablet, enter points by placing the cross hair over the point and pressing ENTER OUTPUT.
- R. When all points have been digitized, enter the last point with negative x and y coordinates to signal the end of the data file for the transformation program. If negative values of points need to be digitized, the final point should be less than the lowest value. The process will function without the negative number at the end of the file, but it prevents any points from being inadvertently entered before the file is closed.
- S. Save the file and exit the editor.
- Control-X S to save
- Control-X Control-C to exit Jove
- T. If another set of data points off the same graph is desired, return to step P.

If points from another graph are desired, repeat steps E through I before moving ahead to step P.

- U. Exit UNIX by typing "exit" <cr> on both terminals. If you wish to view the files that you have saved while in UNIX, type "ls" <cr>.

II. REMOVING DATA FILES FROM UNIX

A. The data files must be removed from UNIX and sent to a disk. While in UNIX, type "ls" <cr> to get a list of the files.

B. To get into the file transfer mode, type

Alt-T (initiates file transfer)

Alt-I (send internet address)

Alt-W (ask for password)

Alt-W (send password)

C. To transfer a file, type

"put" <cr>

At the local file prompt, type the UNIX "*Filename.DAT*" <cr>. At the distant filename prompt, use the drive you would like to send the file to ("*B:Filename.DAT*").

D. To transfer another file, return to step C.

E. Type "quit" <cr> to return to the UNIX operating mode.

F. Type "exit" to leave UNIX.

III. DATA FILE TRANSFORMATION

- A. The program is available in an executable form on the program disk. To run the programs, type MENU. A title screen will appear, followed by a main menu. Select the option to digitize a set of data at the prompt.
- B. Follow the instructions and enter the data that were recorded during the digitization process. The data file that was retrieved from UNIX is not erased by this program. If a mistake is made, run the program again.
- C. If the program needs to be altered due to negative values, or any other reason, follow the steps below.
 - 1. At the *F:login* prompt type "watfor77" <cr>
 - 2. Type "edit DIGITIZE.FOR" <cr> to retrieve the chosen FORTRAN program
 - 3. Use the function key F4 to go into and out of the program.
 - 4. Type "run" <cr> to start the program.
 - 5. "quit" <cr> exits FORTRAN without saving changes in the program, "exit" <cr> exits and saves the changes in the program.

Appendix C: DIGITIZE Program Listing

```
*$noex
      program DIGITIZE
*$nolist
*$include Gksdefn.for
*$list

*   Jonathan M. Pope, Materials Science Department, University of
*   Virginia, June 1993.
*
*   This program is to be used in conjunction with the Numonics
*   2400 Digitablet. The Digitablet output can be transformed
*   into digital data representative of an original graph. Any
*   graph that has been digitized can have the values of its
*   points calculated by using this program and the data
*   requested in the digitization manual. Any combination of
*   linear and logarithmic scales on the X and Y axes can be
*   handled.
*
      Real  X1(1000),X2(1000),Y1(1000),Y2(1000)
      Real  ORX,ORY,ONEX,ONEY,VX,VY
      Real  LOGR,LINEAR
      Integer  I,J,K,AX,AY
      Character*32  INPUT,OUTPUT
*
*   INPUT is the file that was retrieved through the editor when
*   using the Digitablet. OUTPUT should be named by the user.
*
      Call Screen
      print *, 'DIGITIZE Program - Jonathon Pope'
      print *, 'University of Virginia - June 1993'
      print *, 'Department of Mechanical Engineering'
      print *
      print*, 'Enter the drive and name of the source data file'
      read (*,100) INPUT
100 format (a32)
      print*
      print*, 'Enter the drive and name of the desired output file'
      read (*,100) OUTPUT
      print*
      print*, 'If the X axis has a logarithmic scale enter 1,'
      print*, 'or enter 0 for a linear scale'
```

```

read*, AX
print*
print*, 'Enter the X axis value at the origin'
read*, ORX
print*
print*, 'Enter the X axis value at the X axis reference point'
read*, VX
print*
print*, 'Enter the Digitablet console value for the distance'
print*, 'between the origin and the reference point'
read*, ONEX

```

*

AX, AY are a logical operators used to remember if the axis is logarithmic or linear. ORX, ORY are the origin values on each axis. This is the origin as defined by the digitablet, and it may be different than the graph origin. VX, VY are each an additional reference point on each axis, and ONEX, ONEY are the distances from the origin to the reference point. These distances are in centimeters, simply to be consistent with the manual, and are easily read from the console.

*

```

print*
print*
print*
print*, 'If the Y axis has a log scale enter 1,'
print*, 'or enter 0 for a linear scale'
read*, AY
print*
print*, 'Enter the Y axis value at the origin'
read*, ORY
print*
print*, 'Enter the Y axis value at the Y axis reference point'
read*, VY
print*
print*, 'Enter the Digitablet console value for the distance'
print*, 'between the origin and the reference point'
read*, ONEY
open (1,file=INPUT)
open (2,file=OUTPUT)
I=1
X1(1)=.001

```

*

The manual calls for the last point to be entered as a negative value off the graph. It is not necessary for the

```

*      program to function properly, but it is helpful if the file
*      needs to be investigated for errors. In the event that
*      negative valued points are part of the data file, the
*      parameter in the 'while' statement below should be changed
*      to a smaller number.
*
      while (X1(I).ge.-1.0) do
        I=I+1
        read (1,*,end=400) X1(I), Y1(I)
      end while
400 close (1)
*
*      The mathematical functions needed to correct the data
*      for each axis are activated in the statements below.
*
      J=I-1
      do 200 I=2,J
        if (AX.eq.1) then
          X2(I) = LOGR (X1(I),ORX,ONEX,VX)
        else
          X2(I) = LINEAR (X1(I),ORX,ONEX,VX)
        end if
        if (AY.eq.1) then
          Y2(I) = LOGR (Y1(I),ORY,ONEY,VY)
        else
          Y2(I) = LINEAR (Y1(I),ORY,ONEY,VY)
        end if
      200 continue
*
*      The transformed data is written into the output file.
*
      N = J - 1
      Call Sort (X2,Y2,N)
      do 300 K=2,J
        write (2,310) X2(K),Y2(K)
310    format(G12.4,3X,G12.4)
      300 continue

      stop
      end
*
*      *****
*      This function corrects the digitablet values for axes
*      with logarithmic scales.

```

```
* *****
*
```

```
real function LOGR(Z,OR,ONE,V)
real Z,OR,ONE,V
```

```
LOGR = OR*((V/OR)**(Z/ONE))
```

```
return
end
```

```
*
* *****
* This function corrects the digitablet values for axes
* with linear scales.
* *****
*
```

```
real function LINEAR(Z,OR,ONE,V)
real Z,OR,ONE,V
```

```
LINEAR = OR + (V-OR) * Z/ONE
```

```
return
end
```

```
Subroutine Sort (X,Y,N)
```

```
*
* This subroutine sorts the Delta K and da/dN arrays so that the Delta
* K values are placed in ascending order.
*
```

```
Real X(N),Y(N),First,Tempx,Tempy
```

```
Integer I,Index,J
```

```
Do 30 I = 2,(N-1)
```

```
First = X(I)
```

```
Index = I
```

```
Do 40 J = I+1,N
```

```
If (X(J) .lt. First) then
```

```
First = X(J)
```

```
Index = J
```

```
Endif
```

```
40 continue
```

```
If (Index .ne. I) then
```

```
Tempx = X(I)
```

```
X(I) = X(Index)
```

```
X(Index) = Tempx
```

```

        Tempy = Y(I)
        Y(I) = Y(Index)
        Y(Index) = Tempy
    Endif
30 Continue
End

```

```

* -----

Subroutine Screen
*
*   This subroutine clears the screen, and paints the screen blue.
*
    Call Init(0)
    Call Clearscreen
    Call Paint(0.0,0.0,0)
    Call Gscr(1,0,0.0,0.0,0.5)
    Return
End

*$include Gkscover.for

```

Appendix D: Examples for the Interpolative Model

Example 1: Data have been collected for 2090 aluminum in a vacuum environment. The data are to be fit to the Forman Equation with closure, fitting only the parameters C and n . The constant loading variable is K_{max} , which has a value of $537.6 \text{ MPa}\sqrt{\text{mm}}$. The frequency of the load is 5 Hz, and the K_{max} hold time is 0 seconds. The values of K_C and ΔK_{th} are to be optimized, and the values for the material properties are to be loaded from a NASA defined material file. The value of p is to be 0.5, and q is to be entered as 1.00

Note: > indicates keyed input

Interpolative Model Options

-
- 1) Determine Equation Constants,
Interpolate Data
- 2) Prepare Data File
- 3) Quit Program

Please select an option

>1

Enter type of units:

- 1) U.S. Customary Units (inches, ksi, $\text{ksi}\sqrt{\text{in}}$)
- 2) SI Units (mm, MPa, $\text{MPa}\sqrt{\text{mm}}$)

>2

Enter option for Material:

- 1) Manual input
- 2) Input from NASA/FLAGRO Materials File
- 3) Examine data on NASA/FLAGRO Materials File
- 4) Input from User Defined Materials File (UDMF)
- 5) Examine data on User Defined Materials File
- 0) Terminate materials entry

>2

Enter one of the codes in brackets []
to display alloy types.....or 0 to exit

NASA/FLAGRO Materials File

Ferrous Alloys(>=50% Fe)

Iron (alloy or cast)
ASTM Spec. Grade Steel
AISI Steel
Misc. U.S. Spsc. Grade Steel
Trade/Common Name Steel
AISI Type Stainless Steel
Misc Cres/Heat Resistant Steel
High Temperature Steel
Tool Steel

[A]
[B]
[C]
[D]
[E]
[F]
[G]
[H]
[J]

Non-ferrous Alloys

1000-9000 Series Aluminum [M]
Cast and Misc. Aluminum [O]
Titanium Alloys [P]
Nickel Alloys/Superalloys [Q]
Misc. Superalloys [R]
Copper/Bronze Alloys [S]
Magnesium Alloys [T]
Misc. Non-ferrous [U]

Note: Unless specified properties are for
1. Welds not heat treated.
2. 75 deg F Air Environment.
3. Any Crack Orientation except S-T & S-L.

>M

Enter ID Number in brackets to choose a Material Type
or X to return to main material menu.

2000 series	[2]
5000 series	[5]
6000 series	[6]
7000 series	[7]

>2

Enter Code in brackets to choose alloy & HT/Condition.

2014-T6 Al	[AD]	2024-T852 Al	[EK]
2014-T651 Al	[AF]	2024-T861 Al	[EL]
2020-T651 Al	[CB]	2048-T851 Al	[FC]
2024-T3 Al	[EA]	2124-T851 Al	[GC]
2024-T351 Al	[EB]	2219-T62 Al	[IA]
2024-T3511 Al	[EC]	2219-T851 Al	[IC]
2024-T62 Al	[EG]	2219-T87 Al	[IF]
2024-T81 Al	[EI]	2324-T39 Al	[JA]
2024-T851 Al	[EJ]	2090-T8E41 Al-Li	[PA]

>PA

M2PA 2090-T8E41 Al-Li

Enter one of the codes in brackets []
to choose product form, crack orien. & temperature

[1] M2PA11AB1 Plt & sht; L-T

>1

Searching...

Please enter thickness of part (in millimeters) :

>10.0

Material Properties:

:Matl:	UTS :	YS :	K1e :	K1c :	Ak :	Bk :	Thk :	Kc :
: No.:	:	:	:	:	:	:	:	:
:	:	:	:	:	:	:	:	:
: 1 :	586.1:	551.6:	1598.4:	1146.7:	1.00:	1.00:	10.000:	1633.6:

Which equation would you like to use to curvefit data :

- 1) Forman Equation (with closure)
- 2) Forman Equation (without closure)
- 3) Paris Equation
- 4) Hyperbolic Sine Equation (SINH)
- 5) Sigmoidal Equation

>1

Would you like to enter the Forman Equation Constants :

- 1) By file
- 2) Manually

>1

:Matl :	Crack Growth Eqn Constants (closure)								:
: No. :	C	n	p	q	DKo	Rcl	Alpha	Smax/	:
:	:	:	:	:	:	:	:	SIGo	:
:	:	:	:	:	:	:	:	:	:
: 1 :	0.114D-11:	3.267 :	0.50 :	1.00 :	4.0 :	0.70 :	1.50 :	0.3 :	:

The following values were determined for Newman's constants :

A0 = 0.3958
A1 = 0.9255E-01
A2 = 0.6274
A3 = -0.1158

Would you like to use :

- 1) Newman Closure (explicit form of Forman Equation)
- 2) de Koning/Henriksen equation (Forman variant)

>2

Please enter the number of data sets :
>1

Please pick one of the following for the data sets:

- 1) Constant Stress Ratio
 - 2) Varying Stress Ratio - Constant Kmax
 - 3) Varying Stress Ratio - Constant Kmin
- >2

Load Characteristics for Data Set 1

Please enter the frequency of the applied load (in Hertz) :
>5

Please enter the hold time of the applied load (in seconds) :
>0

Would you like to :

- 1) Optimize the parameters for Data Set 1
 - 2) Enter the parameters for Data Set 1
- >1

Determination of Crack Growth Constants

Press: 1 to enter data from a file,
2 to enter data by hand.
>1

Enter complete file name (maximum of 48 characters)
>2090TEST.DAT

Name of data file = 2090TEST.DAT

Press <return> (or C and <return> to change)
>RTN

Data exists for Kmax = 537.6

Press <return> to continue, or C to review and/or edit data.
>RTN

Save current data on disk? (Y or N)

Note : New data must be saved now to be used over again.
>N

Curvefit option for Data Set : 1

$$\frac{da}{dN} = \frac{C (DK_{eff})^n (1 - DK_{th}/DK)^p}{q}$$

$$[1 - DK/\{(1 - R)K_{cr}\}]$$

where $DK_{eff} = (1 - S_o/S_{max})/(1 - R)$
 $DK_{th} = DK_o (4/PI) \arctan(1 - R)$
 $R = K_{min} / K_{max}$
 S_o & S_{max} are crack opening & max stresses
 DK_o is the fatigue threshold at $R=0$

Would you like to curvefit C :
 >Y

Curvefit option for Data Set : 1

$$da/dN = C (DK_{eff})^n (1 - DK_{th}/DK)^p$$

$$[1 - DK/\{(1 - R)K_{cr}\}]^q$$

where $DK_{eff} = (1 - S_o/S_{max})/(1 - R)$
 $DK_{th} = DK_o (4/PI) \arctan(1 - R)$
 $R = K_{min} / K_{max}$
 S_o & S_{max} are crack opening & max stresses
 DK_o is the fatigue threshold at $R=0$

Would you like to curvefit n :
 >Y

Curvefit option for Data Set : 1

$$da/dN = C (DK_{eff})^n (1 - DK_{th}/DK)^p$$

$$[1 - DK/\{(1 - R)K_{cr}\}]^q$$

where $DK_{eff} = (1 - S_o/S_{max})/(1 - R)$
 $DK_{th} = DK_o (4/PI) \arctan(1 - R)$
 $R = K_{min} / K_{max}$
 S_o & S_{max} are crack opening & max stresses
 DK_o is the fatigue threshold at $R=0$

Would you like to curvefit p :
 >N

Curvefit option for Data Set : 1

$$da/dN = C (DK_{eff})^n (1 - DK_{th}/DK)^p$$

$$q$$

$$[1 - DK/\{(1 - R)K_{cr}\}]$$

where $DK_{eff} = (1 - S_o/S_{max})/(1 - R)$
 $DK_{th} = DK_o (4/\pi) \arctan(1 - R)$
 $R = K_{min} / K_{max}$
 S_o & S_{max} are crack opening & max stresses
 DK_o is the fatigue threshold at $R=0$

Would you like to curvefit q :
 >N

Would you like to :
 1) Calculate K_c using NASA Equation
 2) Optimize K_c using Cubic Approximation
 3) Enter K_c Manually
 >2

Optimum $K_c = 0.3297E+09$

p = 0.5000

Press <return> (or C and <return> to change)
 >RTN

q = 1.000

Press <return> (or C and <return> to change)
 >RTN

Enter 1) Enter ΔK_{th} manually,
 2) Calculate ΔK_{th} from DK_o
 3) Optimize ΔK_{th} using Cubic Approximation
 >3

Optimum $\Delta K_{th} = 40.65$

Press <return> to continue
 >RTN

Alpha = 1.50

Press <return> (or C and <return> to change)
 >RTN

$S_{max}/S_{IGo} = 0.30$

Press <return> (or C and <return> to change)
 >RTN

What confidence interval would you like on the coefficients:

- | | |
|----------|----------|
| 1) 99.9% | 6) 90.0% |
| 2) 99.8% | 7) 80.0% |
| 3) 99.5% | 8) 50.0% |
| 4) 99.0% | 9) 20.0% |
| 5) 95.0% | |

Please enter selection.
>6

Computation of Grack Rate Constants

S.I. units [mm, MPa, MPa√mm]
(Crack Closure Considered - Forman Equation)

K_{1c} = 33.00 Ak = 1.000 BK = 1.000
YS = 80.00
Thick = 0.2500

K_c = 0.3297E+09

D_{Ko} = 56.50

S_{max}/S_{IGo} = 0.3000 Alpha = 1.500

Press <return> to continue

>RTN

K_{max} = 537.6

da/dN	:	Delta K

0.2046E-06	:	122.8
0.4104E-06	:	126.1
0.5594E-06	:	129.4
0.1004E-05	:	131.8
0.8274E-06	:	134.4
0.6022E-06	:	137.8
0.6901E-06	:	142.0
0.8955E-06	:	146.1
0.9990E-06	:	151.8
0.2045E-05	:	156.5
0.2255E-05	:	161.9
0.3255E-05	:	168.4
0.2914E-05	:	174.3
0.4019E-05	:	180.5

Press <return> to continue

>RTN

da/dN	:	Delta K
0.4190E-05	:	187.1
0.4424E-05	:	195.2
0.6237E-05	:	201.4
0.8037E-05	:	207.8
0.1171E-04	:	215.2
0.1286E-04	:	222.5
0.1535E-04	:	229.7
0.1613E-04	:	237.6
0.1899E-04	:	244.8
0.2199E-04	:	252.8
0.2506E-04	:	260.6
0.3016E-04	:	267.6
0.2826E-04	:	275.1
0.3398E-04	:	282.0
0.4509E-04	:	290.0
0.5364E-04	:	303.8

Press <return> to continue

>RTN

Growth Rate Constants:

C = 0.2962E-19
n = 6.406
* p = 0.5000
* q = 1.000

* indicates a value input by the user

Press <return> to continue

>RTN

90% Confidence Intervals:

$0.6839\text{e-}20 \leq C \leq 0.1283\text{e-}18$
 $6.120 \leq n \leq 6.692$

Would you like to store the results on a disk :

>N

The data have successfully been fit to the Forman Equation. The coefficient C in the equation has been fit to an equation of the form:

$C = A \cdot \log((1/f) + 1)$

where:

f = frequency of applied load

The following values for the coefficients were determined :

A = 0.37412839471948E-18

Please press <return> to continue

>RTN

The data have successfully been fit to the Forman Equation. The coefficient n in the equation has been fit to an equation of the form:

$$n = A * \log ((1/f) + 1)$$

where:

f = frequency of applied load

The following values for the coefficients were determined :

A = 80.899106556360

Please press <return> to continue

>RTN

The data have successfully been fit to the Forman Equation. The parameter ΔK_{th} in the equation has been fit to an equation of the form:

$$\Delta K_{th} = A * \log ((1/f) + 1)$$

where:

f = frequency of applied load

The following values for the coefficients were determined :

A = 513.38527054904

Please press <return> to continue

>RTN

Comparison of Actual and Predicted Values

ΔK	da/dN(act)	da/dN(pred)	% Error
122.80	0.2046000E-06	0.3674280E-06	79.8
126.10	0.4104000E-06	0.4321204E-06	5.29
129.40	0.5594000E-06	0.5057272E-06	9.59
131.80	0.1004000E-05	0.5653662E-06	43.69
134.40	0.8274000E-06	0.6362456E-06	23.10
137.80	0.6022000E-06	0.7395572E-06	22.81

142.00	0.6901000E-06	0.8853623E-06	28.29
146.10	0.8955000E-06	0.1049106E-05	17.15
151.80	0.9990000E-06	0.1316127E-05	31.74
156.50	0.2045000E-05	0.1574851E-05	22.99
161.90	0.2255000E-05	0.1920417E-05	14.84
168.40	0.3255000E-05	0.2413308E-05	25.86
174.30	0.2914000E-05	0.2942523E-05	0.98
180.50	0.4019000E-05	0.3592812E-05	10.60
187.10	0.4190000E-05	0.4403338E-05	5.09

Please press <return> to continue

>RTN

Comparison of Actual and Predicted Values

ΔK	da/dN(act)	da/dN(pred)	% Error
195.20	0.4424000E-05	0.5584996E-05	26.24
201.40	0.6237000E-05	0.6644315E-05	6.53
207.80	0.8037000E-05	0.7893201E-05	1.79
215.20	0.1171000E-04	0.9552245E-05	18.43
222.50	0.1286000E-04	0.1143533E-04	11.08
229.70	0.1535000E-04	0.1355320E-04	11.71
237.60	0.1613000E-04	0.1619892E-04	0.43
244.80	0.1899000E-04	0.1892519E-04	0.34
252.80	0.2199000E-04	0.2233087E-04	1.55
260.60	0.2506000E-04	0.2605626E-04	3.98
267.60	0.3016000E-04	0.2975805E-04	1.33
275.10	0.2826000E-04	0.3411763E-04	20.73
282.00	0.3398000E-04	0.3850124E-04	13.31
290.00	0.4509000E-04	0.4404544E-04	2.32
303.80	0.5364000E-04	0.5481080E-04	2.18

Please press <return> to continue

>RTN

Data Set	Coefficient of Determination
1	0.9880

>RTN

Would you like to interpolate data using the determined coefficients :

>N

Interpolative Model Options

1) Determine Equation Constants

Interpolate Data

- 2) Prepare Data File
- 3) Quit Program

Please select an option

>3

Example 2: Data have been collected for Ti-6Al-4V in an air environment. The data are to be fit to the Forman Equation without closure, fitting the parameters C , n , p , and q . The parameter m is to have a value of 1.0. The constant loading variable is the stress ratio, which has a value of 0.1. The frequency of the load is 10 Hz, and the K_{max} hold time is 0 seconds. The value of ΔK_{th} is to be 7.27 ksi $\sqrt{\text{in}}$, and the values for the material properties are to be loaded manually, including the value for K_C of 83.27 ksi $\sqrt{\text{in}}$.

Note: > indicates keyed input

Interpolative Model Options

-
- 1) Determine Equation Constants, Interpolate Data
 - 2) Prepare Data File
 - 3) Quit Program

Please select an option

>1

Enter type of units:

- 1) U.S. Customary Units (inches, ksi, ksi $\sqrt{\text{in}}$)
- 2) SI Units (mm, MPa, MPa $\sqrt{\text{mm}}$)

>1

Enter option for Material:

- 1) Manual input
- 2) Input from NASA/FLAGro Materials File
- 3) Examine data on NASA/FLAGro Materials File
- 4) Input from User Defined Materials File (UDMF)
- 5) Examine data on User Defined Materials File
- 0) Terminate materials entry

>1

Enter Yield Strength:
>146.0

Yield Strength = 146.00

Enter Plane strain fracture toughness, K1c:
>50.0

K1c = 50.00

Enter Ak, Bk:
>1.0,0.5

Ak = 1.00 Bk = 0.50

Please enter thickness (in inches):
>0.25

Material Properties:

:Matl:	YS	:	K1c	:	Ak	:	Bk	:	Kc	:
: No.:		:		:		:		:		:
:-----:										
: 1 :	146.0:		50.0:		1.00:		0.50:		62.1:	

Which equation would you like to use to curvefit data :

- 1) Forman Equation (with closure)
- 2) Forman Equation (without closure)
- 3) Paris Equation
- 4) Hyperbolic Sine Equation (SINH)
- 5) Sigmoidal Equation

>2

$$\frac{da}{dN} = C (1 - R)^m DK^n (1 - \frac{DK_{th}}{DK})^p$$

$$(1 - R - \frac{DK}{K_{cr}})^q$$

where: DKth = DKo * (4/PI) * Arctan(1 - R)
R = K min / K max
DKo : fatigue threshold @ R=0

Enter DKo :
>3.5

DKo = 3.50

Please enter the number of data sets :
>1

Please pick one of the following for the data sets:

- 1) Constant Stress Ratio
- 2) Varying Stress Ratio - Constant Kmax
- 3) Varying Stress Ratio - Constant Kmin

>1

Load Characteristics for Data Set 1

Please enter the frequency of the applied load (in Hertz) :

>10

Please enter the hold time of the applied load (in seconds) :

>0

Would you like to :

- 1) Optimize the parameters for Data Set 1
- 2) Enter the parameters for Data Set 1

>1

Determination of Crack Growth Constants

Press: 1 to enter data from a file,
2 to enter data by hand.

>1

Enter complete file name (maximum of 48 characters)

>TT1B.DAT

Name of data file = TT1B.DAT

Press <return> (or C and <return> to change)

>RTN

Data exists for R = 0.1000

Press <return> to continue, or C to review and/or edit data.

>RTN

Save current data on disk? (Y or N)

Note : New data must be saved now to be used over again.

>N

Curvefit option for Data Set : 1

$$\frac{da}{dN} = C (1 - R)^m DK^n (1 - DK_{th}/DK)^p$$

$$(1 - R - DK/K_{cr})^q$$

where: $DK_{th} = DK_o * (4/PI) * \text{Arctan}(1 - R)$

R = K min / K max
 DKo : fatigue threshold @ R=0

Would you like to curvefit C :
 >Y

Curvefit option for Data Set : 1

$$\frac{da}{dN} = C (1 - R)^m DK^n (1 - DKth/DK)^p$$

$$(1 - R - DK/Kcr)^q$$

where: DKth = DKo * (4/PI) * Arctan(1 - R)
 R = K min / K max
 DKo : fatigue threshold @ R=0

Would you like to curvefit n :
 >Y

Curvefit option for Data Set : 1

$$\frac{da}{dN} = C (1 - R)^m DK^n (1 - DKth/DK)^p$$

$$(1 - R - DK/Kcr)^q$$

where: DKth = DKo * (4/PI) * Arctan(1 - R)
 R = K min / K max
 DKo : fatigue threshold @ R=0

Would you like to curvefit p :
 >Y

Curvefit option for Data Set : 1

$$\frac{da}{dN} = C (1 - R)^m DK^n (1 - DKth/DK)^p$$

$$(1 - R - DK/Kcr)^q$$

where: DKth = DKo * (4/PI) * Arctan(1 - R)
 R = K min / K max
 DKo : fatigue threshold @ R=0

Would you like to curvefit q :
>Y

Curvefit option for Data Set : 1

$$da/dN = C (1 - R)^m DK^n (1 - DKth/DK)^p \frac{1}{(1 - R - DK/Kcr)^q}$$

where: DKth = DKo * (4/PI) * Arctan(1 - R)
R = K min / K max
DKo : fatigue threshold @ R=0

Would you like to curvefit m :
>N

Would you like to :

- 1) Calculate Kc using NASA Equation
 - 2) Optimize Kc using Cubic Approximation
 - 3) Enter Kc Manually
- >3

Enter Kc:
>83.27

Enter 1) Enter Delta Kth manually
2) Calculate Delta Kth from DK0
3) Optimize Delta kth Using Cubic Approximation
>1

Delta Kth (R = 0.1000) = 3.266

Press <return> (or C and <return> to change)
>C

Enter Delta Kth (R = 0.1000) :
>7.27

m = 1.000

Press <return> (or C and <return> to change)
>RTN

What confidence interval would you like on the coefficients:

- | | |
|----------|----------|
| 1) 99.9% | 6) 90.0% |
| 2) 99.8% | 7) 80.0% |
| 3) 99.5% | 8) 50.0% |
| 4) 99.0% | 9) 20.0% |

5) 95.0%

Please enter selection.

>6

Computation of Grack Rate Constants

U.S. customary units [inches, ksi, ksi√in]

(Crack Closure Absent - Forman Equation)

K_{1c} = 50.00 Ak = 1.000 BK = 0.5000
YS = 146.0
Thick = 0.2500

K_c = 83.27

DK_o = 6.344

Press <return> to continue

>RTN

R = 0.1000

da/dN	:	Delta K
0.1504E-05	:	8.697
0.1807E-05	:	9.049
0.2390E-05	:	9.662
0.3171E-05	:	9.847
0.4640E-05	:	10.12
0.7561E-05	:	10.78
0.1291E-04	:	12.11
0.1466E-04	:	12.41
0.1372E-04	:	13.18
0.1827E-04	:	13.99
0.2023E-04	:	14.82
0.2700E-04	:	15.63
0.3164E-04	:	16.39
0.3712E-04	:	17.39

Press <return> to continue

>RTN

da/dN	:	Delta K
-----	:	-----

0.4424E-04 :	18.91
0.4232E-04 :	19.36
0.5009E-04 :	21.45
0.6002E-04 :	21.85
0.6819E-04 :	24.46
0.8099E-04 :	25.05
0.8054E-04 :	25.62
0.9050E-04 :	28.07
0.1006E-03 :	28.68
0.1130E-03 :	29.34
0.1785E-03 :	34.31
0.1681E-03 :	34.94
0.1882E-03 :	36.11
0.2449E-03 :	38.03
0.2807E-03 :	40.00
0.2785E-03 :	41.85
0.4012E-03 :	44.04
0.3817E-03 :	45.46
0.4584E-03 :	47.34
0.6988E-03 :	51.98

Press <return> to continue

>RTN

Growth Rate Constants:

C =	0.2910E-04
n =	0.2520
p =	2.257
q =	2.077
* m =	1.000

* indicates a value input by the user

Press <return> to continue

>RTN

90% Confidence Intervals:

$0.7675e-5 \leq C \leq 0.110e-3$
$-0.2194 \leq n \leq 0.7234$
$1.961 \leq p \leq 2.553$
$1.531 \leq q \leq 2.623$

Would you like to store the results on a disk :

>N

The data have successfully been fit to the Forman Equation. The coefficient C in the equation has been fit to an equation of the form:

$$C = A \cdot \log \left(\left(\frac{1}{f} \right) + 1 \right)$$

where:

f = frequency of applied load

The following values for the coefficients were determined :

$$A = 0.70299880016317E-03$$

Please press <return> to continue

>RTN

The data have successfully been fit to the Forman Equation. The coefficient n in the equation has been fit to an equation of the form:

$$n = A \cdot \log \left(\left(\frac{1}{f} \right) + 1 \right)$$

where:

f = frequency of applied load

The following values for the coefficients were determined :

$$A = 6.0878585123169$$

Please press <return> to continue

>RTN

The data have successfully been fit to the Forman Equation. The coefficient p in the equation has been fit to an equation of the form:

$$p = A \cdot \log \left(\left(\frac{1}{f} \right) + 1 \right)$$

where:

f = frequency of applied load

The following values for the coefficients were determined :

$$A = 54.529508388391$$

Please press <return> to continue

>RTN

The data have successfully been fit to the Forman Equation. The coefficient q in the equation has been fit to an equation of the form:

$$q = A \cdot \log \left(\left(\frac{1}{f} \right) + 1 \right)$$

where:

f = frequency of applied load

The following values for the coefficients were determined :

A = 50.178651792115

Please press <return> to continue
>RTN

The data have successfully been fit to the Forman Equation. The parameter ΔK_{th} in the equation has been fit to an equation of the form:

$$\Delta K_{th} = A \cdot \log \left(\left(\frac{1}{f} \right) + 1 \right)$$

where:

f = frequency of applied load

The following values for the coefficients were determined :

A = 175.63485719627

Please press <return> to continue
>RTN

Comparison of Actual and Predicted Values

ΔK	da/dN(act)	da/dN(pred)	% Error
8.70	0.1504000E-05	0.1228642E-05	18.31
9.05	0.1807000E-05	0.1887142E-05	4.44
9.66	0.2390000E-05	0.3291465E-05	37.72
9.85	0.3171000E-05	0.3771017E-05	18.92
10.12	0.4640000E-05	0.4520019E-05	2.59
10.78	0.7561000E-05	0.6509366E-05	13.91
12.11	0.1291000E-04	0.1111932E-04	13.87
12.41	0.1466000E-04	0.1224719E-04	16.46
13.18	0.1372000E-04	0.1526259E-04	11.24
13.99	0.1827000E-04	0.1859967E-04	1.80
14.82	0.2023000E-04	0.2217397E-04	9.61
15.63	0.2700000E-04	0.2580105E-04	4.44
16.39	0.3164000E-04	0.2932364E-04	7.32
17.39	0.3712000E-04	0.3413289E-04	8.05
18.91	0.4424000E-04	0.4183280E-04	5.44

Please press <return> to continue
>RTN

Comparison of Actual and Predicted Values

ΔK	da/dN(act)	da/dN(pred)	% Error
19.36	0.4232000E-04	0.4420718E-04	4.46
21.45	0.5009000E-04	0.5585967E-04	11.52
21.85	0.6002000E-04	0.5821680E-04	3.00
24.46	0.6819000E-04	0.7476238E-04	9.64
25.05	0.8099000E-04	0.7881556E-04	2.68
25.62	0.8054000E-04	0.8285450E-04	2.87
28.07	0.9050000E-04	0.1017637E-03	12.45
28.68	0.1006000E-03	0.1069109E-03	6.27
29.34	0.1130000E-03	0.1127023E-03	0.26
34.31	0.1785000E-03	0.1655161E-03	7.27
34.94	0.1681000E-03	0.1736471E-03	3.30
36.11	0.1882000E-03	0.1898270E-03	0.86
38.03	0.2449000E-03	0.2198689E-03	10.22
40.00	0.2807000E-03	0.2561582E-03	8.74
41.85	0.2785000E-03	0.2965529E-03	6.48

Please press <return> to continue

>RTN

Comparison of Actual and Predicted Values

ΔK	da/dN(act)	da/dN(pred)	% Error
44.04	0.4012000E-03	0.3545201E-03	11.64
45.46	0.3817000E-03	0.3995588E-03	4.68
47.34	0.4584000E-03	0.4707966E-03	2.70
51.98	0.6988000E-03	0.7325326E-03	4.83

Please press <return> to continue

>RTN

Data Set	Coefficient of Determination
1	0.9932

Would you like to interpolate data using the determined coefficients :
>N

Interpolative Model Options

- 1) Determine Equation Constants,
Interpolate Data
- 2) Prepare Data File
- 3) Quit Program

Please select an option

>3

Appendix E: Superposition Program Verification - Integration

To test the accuracy of the linear superposition computer program, it is necessary to compare the numerical integration with exact solutions. Exact solutions for each of the three major types of loading wave forms (sinusoidal, square, and ramp loading) were calculated for a single power law description model of stress corrosion da/dt -K data. The integration was calculated over the period of one cycle of loading. As stated earlier:

$$\frac{da}{dN}_{scc-exact} = \int_{\tau} C K(t)^n dt \quad (E.1)$$

For square wave loading, the program uses the following equations to represent the instantaneous stress intensity $K(t)$:

$$K(t) = \begin{array}{ll} K_{max} & \text{(for the percentage of } \tau \text{ loaded at maximum, } \alpha) \\ K_{min} & \text{(for the remaining percentage of } \tau, 1-\alpha) \end{array}$$

Since K in this case is constant for each separate time period, the exact solution to Equation E.1 is:

$$\frac{da}{dN}_{scc-exact} = C \tau [K_{max}^n * \alpha + K_{min}^n * (1-\alpha)] \quad (E.2)$$

This equation is valid for all C and n . For the tests run, the model was loaded for 50% of the cycle, or $\alpha = 0.50$.

For ramp loading with a total period, τ , the program uses three equations to represent K during a load cycle:

$$\begin{aligned}
K(t) = & \quad (\Delta K / \tau_{load}) * t + K_{min} && \text{(during the loading period)} \\
& K_{max} && \text{(during the hold time)} \\
& K_{max} - (\Delta K / \tau_{unload}) * t && \text{(during the unloading)}
\end{aligned}$$

Each of these time periods was integrated individually and added to create the final solution. Although the solution for the integral during the hold time was the same as for the case of the loaded percent of the square wave, the loading and unloading results differed for each constant n in the stress corrosion power law equation. For simplicity, the exact solutions were calculated and compared with the numerical integration in the program for n values of 1, 2, 3, and 4. The following are the exact solutions for $(da/dN)_{\text{stress corrosion}}$ in Equation E.1 for the loading and unloading $K(t)$ functions and the given exponent:

$$n = 1$$

$$\frac{da}{dN}_{load} = C \tau_{load} \left(\frac{\Delta K}{2} + K_{min} \right) \quad (E.3)$$

$$\frac{da}{dN}_{unload} = C \tau_{unload} \left(K_{max} - \frac{\Delta K}{2} \right) \quad (E.4)$$

$$n = 2$$

$$\frac{da}{dN}_{load} = C \tau_{load} \left(\frac{\Delta K^2}{3} + K_{min} * \Delta K + K_{min}^2 \right) \quad (E.5)$$

$$\frac{da}{dN}_{unload} = C \tau_{unload} \left(K_{max}^2 - K_{max} * \Delta K + \frac{\Delta K^2}{3} \right) \quad (E.6)$$

$$n = 3$$

$$\frac{da}{dN}_{load} = C \tau_{load} \left(\frac{\Delta K^3}{4} + \Delta K^2 * K_{min} + 3 \frac{\Delta K}{2} * K_{min}^2 + K_{min}^3 \right) \quad (E.7)$$

$$\frac{da}{dN}_{unload} = C \tau_{unload} \left(K_{max}^3 - 3 K_{max}^2 \frac{\Delta K}{2} + K_{max} \Delta K^2 - \frac{\Delta K^3}{4} \right) \quad (E.8)$$

$$n = 4$$

$$\frac{da}{dN}_{load} = C \tau_{load} \left(\frac{\Delta K^4}{5} + \Delta K^3 K_{min} + 2 \Delta K^2 K_{min}^2 + 2 \Delta K K_{min}^3 + K_{min}^4 \right) \quad (E.9)$$

$$\frac{da}{dN}_{unload} = C \tau_{unload} \left(K_{max}^4 - 2 K_{max}^3 \Delta K + 2 K_{max}^2 \Delta K^2 - K_{max} \Delta K^3 + \frac{\Delta K^4}{5} \right) \quad (E.10)$$

For the test, the model was statically held for 40% of the period, while loading and unloading each required 30% of the cycle.

For sinusoidal loading with period, τ , the program uses the following equation to represent the loading function:

$$K(t) = \frac{\Delta K}{2} \left[\cos \left(\frac{2\pi t}{\tau} - \pi \right) + 1 \right] + K_{min} \quad (E.11)$$

Integration of Equation E.1 for this loading function yielded unique results for each exponent calculated:

$$n=1$$

$$\frac{da}{dN}_{scc-exact} = C K_{avg} \tau \quad (E.12)$$

n=2

$$\frac{da}{dN}_{scc-exact} = C \tau \left(\frac{\Delta K^2}{8} + K_{avg}^2 \right) \quad (E.13)$$

n=3

$$\frac{da}{dN}_{scc-exact} = C \tau \left(\frac{3}{8} \Delta K^2 * K_{avg} + K_{avg}^3 \right) \quad (E.14)$$

n=4

$$\frac{da}{dN}_{scc-exact} = C \tau \left(\frac{3}{128} \Delta K^4 + \frac{3}{4} K_{avg}^2 \Delta K^2 + K_{avg}^2 \right) \quad (E.15)$$

For evaluation of the integration in the program, the following variables were set:

Frequency = 1 Hz

C constant from Equation III.5 (arbitrary units) = 1

Percent reduction of crack growth in unloading = 0%

For all cases examined, precise agreement was observed between the program numerical integration and the exact solutions presented in equations E.2 through E.15. Specific results are presented in Tables E. 1 through E. 4. Since C was equated to unity, the units for K_{max} , K_{min} , and da/dN are meaningless physically.

Table E.1: Program predictions of $(da/dN)_{stress\ corrosion}$ for n = 1

K_{max}	1×10^{-5}	100,000	20,000	100,000
K_{min}	0	0	10,000	99,999
Sinusoidal	4.9999995×10^{-6}	49,999.995	14,999.999	99,999.50
Exact Solution	5×10^{-6}	50,000	15000	99,999.5
Ramp loading	7.0×10^{-6}	70,000.0	17,000.0	99,999.70
Exact Solution	7×10^{-6}	70,000	17,000	99,999.7
Square loading	5.0×10^{-6}	50,000.0	15,000.0	99,999.50
Exact solution	5×10^{-6}	50,000	15,000	99,999.5

Table E.2: Program predictions of $(da/dN)_{\text{stress corrosion}}$ for $n = 2$

K_{\max}	1×10^{-5}	100,000	20,000	100,000
K_{\min}	0	0	10,000	99,999
Sinusoidal	$3.7499996 \times 10^{-11}$	3.7499996×10^9	2.37499986×10^8	9.99990×10^9
Exact Solution	3.75×10^{-11}	3.75×10^9	2.375×10^8	9.9999×10^9
Ramp loading	6.0×10^{-11}	6.0×10^9	3.0×10^8	9.999940×10^9
Exact Solution	6×10^{-11}	6×10^9	3×10^8	9.99994×10^9
Square loading	5.0×10^{-11}	5.0×10^9	2.50×10^8	9.99990×10^9
Exact Solution	5×10^{-11}	5×10^9	2.5×10^8	9.9999×10^9

Table E.3: Program predictions of $(da/dN)_{\text{stress corrosion}}$ for $n = 3$

K_{\max}	1×10^{-5}	100,000	20,000	100,000
K_{\min}	0	0	10,000	99,999
Sinusoidal	$3.1249997 \times 10^{-16}$	3.1249997×10^{14}	3.9374997×10^{12}	9.999850×10^{14}
Exact Solution	3.125×10^{-16}	3.125×10^{14}	3.9375×10^{12}	9.99985×10^{14}
Ramp loading	5.50×10^{-16}	5.50×10^{14}	5.450×10^{12}	9.99991×10^{14}
Exact Solution	5.5×10^{-16}	5.5×10^{14}	5.45×10^{12}	9.9999099×10^{14}
Square loading	5.0×10^{-16}	5.0×10^{14}	4.50×10^{12}	9.99985×10^{14}
Exact Solution	5×10^{-16}	5×10^{14}	4.5×10^{12}	9.99985×10^{14}

Table E.4: Program predictions of $(da/dN)_{\text{stress corrosion}}$ for $n = 4$

K_{max}	1×10^{-5}	100,000	20,000	100,000
K_{min}	0	0	10,000	99,999
Sinusoidal	$2.7343747 \times 10^{-21}$	2.7343747×10^{19}	6.7734369×10^{16}	9.99980×10^{19}
Exact Solution	2.734375×10^{-21}	2.734375×10^{19}	6.7734375×10^{16}	9.9998×10^{19}
Ramp loading	5.20×10^{-21}	5.20×10^{19}	1.0120×10^{17}	9.999880×10^{19}
Exact Solution	5.2×10^{-21}	5.2×10^{19}	1.012×10^{17}	9.99988×10^{19}
Square loading	5.0×10^{-21}	5.0×10^{19}	8.50×10^{16}	9.99980×10^{19}
Exact Solution	5×10^{-21}	5×10^{19}	8.5×10^{16}	9.9998×10^{19}

Appendix F: Examples for the Superposition Model

This appendix displays the options available to the user in the linear superposition program by proceeding through the program as it predicts corrosion fatigue crack growth rates. The example is intended to duplicate results produced by Speidel for corrosion fatigue in AA 7079-T651 subjected to cyclic loading in a 3.5 % NaCl solution. This material-environment combination is well suited for modeling by linear superposition because of the great influence of environment on crack growth. Speidel noted this and used linear superposition to model the frequency dependence of crack growth²⁸.

Crack Growth Modeling

After an introduction screen is displayed informing the user of the parameters which must be input, the next screen allows the user to decide which model the computer will use to represent fatigue in an inert environment, $(da/dN)_{\text{fatigue}}$. Speidel used the following equation to model fatigue:

$$\frac{da}{dN} = 6 \left(\frac{\Delta K}{E} - 2.7 \times 10^{-5} \right)^2 \frac{K_C}{K_C - \Delta K} \quad (\text{F.1})$$

Where K_C and ΔK are in $\text{MPa}\sqrt{\text{m}}$. For his calculations, however, he neglected the influence of fatigue on crack growth²⁸. Although the current program is not designed to use this equation to model fatigue, data points from either a trend line or specific da/dN - ΔK results can be digitized and input to the program. From these data, constants

can be determined for any of the modeling equations used by the program (Paris, Forman, or Sigmoidal). The Forman Equation with closure was selected for this example and proved to be very accurate. The Forman Equation differs from the other two models in that the equation constants may alternatively be read from a library of material properties on file. It is assumed the user would prefer to read equation constants from the library. Once the Forman Equation is selected as the fatigue model, the program returns the equation constants from a file. After the constants are specified, the program asks if the user would like to change any or all of the constants to values fit from input data.

To begin the search for equation constants, the program asks which units the user would like to use. U.S. customary units are ΔK in ksi $\sqrt{\text{in}}$ and da/dN in in/cycle. For S.I. units, ΔK values are in MPa $\sqrt{\text{mm}}$, while da/dN is given as mm/cycle. If all of the equation constants are to be fit to data, either selection will have no influence on the output since the units of the equation will be determined by the units of the input data.

On the next screen, shown in Figure F.1, the program displays those materials on file for which Forman Equation constants exist. For each class of material listed, further specifications of the material will continue until the specific alloy, heat treatment and product form are selected. The program will then ask which Forman Equation (closure or non-closure) should be used to model data. For this example, the Forman Equation with closure was selected. The program then asks for the thickness of the test specimen, for which 10 mm was input. After displaying material properties, the program will ask if the user would like to input the equation constants manually or read them from the library. In this example,

the constants were read from the library even though they will eventually be determined by data points from the original fatigue plot. By selecting the Forman Equation with closure, the user is required to specify which type of closure to use. The Forman variant was selected.

The program then asks the user whether or not to fit one or more of the Forman Equation constants to a set

of data. After making the appropriate program inputs the user must input the da/dN vs ΔK data digitized from the original graph. After inputting the data and specifying which value (K_{max} , K_{min} , or R) was constant in the data set, the program fits the data to a cubic equation of the form:

$$\frac{da}{dN} = \Delta K^3 + \Delta K^2 + \Delta K + C \quad (F.2)$$

where C is a constant. This is shown in Figure F.2. This is done to approximate ΔK_{th} and K_C values for the data set. When the program asks for ΔK_0 and K_C values which represent ΔK_{th} and ΔK_C , respectively, at $R = 0$, the program displays values from the library file and recommended values calculated from the data. Equation F.2 is used to make recommendations for the threshold and critical stress intensities from the input data. It is

Enter one of the codes in brackets []
To display alloy types....or 0 to exit

NASA/FLAGRO Materials File

Ferrous Alloys (> 50% Fe)		Non-ferrous Alloys	
Iron (alloy or cast)	[A]	1000-9000 Series Aluminum	[M]
ASTM Spec. Grade Steel	[B]	Cast and Misc. Aluminum	[O]
AISI Steel	[C]	Titanium Alloys	[P]
Misc. U.S. Spec. Grade Steel	[D]	Nickel Alloys/Superalloys	[Q]
Trade/Common Name Steel	[E]	Misc. Superalloys	[R]
AISI Type Stainless Steel	[F]	Copper/Bronze Alloys	[S]
Misc. Creep/Heat Resistant Steel	[G]	Magnesium Alloys	[T]
High Temperature Steel	[H]	Misc. Non-ferrous	[U]
Tool Steel	[J]		

Note: Unless specified properties are for
1. Welds not heat treated.
2. 75 deg F Air Environment.
3. Any Crack Orientation except S-T & S-L.

Figure F.1: Materials on file for Forman Equation constants; After NASA FLAGRO¹⁶.

suggested that the values recommended by the program be used unless the operator knows the exact critical and/or threshold values to prevent the program from having a fatal error.

After inputting the data, the program asks if the data should be "flipped". The flipping option allows the program to remove some of the randomness of experimental data. The random nature of the experimental data, when input into the program, can result in equations which do not follow the general trend of crack growth models. Flipping helps the curve fitting subroutine to avoid creating equations which fit the data but do not accurately model crack growth. An

example of inaccurate modeling is an equation where increasing ΔK causes decreasing da/dN for any ΔK . Flipping of data should not be done to data sets with few points (< 15) because the process deletes points outside of the general trend of the data; the resulting number of points after this process may not be sufficient to allow the program to fit the Forman

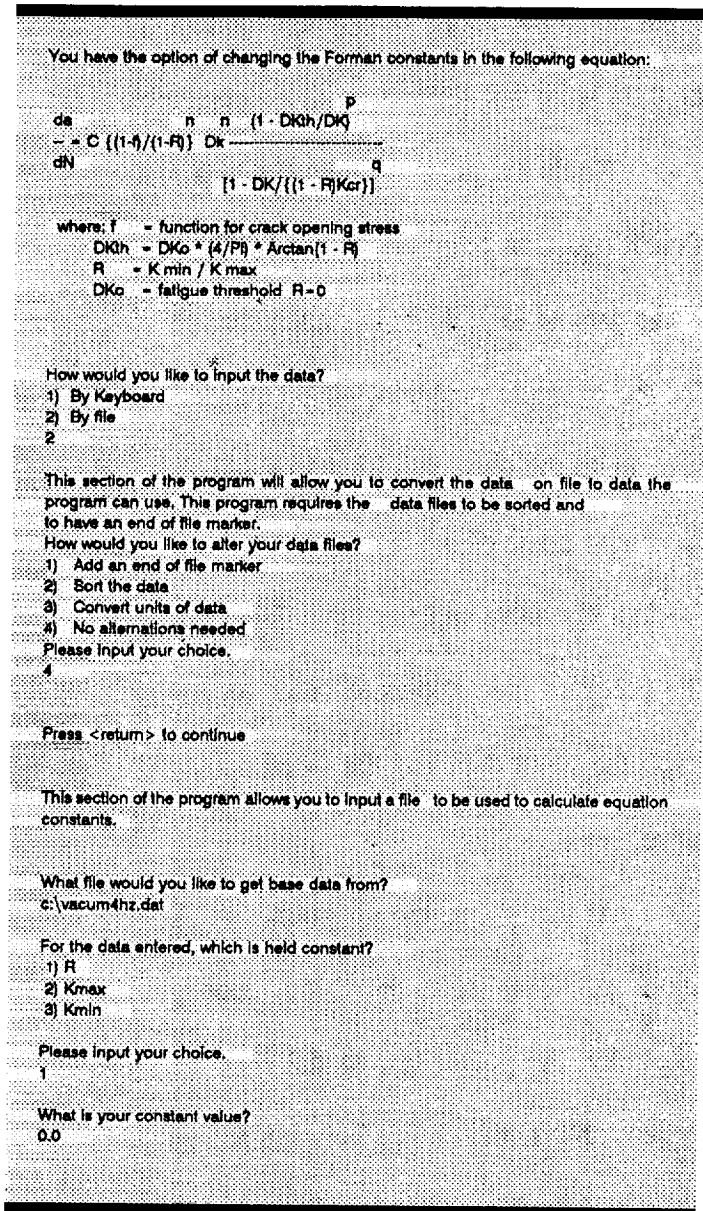


Figure F.2: Input of data modeled by Forman Equation.

Equation to the data. In this situation, the data were not flipped.

Next, the program asks the user if each equation constant should be fit to the data or kept at its current value. For the example problem, all constants were fit to the data, resulting in a maximum error of 3.6% between the Forman Equation and the input data. The program then allows the user to graph the input data and the fitted curve.

At this point, the program begins modeling stress corrosion. For simplicity, the power law model was chosen. Next, the choice between a single and double power law is made, followed by the decision to allow the program to calculate the constants. Stress corrosion data for 7079-T651 in 3.5% NaCl solution are available from the original paper presented by

```

Enter Dk0 :
Current value = 88.50000
Recommended = 1.348401
1.55
Dk0 = 1.55

Enter Ker :
Current value = 1085.573
Recommended = 16.78424
21
Ker = 21.00
Would you like the data flipped?
n
Would you like to fit for C? (currently 0.3120000E-08)
y

Enter Alpha, constraint factor on tensile yielding (Currently = 1.90) :
1.9
Alpha = 1.90

Enter Smax/SiG0, ratio of stress level to flowstress (currently = 0.30) :
0.30
Smax/SiG0 = 0.30

Would you like to fit for n? (currently 2.101000)
y
Would you like to fit for p? (currently 0.5000000)
y
Would you like to fit for q? (currently 1.000000)
y

---Output of Subroutine Curfit1---
Function Code coefficient
1 -9.12537725
15 1.7982318
17 0.756604323
19 1.80457832
Calculated data-----
Maximum Error = 0.34874 Maximum Percent Error = -3.6122
Standard Deviation = 0.1742476

Correlation Coefficient = 0.9820072054883

Press <return> to continue

Forman equation constants
-----
* C = 0.7492E-08
* n = 1.797
* p = 0.7566
* q = 1.805

* - Indicates a value curvefit from data

```

Figure F.3: Specifications for determining Forman Equation constants.

Speidel²⁸. The program was employed to calculate the constants from the input data. The program also allows the user to alter the data before importation into the program. One method of alteration puts an end of file marker in the data set notifying the computer where to stop as it reads in data. Ordering the data from lowest to highest ΔK values is required to insure that the program will not shut down during operation. The conversion of units will allow the user to multiply the stress intensity (X) and the crack growth rate (Y) columns by separate multipliers. The user must calculate the X and Y multipliers to convert the data from current units to the units consistent with inert environment fatigue crack growth rate data.

After the computer imports the stress corrosion cracking data, the program performs the flipping routine and calculates the best fit for a double power law relating da/dt to K. The two sets of constants are output, as well as the stress intensity where the equation changes from using the first set of constants to the second. The program again allows the user to view the data graphed with the model. When data are graphed, the program will ask if the user would like to write the curvefit data to a file. This option allows the user to import the model into a graphing package (Quattro Pro, SigmaPlot, etc.) for later use. This option is also available for the fatigue data.

Output Data Parameters / Calculation

After modeling the two components of crack growth, the program asks a sequence of questions to specify the output data variables for the environmental fatigue crack growth rate prediction. These include the constant loading parameter, range of ΔK

values, spacing of ΔK within this range, and the number of data points. The next screen gives the user the opportunity to reduce the calculation of crack growth due to unloading. Finally, the type of loading is specified. In this example, sinusoidal loading was selected to agree with the loading condition used by Speidel. After inputting the frequency, the program predicts $(da/dN)_{total}$ versus ΔK . The following screen allows the user to type in the X and Y units for the output data file, then a location where the program sends the file. The program then displays the results on the screen, including the contribution of stress corrosion to the total fatigue crack growth rate. The program then asks if the user would like to run the program again. This will only allow the user to alter the loading function; the predefined models and the output parameters will remain the same. After selecting no, the program ends.

Appendix G: Computer Models for Fatigue Analysis

The programs developed by Jonathan Pope, Allen Wilson, and Edward Richey are available in executable form, along with the source codes. To run the programs, place the program disk in drive A:\ and type MENU. A title screen will appear; press <RETURN> and a main menu will appear. The main menu allows the user to choose between digitizing a set of data, or using either the linear superposition or interpolative models.

If the user wishes to run the programs from a drive other than A:\, or from a hard drive, the batch file SETWGKS.BAT must be modified. If the user wishes to install the programs onto a hard drive, the program files must all be copied into the desired directory on the hard drive. The batch file must then be edited. The file should contain:

```
@echo off  
  
set library = drive;drive\watfor;drive\wgks  
  
wgks1
```

where *drive* specifies the location of the GKS (Graphical Kernel System) library files. For example, if the user wishes to install the program on the hard drive (disk C:\) in a directory called NASA, then *drive* = C:\NASA, and setwgks.bat would contain:

```
@echo off  
  
set library = C:\NASA;C:\NASA\watfor;C:\NASA\wgks  
  
wgks1
```

If the user wishes to run the program from a floppy disk in a drive other than A:\, then only the file setwgks.bat must be modified.

The program files found on the program disk include all of the necessary executable files, and the materials files. These files are :

SETWGKS.BAT - defines the location of the WGKS library files

MENU.EXE - executable form of main menu program, written in QBasic

NASA.EXE - executable form of interpolative model program

LINEAR.EXE - executable form of linear superposition model

DIGITIZE.EXE - executable form of graph digitization program

ROTUNDA.EXE - executable program which draws main title screen

WGKS1.EXE - loads WATCOM WGKS into memory

WATFOR.LIB, WGKS.LIB - library files for WGKS

NASAMFM, NASAMFC, USRMFM, USRMFC - materials files

The source code listings are also included on the program disk. The following files are needed for each of the executable programs:

NASA.EXE - Interpolative model

Nasa.for

Graph.for

Filesub.for

Cfit.for

Forman.for

Sig.for

Sinh.for

LINEAR.EXE - linear superposition model

Linear.for

Linear2.for

Inmfil.for

Graph2.for

DIGITIZE.FOR

Digitize.for

ROTUNDA.EXE

Rotunda.for

All of the programs also require the files Gksdefn.for and Gkscover.for.

The source codes for the computer programs are contained in the compressed file SOURCE.EXE located on the program disk. To expand the SOURCE.EXE file, copy the file to the directory you wish to use and type SOURCE.EXE. The datafiles listed in Appendix A are contained in the compressed file DATAFILE.EXE. Both files are self-extracting.

The executable programs were all compiled using the WATFOR-77 compiler from Watcom. The compiler only uses conventional memory, thus, in order for the program to run, there must be at least 570K of free conventional memory before loading WGKS into memory. Unnecessary memory resident programs, such as mouse drivers, should be removed.

REPORT DOCUMENTATION PAGE			Form Approved OMB No. 0704-0188	
Public reporting burden for this collection of information is estimated to average 1 hour per response, including the time for reviewing instructions, searching existing data sources, gathering and maintaining the data needed, and completing and reviewing the collection of information. Send comments regarding this burden estimate or any other aspect of this collection of information, including suggestions for reducing this burden, to Washington Headquarters Services, Directorate for Information Operations and Reports, 1215 Jefferson Davis Highway, Suite 1204, Arlington, VA 22202-4302, and to the Office of Management and Budget, Paperwork Reduction Project (0704-0188), Washington, DC 20503.				
1. AGENCY USE ONLY (Leave blank)		2. REPORT DATE September 1994		3. REPORT TYPE AND DATES COVERED Contractor Report
4. TITLE AND SUBTITLE Computer Modeling the Fatigue Crack Growth Rate Behavior of Metals in Corrosive Environments			5. FUNDING NUMBERS NAG1-745 WU 538-02-10-01	
6. AUTHOR(S) Edward Richey III, Allen W. Wilson, Jonathan M. Pope, and Richard P. Gangloff				
7. PERFORMING ORGANIZATION NAME(S) AND ADDRESS(ES) University of Virginia Charlottesville, VA 22903			8. PERFORMING ORGANIZATION REPORT NUMBER	
9. SPONSORING/MONITORING AGENCY NAME(S) AND ADDRESS(ES) National Aeronautics and Space Administration Langley Research Center Hampton, VA 23681-0001			10. SPONSORING/MONITORING AGENCY REPORT NUMBER NASA CR-194982	
11. SUPPLEMENTARY NOTES Langley Technical Monitor: Robert S. Piascik Final Report				
12a. DISTRIBUTION/AVAILABILITY STATEMENT Unclassified - Unlimited Subject Category - 26			12b. DISTRIBUTION CODE	
13. ABSTRACT (Maximum 200 words) The objective of this task was to develop a method to digitize FCP kinetics data, generally presented in terms of extensive $da/dN-\Delta K$ pairs, to produce a file for subsequent linear superposition or curve-fitting analysis. The method that was developed is specific to the Numonics 2400 Digitab and is comparable to commercially available software products as Digimatic TM 4. Experiments demonstrated that the errors introduced by the photocopying of literature data, and digitization, are small compared to those inherent in laboratory methods to characterize FCP in benign and aggressive environments. The digitizing procedure was employed to obtain fifteen crack growth rate data sets for several aerospace alloys in aggressive environments.				
14. SUBJECT TERMS Fatigue crack growth; Curve-fitting; Digitization; Superposition; Analysis program			15. NUMBER OF PAGES 179	
			16. PRICE CODE A09	
17. SECURITY CLASSIFICATION OF REPORT Unclassified	18. SECURITY CLASSIFICATION OF THIS PAGE Unclassified	19. SECURITY CLASSIFICATION OF ABSTRACT	20. LIMITATION OF ABSTRACT	